



**Maria João Xavier
Ribeiro**

**Formação de Nanomaterial-Corona específica:
avanços para o modo de ação de NMs**

**dyNaMIC – Nanomaterial-corona formation species
targeted, advances for NMs mode of action**



**Maria João Xavier
Ribeiro**

**Formação de Nanomaterial-Corona específica:
avanços para o modo de ação de NMs**

**dyNaMIC – Nanomaterial-corona formation species
targeted, advances for NMs mode of action**

Tese apresentada à Universidade de Aveiro para cumprimento dos requisitos necessários à obtenção do grau de Doutor em Biologia, realizada sob a orientação científica da Doutora Mónica Amorim investigadora principal da Universidade de Aveiro, Departamento de Biologia e CESAM Portugal, e do Professor Doutor Janeck Scott-Fordsmand investigador sénior do Departamento de Biociências da Universidade de Aarhus, Dinamarca.

Apoio financeiro da FCT e do FSE no âmbito do III Quadro Comunitário de Apoio através de uma Bolsa de Doutoramento atribuída a Maria João Xavier Ribeiro (SFRH/BD/95027/2013) e através dos projetos SUN-Sustainable Nanotechnologies 394 (FP7-NMP-2013-LARGE-7, GA No. 604305), e NM_OREO: using a NM-(bio)molecule cOrona approach to undeRstand the mEchanisms of tOxicity - a systems biology environment impact study (POCI-01-0145-FEDER-016771, PTDC/AAG-MAA/4084/2014).

o júri

presidente

Doutor António José Arsénia Nogueira
Professor Catedrático da Universidade de Aveiro

vogais

Doutor Amadeu Mortágua Velho da Maia Soares
Professor Catedrático da Universidade de Aveiro

Doutora Lúcia Maria das Candeias Guilhermino
Professora Catedrática da Universidade do Porto

Doutor Jörg Römbke
Diretor Executivo (CEO), Ect Oekotoxikologie, Alemanha

Doutora Mónica João de Barros Amorim (orientadora)
Investigadora Principal do Departamento de Biologia e Centro de Estudos do Ambiente e do Mar (CESAM) da Universidade de Aveiro

agradecimentos

Agradeço aos meus orientadores, Dra. Mónica Amorim e Dr. Janeck Scott-Fordsmand, por me terem dado a possibilidade de realizar esta etapa de crescimento pessoal e profissional.

Agradeço também:

À equipa técnica (de Aveiro, Silkeborg e Aarhus) pela ajuda e disponibilidade, em especial ao Abel.

Às minhas meninas do coração, por todo o apoio, partilha e amizade.

Aos meus pais, por tudo. À minha irmã, pela cumplicidade. Ao João, por ser o meu porto seguro.

palavras-chave

Contaminantes emergentes, stress oxidativo, genotoxicidade, sobrevivência, reprodução, multigeração, avaliação de risco, nanomaterial, invertebrados de solo, oligochaeta, *in vitro*.

resumo

A crescente utilização de nanomateriais (NMs) numa grande variedade de setores é devida às melhores e mais inovadoras propriedades que estes podem oferecer, por exemplo, à indústria de uso final ou à biomedicina. A libertação de NMs no ambiente durante o seu ciclo de vida é um cenário actual. Ao entrarem no ambiente, os NMs irão interagir com os organismos, e apesar dos crescentes esforços para fornecer resultados conclusivos sobre a segurança dos NMs, o seu impacto ainda é pouco conhecido, particularmente no compartimento terrestre. Existem várias lacunas no conhecimento que necessitam de ser preenchidas de forma a entender melhor os mecanismos que levam à toxicidade dos NMs; assim, esta tese pretende aumentar o conhecimento dos efeitos de NMs seleccionados em invertebrados de solo. Perceber o mecanismo de acção dos NMs é a chave para estratégias safer-by-design, fundamentais para melhorar a sustentabilidade da nanotecnologia.

A avaliação dos efeitos dos NMs foi realizada a vários níveis de organização biológica, cobrindo diferentes endpoints, que, sendo integrados, permitem perceber os mecanismos de toxicidade. Os efeitos a longo-prazo e multigeneracionais foram também considerados, uma vez que são possíveis cenários de exposição aos NMs. Os NMs seleccionados – prata (Ag), liga de carboneto de tungsténio-cobalto (WCCo) e o caso estudo de óxido de cobre (CuO) (usando diferentes modificações da superfície), juntamente com os correspondentes sais, foram usados a diferentes níveis: molecular (stress oxidativo e genotoxicidade) e do organismo (sobrevivência e reprodução). Os invertebrados modelo de solo *Enchytraeus crypticus* e *Eisenia fetida* foram usados em exposições *in vivo* e *in vitro*, respectivamente.

Concentrações sub-letais de Ag NMs induziram efeitos bioquímicos (de stress oxidativo e genotoxicidade) em *E. crypticus*, distintos e mais tardios comparados com a forma não-nano (AgNO₃). Enquanto diferentes respostas apontam para efeitos nano-específicos, a possível dissolução de Ag NMs e consequente toxicidade induzida pelos iões também pode ocorrer. WCCo NMs comprometeram a reprodução de *E. crypticus* de forma superior comparado com CoCl₂ (assumindo concentrações de Co semelhantes). Menores concentrações de Co na interface solo-água e a menor internalização de Co nos organismos expostos a WCCo, sugere que a toxicidade resulta do efeito combinado entre WC e Co. Apesar da internalização de Co, a exposição multigeneracional não aumentou a toxicidade em termos de sobrevivência e reprodução. A monitorização da quantidade de Co nos organismos aponta para a eliminação e armazenamento como estratégias de detoxificação nos organismos expostos a WCCo NMs e CoCl₂, respectivamente. Os CuO NMs não diminuíram a viabilidade das células dos sistema imunitário de *Eisenia fetida*, quer na forma pristina ou com diferentes modificações da superfície. A interacção com as biomoléculas presentes no fluido celómico terá levado à formação de uma corona nativa que interferiu com o potencial de toxicidade, independentemente da modificação da superfície, mas o impacto dessa interacção não é claro. Alguns aspectos técnicos necessitam de optimização devido à possibilidade dos efeitos terem sido subestimados, mas este constitui um sistema de teste promissor para a bateria de testes *in vitro*.

keywords

Emerging contaminants, oxidative stress, genotoxicity, survival, reproduction, multigeneration, risk assessment, nanomaterial , soil invertebrates, oligochaeta, *in vitro*.

abstract

The growing use of nanomaterials (NMs) in a wide variety of fields is due to the better and innovative properties that they can offer to, e.g., the end-use industry or biomedicine. The release of NMs into the environment during their life-cycle is an actual scenario. Reaching the environment, the NMs will interact with the organisms, but despite the growing efforts to provide conclusive results on the safety of NMs, their impact is still poorly understood, particularly in the terrestrial compartment. There are many knowledge gaps that need to be covered to better understand the mechanisms that drive NMs toxicity, hence this thesis aims to increase the knowledge on the effects of selected NMs in soil invertebrates. Understanding NMs mode of action is key to safer-by-design strategies that will contribute to improve nanotechnology sustainability.

Effect assessment of NMs was done at several levels of biological organization, covering different endpoints, which can be integrated in order to understand the toxicity mechanisms. Further, long-term and multigenerational effects were also considered, as they are likely scenarios for NMs exposure. Selected NMs - silver (Ag), tungsten carbide cobalt (WCCo) and copper oxide (CuO) case study (using different surface modifications), along with the corresponding salt forms, were tested at different levels: molecular (oxidative stress and genotoxicity) and organism (survival and reproduction). The standard soil invertebrates *Enchytraeus crypticus* and *Eisenia fetida* were used for *in vivo* and *in vitro* exposures, respectively.

Sub-lethal concentrations of Ag NMs induced distinct and later biochemical effects (oxidative stress and genotoxicity) in *E. crypticus* compared to the non-nano form (AgNO₃). While different responses point to nano-specific effects, possible dissolution of Ag NMs and consequent ion-driven toxicity can also be occurring. WCCo NMs impaired reproduction in *E. crypticus*, at a higher extent compared to CoCl₂ (assuming similar Co concentrations). The lower Co concentrations in the soil:water interface and lower uptake in WCCo exposed organisms suggest that toxicity resulted from a combined effect between WC and Co. Multigenerational exposure did not increase toxicity in terms of survival and reproduction, in spite of Co internalization. Monitoring of Co body burden pointed to Co elimination and storage as the detoxifying strategies in WCCo and CoCl₂ exposed organisms, respectively. CuO NMs did not decrease viability of *Eisenia fetida*'s immune cells, either in the pristine form or with different surface modifications. The interaction with the biomolecules present in the coelomic fluid may have led to the formation of a native corona that interfered with the toxic potential, independently of the surface modification, but the impact of such interaction is unclear. Some technical aspects need further optimization due to the possibility that the effects could have been underestimated, but this constitutes a promising test system for *in vitro* testing battery.

TABLE OF CONTENTS

Introduction and outline of the thesis	12
Nanotoxicology.....	13
Gaps and challenges in Nanotoxicology.....	16
Environmental hazard of Nanomaterials – Soil Ecotoxicology	17
Test materials.....	18
Test organisms.....	19
Thesis structure.....	19
Chapter I: Oxidative stress mechanisms caused by Ag nanoparticles (NM300K) are different from AgNO₃: effects in the soil invertebrate <i>Enchytraeus crypticus</i>	
Abstract.....	34
Introduction	34
Materials and Methods	35
Results	38
Discussion.....	43
Conclusions.....	47
References.....	48
Chapter II: Silver (nano)materials cause genotoxicity in <i>Enchytraeus crypticus</i> – as determined by the comet assay	
Abstract.....	58
Introduction	58
Materials and Methods	60
Results and Discussion	64
Conclusions.....	70
References.....	71
Supporting Information	78

Chapter III: Fate and effect of nano tungsten carbide cobalt (WCCo) in the soil environment: observing a nanoparticle specific toxicity in *Enchytraeus crypticus*

Abstract.....	86
Introduction	86
Materials and Methods	88
Results	91
Discussion.....	97
Conclusions.....	99
References.....	99
Supporting Information	107

Chapter IV: Multigenerational exposure to Cobalt (CoCl₂) and WCCo nanoparticles in *Enchytraeus crypticus*

Abstract.....	111
Introduction	111
Materials and Methods	113
Results	115
Discussion.....	120
Conclusions.....	122
References.....	123

Chapter V: Cell *in vitro* testing with soil invertebrates - challenges and opportunities to model the effect of nanomaterials – CuO surface modified case study

Abstract.....	131
Introduction	131
Materials and Methods	133
Results	137
Discussion.....	140
Conclusions.....	143

References.....	144
Supporting Information	151
General discussion and conclusions.....	154

INTRODUCTION AND OUTLINE OF THE THESIS

Nanomaterials (NMs) can be roughly defined as materials with one or more dimensions in the 1-100 nm range, and their higher surface to volume ratio endow them distinct physico-chemical properties (e.g. electrochemical reactivity, possible surface functionalisation) from the bulk materials (Ahlbom et al., 2008). Such properties have given NMs potential for application in a myriad of fields such as electronics (Mahian et al., 2013), cosmetics (Mu and Sprando, 2010), biomedicine (Pankhurst et al., 2003), bioremediation (Liu, 2006), etc., which has pushed the field of nanotechnology to grow at an increasing, yet concerning, pace. It's highly likely that at any stage of their life-time NMs can enter the environment *via* air, water and soil, and interaction with organisms is therefore an actual scenario (Gupta et al., 2015). In fact, Europe is expected to release to the different environmental compartments about 50.000 tons/year of NMs and their transformation products (Keller et al., 2013). The risk assessment on NMs has been a major concern for researchers, however the hazard related to NMs applications is still far from being definitively addressed, hence, research on the toxicity of NMs is a pressing matter.

The present thesis aims to provide additional information on the risk that NMs pose to the organisms, by studying the effects of selected nano-materials in soil invertebrates. This introductory chapter was divided in 5 sections, in order to provide a contextualization of the studies performed, being divided as follows:

1. Nanotechnology
2. Gaps and challenges in Nanotoxicology
3. Environmental hazard of Nanomaterials – Soil Ecotoxicology
4. Test materials
5. Test organisms
6. Thesis structure

1. NANOTOXICOLOGY

Given the possible interaction of NMs with living organisms, extensive research has been done to assess the risk of NMs using different model organisms and different materials. Nanotoxicological studies have exponentially increased in the last decades, providing much information on the NMs toxicity mechanisms, but the information available is still not enough to correctly evaluate NMs safety as many aspect of the mechanisms of action are still poorly understood.

The ability to cross biological internal barriers, such the lung epithelium (Yacobi et al., 2007) or the blood-brain barrier (Kreuter et al., 1995), due to their nano-size has proven NMs to be a threaten to living organisms. Once inside the organism, the NMs can be translocated to other parts of the body and be taken up by cells by different mechanisms (Chithrani et al., 2006; De Jong et al., 2008), with implications to the normal cellular metabolism.

Of the molecular-level endpoints related to NMs toxicity mechanisms, two of the most relevant are detailed:

I. OXIDATIVE STRESS

Generally speaking, NMs-derived toxicity is thought to occur primarily via enhanced generation of reactive oxygen species (ROS) that disturbs the redox status of the cell, activating oxidative stress (Choi et al., 2010; Dasari et al., 2013). ROS include superoxide anion ($O_2^{\cdot-}$) and hydroxyl ($\cdot OH$) radicals, hydrogen peroxide (H_2O_2) and singlet oxygen ($^1/2 O_2$) that, when in excess, can disturb the normal functioning of the cell (Apel and Hirt, 2004). To prevent cellular ROS accumulation, cells have an antioxidant system composed of enzymes (e.g. catalase (CAT), superoxide dismutase (SOD), glutathione peroxidase (GPx)) and low molecular mass compounds scavengers (e.g. glutathione, metallothioneins) that counteracts overproduction of ROS by converting them into non radical products (Pisoschi and Pop, 2015) (Fig.1).

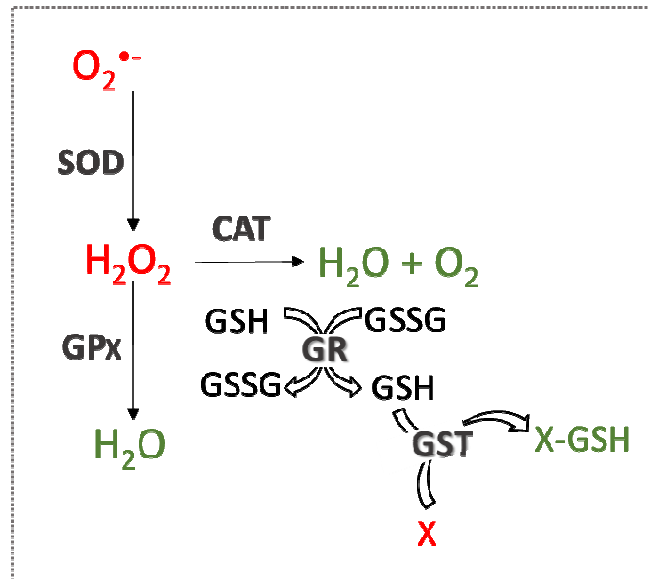


Figure 1: Schematic overview of the detoxifying enzymatic reactions where radicals (in red) are converted to stable compounds (in green). Main enzymes are shown in bold grey: SOD – SuperOxide Dismutase, CAT – CATalase, GPx – Glutathione PeroXidase, GR – Glutathione Reductase, Glutathione S-Transferase.

When the antioxidant system fails to balance ROS production, radicals can interfere with biomolecules causing secondary cellular injuries, such as, cell membrane (Jeng and Swanson, 2006) and DNA damage (Ahamed et al., 2008), mitochondrial membrane permeability alteration (Hussain et al., 2005) and inflammation (Yazdi et al., 2010) (Fig.2). If the cell defenses are not enough to overcome the cellular injuries, it can ultimately lead to cell death, either *via* apoptosis (Choi et al., 2010; Hsin et al., 2008) or necrosis (Pan et al., 2009). Nonetheless, NMs toxicity may also be directly related to NMs, i.e., oxidative stress-independent. For instance, carbonaceous NMs may physically interact with cell membranes (Hirano et al. 2008) and the cytoskeleton (Holt et al. 2010), compromising the normal cell functions.

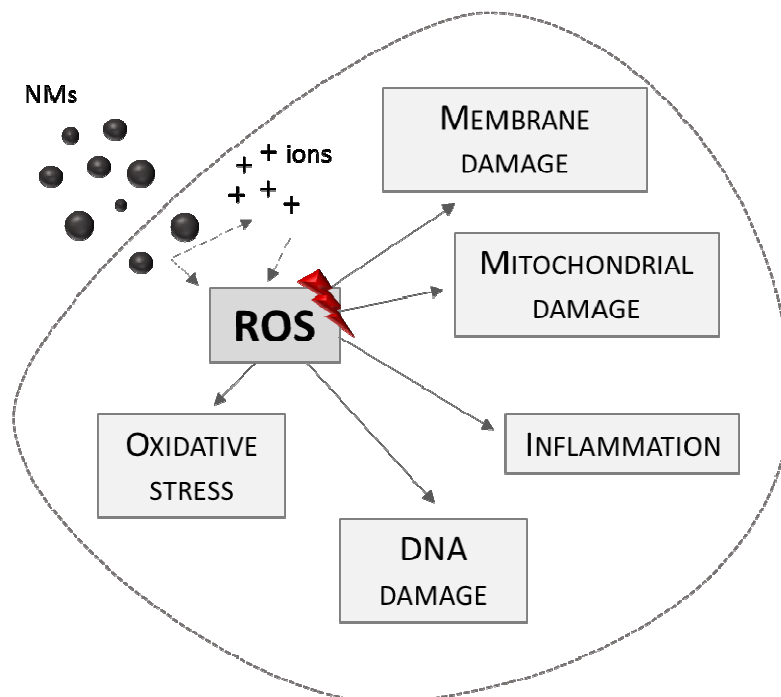


Figure 2: Main cellular events involved in nanomaterials toxicity (adapted from Sanvicens et al. (2008)), where Reactive Oxygen Species (ROS) imbalance is pointed as the initiating event that leads to subsequent cellular effects.

Given the pivotal role of ROS production in the NMs toxicity mechanism, evaluation of oxidative stress was included in the studies of this thesis to understand toxicity of selected NMs (Chapter I).

II. DNA DAMAGE

DNA damage has been also linked to NMs toxicity (Fig. 2) and primarily genotoxicity can be a direct or indirect consequence of NMs cellular internalization:

- a. Direct interaction with DNA or chromosomes is facilitated by NMs small size that allow them to cross the nuclear membrane, or by the disappearance of the nuclear membrane during mitosis, potentially affecting DNA replication and mitosis (An et al., 2010; Yang et al., 2009).
- b. DNA-ROS and/or DNA-released transition metals interaction (Asharani et al., 2009), NMs interference with nuclear proteins (Chen and von Mikecz, 2005) and deregulation of mitotic check points (Huang et al., 2009) are ways of indirect NMs genotoxicity.

Secondary genotoxicity may also arise when DNA is indirectly damaged by ROS overproduced not by the cell itself but by inflammatory cells (Trouiller et al., 2009).

Such damages in the DNA will profoundly affect the correct functioning of the cells, especially if the damage is done in the germline cells due to the potential to change heritable characteristics. Hence, genotoxicity is another endpoint usually included in NMs toxicology studies, and will also be in the scope of the present thesis (Chapter II).

Because the effects of NMs on a molecular level will interfere with higher levels of biological organisation, organism-level endpoints are also needed to understand the NMs impact. In fact, most of data available in regulatory risk assessment involves animal testing using standardized protocols and guidelines developed by international organizations such as Organisation for Economic Co-operation and Development (OECD) and the International Organization for Standardization (ISO), that focus on organism level endpoints - e.g. survival, reproduction, growth. Obtaining and integrating data across multiple levels of organization is of paramount importance, for a more precise and predictive risk assessment approach, which is a present challenge (Sturla et al., 2014). In the present thesis, survival and reproduction were the organism-level endpoints selected for NMs testing (Chapter III and IV).

2. GAPS AND CHALLENGES IN NANOTOXICOLOGY

Despite the growth of nanotoxicology in the last decades, the current uncertainty in NMs safety is due to the existing gaps in knowledge that still concern researchers in the field (see (Amorim et al., 2016; Dhawan and Sharma, 2010; Fadeel et al., 2015; Hu et al., 2016)), some of which are addressed in the present and following sections.

Research has shown that NMs toxicity is, in fact, multiparametric, i.e. toxicity of a particular NMs can be modulated by several factors, such as, intrinsic physicochemical characteristics (Ispas et al., 2009; Uski et al., 2017) and the biological media (Lesniak et al., 2012). Nonetheless, multiparametric testing is usually hampered by logistic limitations, thus, for the purpose of this thesis, only the effect on the surface coating will be considered. The coating on NMs surface can have a major impact in the biological effects, as changes in the surface will influence the mechanisms for cellular entry and, consequently, the cytotoxicity (Javed et al., 2017; Schaeublin et al., 2011; Xia et al., 2009). Even though surface engineering is key to design safer NMs and nano-enable products, results still fail to predict the behaviour and fate in living organisms and no clear correlations could be established (Hussain et al., 2015). It is also included in the present

thesis a study for effect comparison of differently coated NMs to understand toxicity's modulation (Chapter V).

Another current challenge in understanding NMs mode of action is related to the origin of the toxicity. Many studies with metallic NMs have attributed the toxicity to the released ions delivered by the NMs upon intracellular dissolution. Such "Trojan-horse" effect was proposed for several NMs such as silver (Ag) (Park et al., 2010) or copper oxide (CuO) (Studer et al., 2010); however, in other cases, the sole action of the ions doesn't explain the whole toxicity, as effect comparison with salt forms also point to a direct NP-specific effect (e.g. Ag NMs (Bicho et al., 2016; Chae et al., 2009) or CuO NMs (Cho et al., 2012; Gomes et al., 2015). Thus, and having in mind the role that the ions may display in NMs toxicity, in this thesis the biological effects exerted by the NMs were compared to those of the equivalent ions.

3. ENVIRONMENTAL HAZARD OF NANOMATERIALS – SOIL ECOTOXICOLOGY

Soil is considered a sink where NMs can be released and accumulate over time (Cornelis et al., 2014). This poses a threat to soil organisms, particularly the invertebrates, that are of prime importance in the soil ecosystem, by, for instance, maintaining the nutrient cycle, mixing minerals and organic matter and sustaining the porosity and structure of the soil), this way influencing other soil organisms' habitats (Jouquet et al., 2006; Lavelle et al., 2006).

The majority of the *in vivo* studies using soil-dwelling organisms focus on short-term exposures to NMs e.g. the standard toxicity tests for acute or short chronic effects. However, the release of NMs and NMs-containing products to the environment is more related to slower, continuous processes, which make low-dose, chronic and multigenerational exposures considered a most likely and relevant scenario (Amorim et al., 2016; Comfort and Braydich-Stolle, 2014; Diez-Ortiz et al., 2015) but such studies are still very limited mainly due to the time they require. Considering only acute, short-term effects will not allow the correct understanding of the toxicity mechanisms and consequent risk assessment, as delayed toxicity, transgenerational effects or even the recovery ability of the organisms can be overlooked. Hence, this thesis was also intended to include in the current paradigm most likely scenarios of exposure to NMs, by considering prolonged exposure periods in established test guidelines (Chapter III) and the potential for multigenerational toxicity (Chapter IV).

One additional difficulty when considering soil exposures to NMs is the characterization and fate within the soil matrixes. NMs properties and bioavailability can be affected by the soil characteristics, such as the ionic strength, pH or organic matter, but may also vary depending on the organism and route of uptake (Cornelis et al., 2014; Shoults-Wilson et al., 2011). Hence, relating the behaviour of NMs in the soil compartment (and the consequent bioavailability) with the biological effects is of major importance in the risk assessment, however, the current lack of proper techniques and/or equipment difficult such task (Amorim et al., 2016; Gomes et al., 2015). When considering soft-bodied soil invertebrates, two possible routes for NMs entry in the organism are at play, one of which being the gastrointestinal tract (via ingestion of contaminated soil particles and food), and the other dermal uptake (via the skin) (Garcia-Velasco et al., 2016; Laycock et al., 2015). As these organisms are exposed to NMs in both the soil and the soil:pore water, it becomes also important to understand which is the critical soil constituent to understand NMs bioavailability. Even though it's not possible in these studies to fully characterize the NMs, chemical analyses in the soil, the soil:water biofilm and in the organisms were performed to add to the interpretation of NMs toxicity (Chapter III and IV).

4. TEST MATERIALS

The materials used in this thesis were selected based on relevance given the long-time, widespread use (Ag NMs and CuO NMs) and the potential for environmental release (WCCo NP):

Silver nanomaterials (Ag NMs) are the most widely used NMs, mostly owed to the antimicrobial property (Rai et al., 2009). They can be applied in a myriad of consumer items, e.g. house holding products (Zhang et al., 2007), textiles (Emam et al., 2013) or paints (Holtz et al., 2012) and in medical equipment (Cheng et al., 2004).

Copper Oxide nanomaterials (CuO NMs) have applications in antimicrobial preparations (Ren et al., 2009), heat-transfer fluids (Chang et al., 2011), electrochemical and bio sensors (Luo et al., 2006), and batteries (Park et al., 2009).

Tungsten Carbide Cobalt (WCCo) are a class of cemented carbides of great interest to several industrial fields, as it increases hardness and wear resistance in cutting and drilling tools (Prakash, 1995; Yao et al., 1998).

5. TEST ORGANISMS

Enchytraeids (Oligochaeta, Enchytraeidae) are extremely relevant ecotoxicological models with established guidelines (ISO, 2014; OECD, 2016). The species *Enchytraeus crypticus* in particular present several advantages over other enchytraeid species (e.g., shorter generation and test time) (Castro-Ferreira et al., 2012), and numerous molecular and organism-level endpoints are currently available for this species. Molecular-level techniques already implemented include evaluation of energy reserves (Gomes et al., 2015), oxidative stress (Ribeiro et al., 2015), genotoxicity (Maria et al., 2017), transcriptomics (Castro-Ferreira et al., 2014) and metabolomics (Maria et al., 2018). A full life cycle test was also developed, allowing the discrimination of effects in early developmental stages (Bicho et al., 2015), and more recently, a multigenerational test was optimized (Bicho et al., 2017a). As several biological organization levels endpoints were optimized for *E. crypticus*, integration of the different results will aid in the construction of Adverse Outcome Pathways (AOP) for NMs, important to completely understand the toxicity mechanisms (Ankley et al., 2010), and was already proposed for CuO NMs (Bicho et al., 2017b).

6. THESIS STRUCTURE

The present thesis will be structured in five chapters, each covering a particular study related to NMs toxicity:

Chapter I: "Oxidative stress mechanisms caused by Ag nanoparticles (NM300K) are different from AgNO₃: effects in the soil invertebrate *Enchytraeus crypticus*" published in the International Journal of Environmental Research and Public Health, 12, (2015), 9589-9602.

This study aimed to assess the effect of silver nanoparticles (Ag NMs) in terms of oxidative stress in the enchytraeid *E. crypticus*. The salt AgNO₃ was also tested to ascertain the source of toxicity.

Chapter II: “Silver (nano)materials cause genotoxicity in *Enchytraeus crypticus* – as determined by the comet assay” published in *Environmental Toxicology and Chemistry*, 37(1), (2018), 184-191. This work was a follow-up of Chapter I.

Knowing the oxidative potential of Ag NMs, the genotoxic effect was studied using the comet assay, a tool that was not yet implemented in *E. crypticus*. First, the Comet assay was optimized, and then validated using organisms previously exposed to Ag NMs and AgNO₃.

Chapter III: “Fate and effect of nano tungsten carbide cobalt (WCCo) in the soil environment: observing a nanoparticle specific toxicity in *Enchytraeus crypticus*” published in *Environmental Science and Technology*, 52 (19), (2018), 11394-11401.

This study aimed to assess the effect of the nanomaterial Tungsten Carbide Cobalt (WCCo) in *E. crypticus*, in terms of survival and reproduction, with a prolonged exposure period to evaluate longer term effects in total population. To understand the potential role of cobalt ions, the salt CoCl₂ was used for effect comparison.

Chapter IV: “Multigenerational exposure to Cobalt (CoCl₂) and WCCo nanoparticles in *Enchytraeus crypticus*” – submitted in *Nanotoxicology* (major revisions).

This study focused on another level of long term effects of WCCo and CoCl₂ in *E. crypticus*, using a multigenerational exposure. The occurrence of transgenerational toxicity was also considered, and the two last generations were reared in non-contaminated soil.

Chapter V: “Cell *in vitro* testing with soil invertebrates - challenges and opportunities to model the effect of nanomaterials – CuO surface modified case study” - submitted.

This *in vitro* study assessed the cytotoxicity of different coatings in copper oxide NMs (CuO NMs) in a particular type of immune cells – coelomocytes to understand the potential modulatory effect of the surface coating. The cells were extracted from the earthworm *Eisenia fetida*.

REFERENCES

- Ahamed, M., Karns, M., Goodson, M., Rowe, J., Hussain, S.M., Schlager, J.J., Hong, Y., 2008. DNA damage response to different surface chemistry of silver nanoparticles in mammalian cells. *Toxicol. Appl. Pharmacol.* 233, 404–410. doi:10.1016/j.taap.2008.09.015
- Ahlbom, A., Bridges, J., De Jong, W., Jung, T., Hajslova, J., Hartemann, P., Pagés, J., Mattsson, M.-O., Rydzynski, K., Stahl, D., Williams, D., 2008. Opinion on the scientific aspects of the existing and proposed definitions relating to products of nanoscience and nanotechnologies. *Eur. Comm.* 1–22.
- Amorim, M.J.B., Roca, C.P., Scott-Fordsmand, J.J., 2016. Effect assessment of engineered nanoparticles in solid media - Current insight and the way forward. *Environ. Pollut.* 218, 1370–1375. doi:10.1016/j.envpol.2015.08.048
- An, H., Liu, Q., Ji, Q., Jin, B., 2010. DNA binding and aggregation by carbon nanoparticles. *Biochem. Biophys. Res. Commun.* 393, 571–576.
- Ankley, G.T., Bennett, R.S., Erickson, R.J., Hoff, D.J., Hornung, M.W., Johnson, R.D., Mount, D.R., Nichols, J.W., Russom, C.L., Schmieder, P.K., 2010. Adverse outcome pathways: a conceptual framework to support ecotoxicology research and risk assessment. *Environ. Toxicol. Chem.* 29, 730–741.
- Apel, K., Hirt, H., 2004. Reactive oxygen species: metabolism, oxidative stress, and signal transduction. *Annu. Rev. Plant Biol.* 55, 373–99. doi:10.1146/annurev.arplant.55.031903.141701
- Asharani, P. V, Low, G., Mun, K., Hande, M.P., Valiyaveetil, S., 2009. Cytotoxicity and Genotoxicity of Silver in Human cells 3, 279–290.
- Bicho, R.C., Ribeiro, T., Rodrigues, N.P., Scott-Fordsmand, J.J., Amorim, M.J.B., 2016. Effects of Ag nanomaterials (NM300K) and Ag salt (AgNO₃) can be discriminated in a full life cycle long term test with *Enchytraeus crypticus*. *J. Hazard. Mater.* 318, 608–614. doi:10.1016/j.jhazmat.2016.07.040

Bicho, R.C., Santos, F.C.F., Gonçalves, M.F.M., Soares, A.M.V.M., Amorim, M.J.B., 2015. Enchytraeid Reproduction TestPLUS: hatching, growth and full life cycle test-an optional multi-endpoint test with *Enchytraeus crypticus*. *Ecotoxicology* 24, 1053–1063. doi:10.1007/s10646-015-1445-5

Bicho, R.C., Santos, F.C.F., Scott-Fordsmand, J.J., Amorim, M.J.B., 2017a. Multigenerational effects of copper nanomaterials (CuONMs) are different of those of CuCl₂: exposure in the soil invertebrate *Enchytraeus crypticus*. *Sci. Rep.* 7, 8457. doi:10.1038/s41598-017-08911-0

Bicho, R.C., Santos, F.C.F., Scott-Fordsmand, J.J., Amorim, M.J.B., 2017b. Effects of copper oxide nanomaterials (CuONMs) are life stage dependent - full life cycle in *Enchytraeus crypticus*. *Environ. Pollut.* 224, 117–124. doi:10.1016/j.envpol.2017.01.067

Castro-Ferreira, M.P., de Boer, T.E., Colbourne, J.K., Vooijs, R., van Gestel, C.A.M., van Straalen, N.M., Soares, A.M.V.M., Amorim, M.J.B., Roelofs, D., 2014. Transcriptome assembly and microarray construction for *Enchytraeus crypticus*, a model oligochaete to assess stress response mechanisms derived from soil conditions. *BMC Genomics* 15. doi:10.1186/1471-2164-15-302

Castro-Ferreira, M.P., Roelofs, D., van Gestel, C. a M., Verweij, R. a, Soares, A.M.V.M., Amorim, M.J.B., 2012. *Enchytraeus crypticus* as model species in soil ecotoxicology. *Chemosphere* 87, 1222–7. doi:10.1016/j.chemosphere.2012.01.021

Chae, Y.J., Pham, C.H., Lee, J., Bae, E., Yi, J., Gu, M.B., 2009. Evaluation of the toxic impact of silver nanoparticles on Japanese medaka (*Oryzias latipes*). *Aquat. Toxicol.* 94, 320–327. doi:10.1016/j.aquatox.2009.07.019

Chang, M.-H., Liu, H.-S., Tai, C.Y., 2011. Preparation of copper oxide nanoparticles and its application in nanofluid. *Powder Technol.* 207, 378–386.

Chen, M., von Mikecz, A., 2005. Formation of nucleoplasmic protein aggregates impairs nuclear function in response to SiO₂ nanoparticles. *Exp. Cell Res.* 305, 51–62.

Cheng, D., Yang, J., Zhao, Y., 2004. Antibacterial materials of silver nanoparticles application in medical appliances and appliances for daily use. *Chin Med Equip J* 4, 26–32.

Chithrani, B.D., Ghazani, A.A., Chan, W.C.W., 2006. Determining the Size and Shape Dependence of Gold Nanoparticle Uptake into Mammalian Cells. *Nano Lett.* 6, 662–668.

Cho, W.S., Duffin, R., Poland, C.A., Duschl, A., Oostingh, G.J., MacNee, W., Bradley, M., Megson, I.L., Donaldson, K., 2012. Differential pro-inflammatory effects of metal oxide nanoparticles and their soluble ions *in vitro* and *in vivo*; Zinc and copper nanoparticles, but not their ions, recruit eosinophils to the lungs. *Nanotoxicology* 6, 22–35. doi:10.3109/17435390.2011.552810

Choi, J.E., Kim, S., Ahn, J.H., Youn, P., Kang, J.S., Park, K., Yi, J., Ryu, D.-Y., 2010. Induction of oxidative stress and apoptosis by silver nanoparticles in the liver of adult zebrafish. *Aquat. Toxicol.* 100, 151–9. doi:10.1016/j.aquatox.2009.12.012

Comfort, K., Braydich-Stolle, L., 2014. Less is more: Long-term *in vitro* exposure to low levels of silver nanoparticles provides new insights for nanomaterial evaluation. *ACS Nano* 8, 3260–3271.

Cornelis, G., Hund-Rinke, K., Kuhlbusch, T., van den Brink, N., Nickel, C., 2014. Fate and Bioavailability of Engineered Nanoparticles in Soils: A Review. *Crit. Rev. Environ. Sci. Technol.* 44, 2720–2764. doi:10.1080/10643389.2013.829767

Dasari, T.P., Pathakoti, K., Hwang, H.M., 2013. Determination of the mechanism of photoinduced toxicity of selected metal oxide nanoparticles (ZnO, CuO, Co₃O₄ and TiO₂) to *E. coli* bacteria. *J. Environ. Sci. (China)* 25, 882–888. doi:10.1016/S1001-0742(12)60152-1

De Jong, W.H., Hagens, W.I., Krystek, P., Burger, M.C., Sips, A.J.A.M., Geertsma, R.E., 2008. Particle size-dependent organ distribution of gold nanoparticles after intravenous administration. *Biomaterials* 29, 1912–1919. doi:10.1016/j.biomaterials.2007.12.037

Dhawan, A., Sharma, V., 2010. Toxicity assessment of nanomaterials: methods and challenges. *Anal. Bioanal. Chem.* 398, 589–605. doi:10.1007/s00216-010-3996-x

Diez-Ortiz, M., Lahive, E., George, S., Ter Schure, A., Van Gestel, C.A.M., Jurkschat, K., Svendsen, C., Spurgeon, D.J., 2015. Short-term soil bioassays may not reveal the full toxicity potential for nanomaterials; Bioavailability and toxicity of silver ions (AgNO₃) and silver nanoparticles to earthworm *Eisenia fetida* in long-term aged soils. *Environ. Pollut.* 203, 191–198. doi:10.1016/j.envpol.2015.03.033

Emam, H.E., Manian, A.P., Široká, B., Duelli, H., Redl, B., Pipal, A., Bechtold, T., 2013. Treatments to impart antimicrobial activity to clothing and household cellulosic-textiles—why “Nano”-silver? *J. Clean. Prod.* 39, 17–23.

Fadeel, B., Fornara, A., Toprak, M.S., Bhattacharya, K., 2015. Keeping it real: The importance of material characterization in nanotoxicology. *Biochem. Biophys. Res. Commun.* 468, 498–503. doi:10.1016/j.bbrc.2015.06.178

Garcia-Velasco, N., Gandariasbeitia, M., Irizar, A., Soto, M., 2016. Uptake route and resulting toxicity of silver nanoparticles in *Eisenia fetida* earthworm exposed through Standard OECD Tests. *Ecotoxicology* 25, 1543–1555.

Gomes, S.I.L., Murphy, M., Nielsen, M.T., Kristiansen, S.M., Amorim, M.J.B., Scott-Fordsmand, J.J., 2015. Cu-nanoparticles ecotoxicity - Explored and explained? *Chemosphere* 139, 240–245. doi:10.1016/j.chemosphere.2015.06.045

Gomes, S.I.L., Scott-Fordsmand, J.J., Amorim, M.J.B., 2015. Cellular energy allocation to assess the impact of nanomaterials on soil invertebrates (Enchytraeids): the effect of Cu and Ag. *Int. J. Environ. Res. Public Health* 12, 6858–6878.

Gupta, N., Fischer, A.R.H., Frewer, L.J., 2015. Ethics, Risk and Benefits Associated with Different Applications of Nanotechnology: a Comparison of Expert and Consumer Perceptions of Drivers of Societal Acceptance. *Nanoethics* 9, 93–108. doi:10.1007/s11569-015-0222-5

Hirano, S., Kanno, S., Furuyama, A. 2008. Multi-walled carbon nanotubes injure the plasma membrane of macrophages. *Toxicology and applied pharmacology*, 232, 244-251.

Holt, B. D., Short, P. A., Rape, A. D., Wang, Y. L., Islam, M. F., Dahl, K. N., 2010. Carbon nanotubes reorganize actin structures in cells and *ex vivo*. *ACS nano*, 4, 4872-4878.

Holtz, R.D., Lima, B.A., Souza Filho, A.G., Brocchi, M., Alves, O.L., 2012. Nanostructured silver vanadate as a promising antibacterial additive to water-based paints. *Nanomedicine Nanotechnology, Biol. Med.* 8, 935–940.

Hsin, Y.-H., Chen, C.-F., Huang, S., Shih, T.-S., Lai, P.-S., Chueh, P.J., 2008. The apoptotic effect of nanosilver is mediated by a ROS- and JNK-dependent mechanism involving the mitochondrial pathway in NIH3T3 cells. *Toxicol. Lett.* 179, 130–9. doi:10.1016/j.toxlet.2008.04.015

Hu, X., Li, D., Gao, Y., Mu, L., Zhou, Q., 2016. Knowledge gaps between nanotoxicological research and nanomaterial safety. *Environ. Int.* 94, 8–23. doi:10.1016/j.envint.2016.05.001

Huang, S., Chueh, P.J., Lin, Y.-W., Shih, T.-S., Chuang, S.-M., 2009. Disturbed mitotic progression and genome segregation are involved in cell transformation mediated by nano-TiO₂ long-term exposure. *Toxicol. Appl. Pharmacol.* 241, 182–194.

Hussain, S.M., Hess, K.L., Gearhart, J.M., Geiss, K.T., Schlager, J.J., 2005. In vitro toxicity of nanoparticles in BRL 3A rat liver cells. *Toxicol. In Vitro* 19, 975–83. doi:10.1016/j.tiv.2005.06.034

Hussain, S.M., Warheit, D.B., Ng, S.P., Comfort, K.K., Grabinski, C.M., Braydich-Stolle, L.K., 2015. At the crossroads of nanotoxicology *in vitro*: Past achievements and current challenges. *Toxicol. Sci.* 147, 5–16. doi:10.1093/toxsci/kfv106

ISO, I.O. for S.S.Q., 2014. Soil quality—Effects of contaminants on Enchytraeidae (Enchytraeus sp.)—Determination of effects on reproduction. ISO 16387.

Ispas, C., Andreescu, D., Patel, A., Goia, D. V, Andreescu, S., Wallace, K.N., 2009. Toxicity and developmental defects of different sizes and shape nickel nanoparticles in zebrafish. *Environ. Sci. Technol.* 43, 6349–6356.

Javed, R., Ahmed, M., Haq, I. ul, Nisa, S., Zia, M., 2017. PVP and PEG doped CuO nanoparticles are more biologically active: Antibacterial, antioxidant, antidiabetic and cytotoxic perspective. *Mater. Sci. Eng. C* 79, 108–115. doi:10.1016/j.msec.2017.05.006

Jeng, H.A., Swanson, J., 2006. Toxicity of Metal Oxide Nanoparticles in Mammalian Cells. *J. Environ. Sci. Heal. Part A* 41, 2699–2711. doi:10.1080/10934520600966177

Jouquet, P., Dauber, J., Lagerlöf, J., Lavelle, P., Lepage, M., 2006. Soil invertebrates as ecosystem engineers: Intended and accidental effects on soil and feedback loops. *Appl. Soil Ecol.* 32, 153–164. doi:10.1016/j.apsoil.2005.07.004

Keller, A.A., McFerran, S., Lazareva, A., Suh, S., 2013. Global life cycle releases of engineered nanomaterials. *J. Nanoparticle Res.* 15. doi:10.1007/s11051-013-1692-4

Kreuter, J., Alyautdin, R.N., Kharkevich, D.A., Ivanov, A.A., 1995. Passage of peptides through the blood-brain barrier with colloidal polymer particles (nanoparticles). *Brain Res.* 674, 171–174.

Lavelle, P., Decaëns, T., Aubert, M., Barot, S., Blouin, M., Bureau, F., Margerie, P., Mora, P., Rossi, J.P., 2006. Soil invertebrates and ecosystem services. *Eur. J. Soil Biol.* 42. doi:10.1016/j.ejsobi.2006.10.002

Laycock, A., Diez-Ortiz, M., Larner, F., Dybowska, A., Spurgeon, D., Valsami-Jones, E., Rehkämper, M., Svendsen, C., 2015. Earthworm uptake routes and rates of ionic Zn and ZnO nanoparticles at realistic concentrations, traced using stable isotope labeling. *Environ. Sci. Technol.* 50, 412–419.

Lesniak, A., Fenaroli, F., Monopoli, M.P., Åberg, C., Dawson, K. a, Salvati, A., 2012. Effects of the presence or absence of a protein corona on silica nanoparticle uptake and impact on cells. *ACS Nano* 6, 5845–57. doi:10.1021/nn300223w

Liu, W.-T., 2006. Nanoparticles and their biological and environmental applications. *J. Biosci. Bioeng.* 102, 1–7. doi:10.1263/jbb.102.1

Luo, X., Morrin, A., Killard, A.J., Smyth, M.R., 2006. Application of nanoparticles in electrochemical sensors and biosensors. *Electroanalysis* 18, 319–326.

Mahian, O., Kianifar, A., Kalogirou, S.A., Pop, I., Wongwises, S., 2013. A review of the applications of nanofluids in solar energy. *Int. J. Heat Mass Transf.* 57, 582–594. doi:10.1016/j.ijheatmasstransfer.2012.10.037

Maria, V.L., Licha, D., C., R., Scott-Fordsmand, J.J., Huber, C., Amorim, M.J.B., 2018. The *Enchytraeus crypticus* stress metabolome – CuO NM case study. *Nanotoxicology*.

Maria, V.L., Ribeiro, M.J., Guilherme, S., M. Soares, A.M.V., Scott-Fordsmand, J.J., Amorim, M.J.B., 2017. Silver (Nano)Materials cause genotoxicity in *Enchytraeus crypticus* – as determined by the comet assay. *Environ. Toxicol. Chem.* 9999, 1–8. doi:10.1002/etc.3944

Mu, L., Sprando, R.L., 2010. Application of nanotechnology in cosmetics. *Pharm. Res.* 27, 1746–1749.

OECD, 2016. Test No. 220: Enchytraeid Reproduction Test / Organisation for Economic Co-operation and Development, OECD Guidelines for the Testing of Chemicals, Section 2,. Paris: OECD Publishing.

Pan, Y., Leifert, A., Ruau, D., Neuss, S., Bornemann, J., Schmid, G., Brandau, W., Simon, U., Jahnen-Dechent, W., 2009. Gold nanoparticles of diameter 1.4 nm trigger necrosis by oxidative stress and mitochondrial damage. *Small* 5, 2067–76. doi:10.1002/smll.200900466

Pankhurst, Q.A., Connolly, J., Jones, S.K., Dobson, J., 2003. Applications of magnetic nanoparticles in biomedicine. *J. Phys. D. Appl. Phys.* 36. doi:10.1088/0022-3727/36/13/201

Park, E.-J., Yi, J., Kim, Y., Choi, K., Park, K., 2010. Silver nanoparticles induce cytotoxicity by a Trojan-horse type mechanism. *Toxicol. In Vitro* 24, 872–8. doi:10.1016/j.tiv.2009.12.001

Park, J.C., Kim, J., Kwon, H., Song, H., 2009. Gram-scale synthesis of Cu₂O nanocubes and subsequent oxidation to CuO hollow nanostructures for lithium-ion battery anode materials. *Adv. Mater.* 21, 803–807.

Pisoschi, A.M., Pop, A., 2015. The role of antioxidants in the chemistry of oxidative stress: A review. *Eur. J. Med. Chem.* 97, 55–74. doi:10.1016/j.ejmech.2015.04.040

Prakash, L.J., 1995. Application of fine grained tungsten carbide based cemented carbides. *Int. J. Refract. Met. Hard Mater.* 13, 257–264. doi:10.1016/0263-4368(95)92672-7

Rai, M., Yadav, A., Gade, A., 2009. Silver nanoparticles as a new generation of antimicrobials. *Biotechnol. Adv.* 27, 76–83. doi:10.1016/j.biotechadv.2008.09.002

Ren, G., Hu, D., Cheng, E.W.C., Vargas-Reus, M.A., Reip, P., Allaker, R.P., 2009. Characterisation of copper oxide nanoparticles for antimicrobial applications. *Int. J. Antimicrob. Agents* 33, 587–590.

Ribeiro, M., Maria, V., Scott-Fordsmand, J., Amorim, M., 2015. Oxidative Stress Mechanisms Caused by Ag Nanoparticles (NM300K) are Different from Those of AgNO₃: Effects in the Soil Invertebrate *Enchytraeus Crypticus*. *Int. J. Environ. Res. Public Health* 12, 9589–9602. doi:10.3390/ijerph120809589

Sanvicens, N., Marco, M.P., 2008. Multifunctional nanoparticles - properties and prospects for their use in human medicine. *Trends Biotechnol.* 26, 425–433. doi:10.1016/j.tibtech.2008.04.005

Schaeublin, N.M., Braydich-Stolle, L.K., Schrand, A.M., Miller, J.M., Hutchison, J., Schlager, J.J., Hussain, S.M., 2011. Surface charge of gold nanoparticles mediates mechanism of toxicity. *Nanoscale* 3, 410–20. doi:10.1039/c0nr00478b

Shoults-Wilson, W.A., Reinsch, B.C., Tsyusko, O. V, Bertsch, P.M., Lowry, G. V, Unrine, J.M., 2011. Role of particle size and soil type in toxicity of silver nanoparticles to earthworms. *Soil Sci. Soc. Am. J.* 75, 365–377.

Studer, A.M., Limbach, L.K., Van Duc, L., Krumeich, F., Athanassiou, E.K., Gerber, L.C., Moch, H., Stark, W.J., 2010. Nanoparticle cytotoxicity depends on intracellular solubility: comparison of stabilized copper metal and degradable copper oxide nanoparticles. *Toxicol. Lett.* 197, 169–174.

Sturla, S.J., Boobis, A.R., Fitzgerald, R.E., Hoeng, J., Kavlock, R.J., Schirmer, K., Whelan, M., Wilks, M.F., Peitsch, M.C., 2014. Systems toxicology: From basic research to risk assessment. *Chem. Res. Toxicol.* 27, 314–329. doi:10.1021/tx400410s

Trouiller, B., Reliene, R., Westbrook, A., Solaimani, P., Schiestl, R.H., 2009. Titanium dioxide nanoparticles induce DNA damage and genetic instability *in vivo* in mice. *Cancer Res.* 69, 8784–8789.

Uski, O., Torvela, T., Sippula, O., Karhunen, T., Koponen, H., Peräniemi, S., Jalava, P., Happonen, M., Jokiniemi, J., Hirvonen, M.R., Lähde, A., 2017. *In vitro* toxicological effects of zinc containing nanoparticles with different physico-chemical properties. *Toxicol. Vitro.* 42, 105–113. doi:10.1016/j.tiv.2017.04.010

Xia, T., Kovichich, M., Liong, M., Meng, H., Kabehie, S., George, S., Zink, J.I., Nel, A.E., 2009. Polyethyleneimine coating enhances the cellular uptake of mesoporous silica nanoparticles and allows safe delivery of siRNA and DNA constructs. *ACS Nano* 3, 3273–3286.

Xu, M., Huang, N., Xiao, Z., Lu, Z., 1998. Photoexcited TiO₂ nanoparticles through •OH-radicals induced malignant cells to necrosis. *Supramol. Sci.* 5, 449–451. doi:10.1016/S0968-5677(98)00048-0

Yacobi, N.R., Phuleria, H.C., Demaio, L., Liang, C.H., Peng, C.-A., Sioutas, C., Borok, Z., Kim, K.-J., Crandall, E.D., 2007. Nanoparticle effects on rat alveolar epithelial cell monolayer barrier properties. *Toxicol. Vitro.* 21, 1373–1381.

Yang, W., Shen, C., Ji, Q., An, H., Wang, J., Liu, Q., Zhang, Z., 2009. Food storage material silver nanoparticles interfere with DNA replication fidelity and bind with DNA. *Nanotechnology* 20, 85102.

Yao, Z., Stiglich, J.J., Sudarshan, T., 1998. Nanosized WC-Co holds promise for the future. *Met. Powder Rep.* 53, 26–33.

Yazdi, A.S., Guarda, G., Riteau, N., Drexler, S.K., Tardivel, A., Couillin, I., Tschopp, J., 2010. Nanoparticles activate the NLR pyrin domain containing 3 (Nlrp3) inflammasome and cause pulmonary inflammation through release of IL-1 α and IL-1 β . *Proc. Natl. Acad. Sci.* 107, 19449–19454.

Zhang, Z., Yang, M., Huang, M., Hu, Y., Xie, J., 2007. Study on germicidal efficacy and toxicity of compound disinfectant gel of nanometer silver and chlorhexidine acetate. *Chinese J. Heal. Lab. Technol.* 17, 1403–1406.

CHAPTER I

Oxidative stress mechanisms caused by Ag nanoparticles (NM300K) are different from AgNO₃: effects in the soil invertebrate *Enchytraeus crypticus*

Maria J. Ribeiro ^{1,†}, Vera L. Maria ^{1,†}, Janeck J. Scott-Fordsmand ² and
Mónica J. B. Amorim ^{1,*}

¹Department of Biology & CESAM (Centre for Environmental and Marine Studies), University of Aveiro, 3810-193 Aveiro, Portugal ² Department of Bioscience, Aarhus University, Vejlsovej 25, DK-8600 Silkeborg, Denmark.

[†]These authors contributed equally to this work

* corresponding author: mjamorim@ua.pt

International Journal of Environmental Research and Public Health 12 (2015) 9589-9602.
DOI:10.3390/ijerph120809589

ABSTRACT

The mechanisms of toxicity of Ag nanoparticles (NMs) are unclear in particular in the terrestrial environment. In this study the effects of AgNP (Ag NM300K) were assessed in the soil worm *Enchytraeus crypticus* in terms of oxidative stress, using a range of biochemical markers [Catalase (CAT), Glutathione Peroxidase (GPx), Glutathione S-Transferase (GST), Glutathione Reductase (GR), Total Glutathione (TG), Metallothionein (MT), Lipid Peroxidation (LPO)]. *E. crypticus* were exposed during 3 and 7 days (d) to the reproduction EC20, EC50 and EC80 of both AgNP and AgNO₃. AgNO₃ induced oxidative stress earlier (3d) than AgNP (7d), both leading to LPO despite the activation of the anti-redox system. MT increased only for AgNP. The Correspondence Analysis showed a clear separation between AgNO₃ and AgNP, with e.g. CAT being the main descriptor for AgNP for day 7. LPO, GST and GPx were for both 3 and 7 days associated with AgNO₃, whereas MT and TG were associated with the AgNP. The present can reflect a delay in effects of AgNP compared to AgNO₃ due to the release of Ag⁺ ions from the particles, although this does not fully explain the observed differences.

Keywords: antioxidant system; reactive oxygen species; metallothionein; lipid damage; soil

INTRODUCTION

In addition to the bactericidal properties, silver nanoparticles (Ag NPs) have been reported to cause *in vitro* and *in vivo* effects in organisms other than bacteria, e.g. in vertebrates [*Danio rerio* and *Mus musculus* (Ghosh et al., 2012; Massarsky et al., 2013)] and invertebrates [*Drosophila melanogaster*, *Caenorhabditis elegans*, and *Eisenia fetida* (Ahamed et al., 2010; Ahn et al., 2014; Hayashi et al., 2013)].

AgNP toxicity has been mostly attributed to the generation of reactive oxygen species (ROS) in cells (Ahamed et al., 2010; Arora et al., 2008; Choi et al., 2010). Park et al. (2010) proposed that Ag NPs' toxicity may partly follow a Trojan-horse type mechanism i.e. AgNP are taken up by the cell as particles and dissolution occurs inside the cell causing a high local concentration of Ag⁺, however there may also be an external dissolution of AgNP with subsequent ion related Ag⁺ toxicity. Hence, it seems that both particulate and ion-based mechanism of action may be at play, as further discussed by other authors (Gomes et al., 2013; Hayashi et al., 2012; Yang et al., 2012).

Few studies have been performed on terrestrial oligochaetes. For example, the time-response tests with *Eisenia andrei* (Hayashi et al., 2013), a 7-day tests with *E. fetida* (Kwak et al., 2014), or the growth and survival test with *Lumbricus rubellus* (van der Ploeg et al., 2014). Recently, a study on the oxidative stress response in *E. fetida* (Gomes et al., 2015a) comparing short- and longer-term (4 and 28 days) exposure period showed a time dependent response and differences in the redox mechanisms sequence between Ag salt and Ag nano. Despite the activation of the anti-redox enzymes for both Ag forms, lipid peroxidation occurred for longer-term exposures. Further, Hayashi et al. (2013) showed a faster induction of oxidative stress markers in *E. fetida* when exposed to Ag salt than when exposed to Ag NPs. More comprehensive differential gene expression response was studied in *Enchytraeus albidus* (Gomes et al., 2013), linking short to longer term effect, i.e. gene and reproduction. The authors highlight that testing of Ag NPs seem to require longer exposure period to be comparable in terms of effect/risk assessment with other chemicals.

In the present study we aimed to characterize the antioxidant system in the omnipresent standard soil species *Enchytraeus crypticus* (Castro-Ferreira et al., 2012; ISO, 2005; OECD, 2004a) exposed to AgNP. This involved the exposure to dispersed Ag NPs (NM300K, JRC standard particles) and Ag salt (AgNO₃) at the reproduction effect concentration (EC20, EC50 and EC80) during a short time series exposure: 0, 3 and 7 days. A set of oxidative stress biomarkers was used, which included catalase (CAT), glutathione peroxidase (GPx), glutathione reductase (GR) and glutathione-S-transferase (GST) activities, the total glutathione (TG), metallothionein (MT) and lipid peroxidation (LPO) levels.

MATERIALS AND METHODS

Test organism

Enchytraeus crypticus (Oligochaeta: Enchytraeidae) were maintained in laboratory conditions, 19 ± 1 °C and 16:8 h (light:dark) photoperiod regime in agar plates, consisting of a sterile mixture of four solutions (CaCl₂·2H₂O, MgSO₄, KCl, NaHCO₃) and Bacti-Agar medium as a substrate. The animals were fed on autoclaved dried oats. Adult organisms with visible clitellum and similar size were selected for the experiment.

Test Materials

The AgNO₃ (high-grade, 98.5–99.9% purity) was purchased from Sigma–Aldrich (USA). The silver nanoparticles (Ag NPs) used were the standard reference materials Ag NM300K from the European Commission Joint Research Centre (JRC), fully characterized (Klein et al., 2011). The Ag NM300K is dispersed in 4% polyoxyethylene glycerol triolaete and polyoxyethylene (20) sorbitan mono-laurate (Tween 20), thus the dispersant was also tested alone.

Test soil and spiking

The natural standard soil LUFA 2.2 (Speyer, Germany) was used and has the following main characteristics: grain size distribution of 7.2 % clay, 8 % silt and 77.5 % sand, pH (CaCl₂) = 5.5, water holding capacity (WHC) of 45 g/100 g, a cation exchange capacity (CEC) of 10 meq/100 g, and an organic carbon (OC) content of 1.77%.

The soil was dried (72 h, 80 °C) before use. Spiking was performed as aqueous solution onto pre-moistened soil and homogeneously mixed. The soil was left to equilibrate for 3 days prior test start. For AgNP spiking was performed individually per replicate. Test concentrations used (Table 1) corresponded to the EC₂₀, EC₅₀ and EC₈₀ for reproduction. The control soil was prepared by adding deionized water to adjust to the adequate moisture content (50% of the WHC_{max}). A control dispersant was also performed by adding the equivalent to the maximum dispersant volume as added with the AgNP spiking.

Table 1: Test exposure concentrations of AgNO₃ and AgNP, corresponding to the estimated reproduction effect concentrations (ECs), expressed as mg Ag / kg soil dry weight.

Test material	EC₂₀	EC₅₀	EC₈₀
AgNO ₃	45	60	96
AgNP (NM 300K)	60	170	225

Test procedures

Test procedures followed the standard Enchytraeid Reproduction Test (ERT) guideline (OECD, 2004a). In short, each replicate consisted of a glass vessel (Ø 4 cm, 45 ml

volume) containing 20 g soil ww (wet weight) with food supply. Fifty organisms were added in each test vessel and covered with a lid with small holes. Test conditions were 20 ± 1 °C and 16:8 h photoperiod. Five replicates per treatment were used. At each sampling time (0, 3 and 7 days), organisms were carefully collected from soil, rinsed in water, introduced into a microtube, weighed, frozen in liquid nitrogen and stored at -80 °C until further analysis.

Biochemical analysis

Procedures followed the described for *E. albidus* (Gomes et al., 2012) with adaptations. Pools of 40 organisms were homogenized using an ultrasonic homogenizer (Sonifier 250, Branson sonicator) in 2000 μ l of potassium phosphate buffer (0.1 mM, pH 7.4 containing EDTA 1 mM and DTT 1 mM). Part of the homogenate (150 μ l) was separately stored (- 80 °C) with 2.5 μ l BHT (2,6-dieter-butyl-4-metylphenol) 4 % in methanol to block tissue oxidation for later LPO measurement. The rest of the homogenate was centrifuged at 10.000g for 20 min at 4 °C and the post mitochondrial supernatant (PMS) was kept at - 80 °C for further analysis. All biomarkers procedures were based spectrometric methods and a Thermo Scientific, Multiskan Spectrum microplate reader was used. Protein concentration was assayed using the Bradford method (Bradford, 1976), adapted from BioRad's Bradford microassay set up in a 96-well flat bottom plate, using bovine γ - globuline as a standard. Catalase (CAT) activity was measured following the method of Clairborne (1985) as described by Giri et al. (1996). Changes in absorbance were recorded at 240 nm and CAT activity was calculated in terms of μ mol H₂O₂ consumed min⁻¹ mg⁻¹ protein. Glutathione Reductase (GR) activity was measured in accordance to the method of Carlberg and Mannervik (1975) being quantified by the NADPH loss at 340 nm and expressed as nmol of NADP⁺ formed min⁻¹ mg⁻¹ protein. Glutathione S-Transferase (GST) activity was assessed using 1-chloro-2,4- dinitrobenzene (CDNB) as substrate according to the method of Habig et al. (1974). The enzyme activity was recorded at 340 nm and calculated as nmol GS-DNB conjugate min⁻¹ mg⁻¹ protein.

Total Glutathione (TG) levels were measured at 412 nm, using the recycling reaction of reduced glutathione (GSH) with dithionitrobenzoate (DTNB) in the presence of GR excess (Baker et al., 1990; Tietze, 1969). The results were expressed as nmol of 5-thio-2-nitrobenzoic acid (TNB) formed min⁻¹ mg⁻¹ protein. Lipid Peroxidation (LPO) occurrence was evaluated according to the procedure of Ohkawa (1979) and Bird et al. (1984), as adapted by Wilhelm Filho et al. (2001). Absorbance was measured at 535 nm and results

were expressed as μmol of thiobarbituric acid reactive substances (TBARS) formed per milligram of fresh weight.

Metallothionein (MT) levels were determined by using the method described by Viarengo et al. (1997). Briefly, 500 μL of the PMS was added to 500 μL 95 % ethanol with 8 % chloroform. After mixing it was centrifuged at $6000 \times g$ for 10 min at 4 °C. 50 μL RNA, 10 μL HCl and 1.2 mL of cold ethanol were added to the 700 μL of the supernatant (S6) and frozen for 15 min at -80 °C. After centrifuging at $6000 \times g$ for 1 min (at 4 °C) the supernatant was removed and the pellet was re-suspended in 300 μL of 87 % ethanol in 1 % chloroform. The last centrifuge step was repeated and the pellet was re-suspended in 150 μL NaCl, 150 μL HCl containing 4 mM ethylenediaminetetra acetic acid (EDTA) and 300 μL Ellmans reactive with 0.4 mM DTNB, 2 M NaCl and 0.2 M potassium phosphate with a pH 8. After 5 min, the absorbance was read at 412 nm. 1 mM GSH in 0.1 M HCl was used as a standard and the amount of MT was expressed as nmol mg^{-1} protein.

Data analysis

Univariate one-way analysis of variance (ANOVA) followed by Dunnett's Post-Hoc test ($p < 0.05$) (SigmaPlot, 1997) was used to test differences between treatments (between day 0 and 3 and 7 and, between control and concentrations).

Multivariate analysis was done to explore the patterns in correlations between the data, using Correspondence Analysis (CA) including all treatments and also when divided per days. The analysis was performed using the software SAS enterprise guide 5.1 (SAS Enterprise Guide 5.1, 2012). To compensate for the different scales of the biomarkers, the response was normalised using several different normalisation methods all giving the same pattern; in the present normalisation based on averaging is displayed.

RESULTS

Materials characterisation

As mentioned, in methods, the silver nanoparticles (Ag NPs) used were the standard reference materials Ag NM300K from the European Commission Joint Research Centre (JRC), fully characterized (Klein et al., 2011). In short, Ag NM300K are spherical and consist of a colloidal dispersion with a nominal silver content of 10.2 w/w %, dispersed in 4% w/w of polyoxyethylene glycerol trioleate and polyoxyethylene (20) sorbitan mono-

laurat (Tween 20), having > 99 % number of particles with a nominal size of about 15 nm, with no coating. Transmission Electron Microscopy (TEM) indicated a size of 17 ± 8 nm. Smaller nanoparticles of about 5 nm are also present.

Biological characterisation

The results obtained for the various biomarkers (univariate) can be depicted in figure 1.

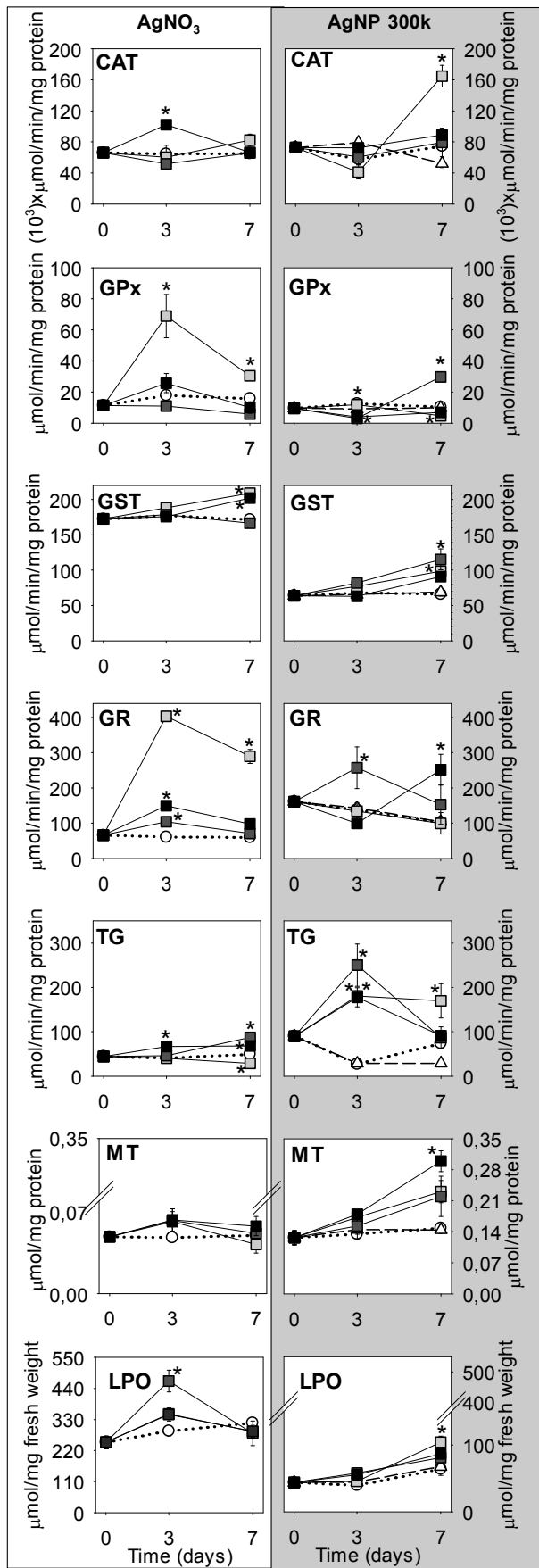


Figure 1: Results from *Enchytraeus crypticus* exposed to Ag NM300K [60 (EC20), 170 (EC50) and 225 (EC80) mg Ag/Kg soil] and AgNO₃ [45 (EC20), 60 (EC50) and 96 (EC80) mg Ag/Kg soil], as sampled at 0-3-7 days, in terms of Catalase (CAT), Glutathione Peroxidase (GPx), Glutathione S-Transferase (GST), Glutathione Reductase (GR), Total Glutathione (TG), Metallothionein (MT) and Lipid Peroxidation (LPO). Values are expressed as mean ± standard error (n=5). * (p<0.05, Dunnett's) for differences between control and treatments.

Summarising, CAT shows a significant increase at the AgNP_EC20_7d, whereas for AgNO₃ mostly the EC80_3d is increased but all is balanced at 7d. GPx and GR seems to have a bell shape pattern for the Ag salt between 0-3-7 days, being most pronounced for AgNO₃_EC20. For AgNP an increase is observed for GPx at AgNP_EC50_7d; GR shows a bell shape (0-3-7d) for EC50 exposure and the opposite shape for the EC80. GST shows a steady increase from 0-7d for both Ag forms, but with higher absolute values for AgNO₃. TG shows bell shape (0-3-7d) for AgNP for all ECs whereas for AgNO₃ changes are minor. MT exhibits a small increase and stabilization for AgNO₃ along the test period for all tested ECs. For AgNP there is a continuous increase in MT levels from 0-7 days, this being highest for the EC80_7d. LPO levels are increased for AgNP_EC20_7d. For AgNO₃, LPO levels get back to normal after an increase at day 3 (significant for EC50). The multivariate analysis of the data (Correspondence Analysis) enabled an identification of the overall differences between the AgNO₃ and AgNP exposures (Fig 2A), with a clear separation of the AgNO₃ and AgNP. It should be noted that whereas Fig. 1 shows mean values and standard errors, the multivariate plot displays the individual replicates. When treating the days separately (Fig 2B, C), an even clearer difference was observed. Whereas CAT has no importance for the separation between the exposures on day 3 it was the main descriptor for AgNP for the day 7. LPO, GST and GPx were for both days associated with AgNO₃, whereas MT and TG was associated with the AgNP over both days.

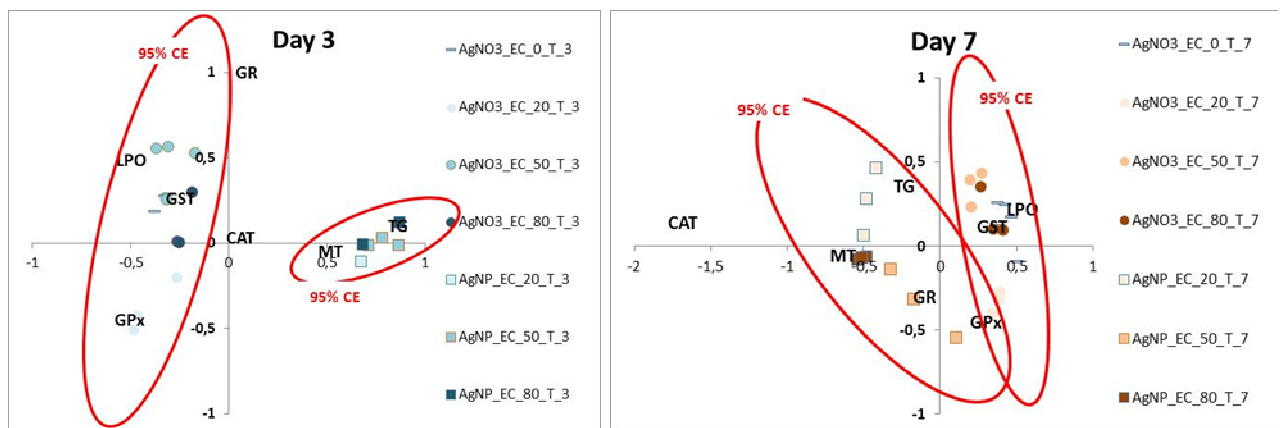
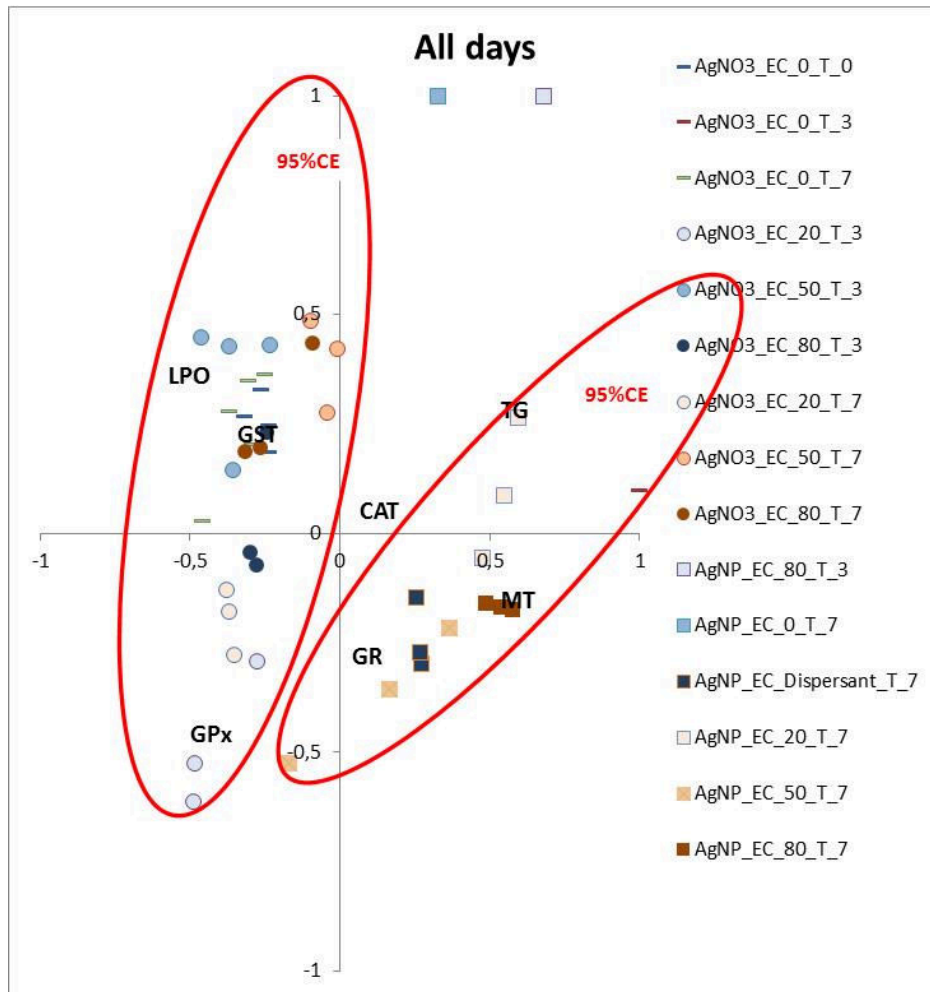


Figure 2: Correspondence analysis of data from *Enchytraeus crypticus* exposed to AgNP (Ag NM300K) [60 (EC20), 170 (EC50) and 225 (EC80) mg Ag/Kg soil] and AgNO₃ [45 (EC20), 60 (EC50) and 96 (EC80) mg Ag/Kg soil], as sampled at 0-3-7 days (designated T₀, T₃ and T₇), in terms of Catalase (CAT), Glutathione Peroxidase (GPx), Glutathione S-Transferase (GST), Glutathione Reductase (GR), Total Glutathione (TG), Metallothionein (MT) and Lipid Peroxidation (LPO). CE: Confidence Ellipses.

DISCUSSION

The results show different biomarker response-patterns for organisms exposed to AgNP and to AgNO₃, both across all time-points and within each time-point. In the following we first discuss responses to each of the materials and then compare the responses across materials.

AgNO₃ mechanisms

At low concentration, GPx was increased during the entire exposure period with a peak response after 3 days. The CAT activity also peaked after 3 days but was only generated by the EC80 exposures. Since both CAT and GPx are related to H₂O₂ cleavage, it seems that GPx is the initial response, concentration wise, whereas CAT is activated at higher oxidation level [i.e. assuming that higher oxidation level is linked to higher exposure concentrations levels]. The cooperation between CAT and GPx has been suggested by Baud et al. (2004) when the action of the enzymes by themselves is not enough for H₂O₂ clearance, being both required in the process. Moreover, for higher cellular H₂O₂ concentrations, GPx activity is mandatory to avoid CAT inactivation, as also seen in the present experiment. The cellular presence of lipid peroxides and other hydroperoxides can also act as stimulant substrates of GPx. In addition, the lower trend in the GPx activity for higher concentrations (EC50 and EC80) could reflect the occurrence of hormesis, i.e., an overcompensation response to low dose is elicited (Calabrese, 2008). This effect has been reported in several studies regarding Ag toxicity, and for both forms (Arora et al., 2008; Braydich-Stolle et al., 2005; Kawata et al., 2009; Xiu et al., 2012).

The increase in GST activity for EC20 and EC80 may be due to the conjugation of GSH with Ag⁺ ions. Induction in GST genes for both AgNP and Ag⁺ was reported in *E. fetida* after 7 d exposure to 100 mg Ag/kg (Tsyusko et al., 2012). A concentration-dependent increase in GST activity was found in *E. fetida* after 14 d exposure to AgNO₃ (Hu et al., 2012). Considering that antioxidant enzyme's activities didn't change for EC50 at 7 d, but TG values were increased, possibly Ag⁺ were forming complexes with GSH molecules. All tested concentrations promptly elevated GR activity, which should increase the GSH levels due to the recycling reaction of GSSG. However, TG content does not reflect this, as only EC80 caused an increase in TG levels. It is known that GSH can interact with certain metal ions, having high affinity to Ag and complexes can be formed (Wang and Ballatori, 1998). Considering that neither GPx nor GST is requiring GSH in EC50 and

EC80 exposures, GSH could be directly binding to Ag⁺ ions and perform an alternative mechanism of response against oxidative stress. An increase in GR activity coupled with the occurrence of Ag⁺ chelation by GSH was also proposed for *E. fetida* (75-100 mg Ag/kg, 4 days exposure) (Gomes et al., 2015a). For EC20, since GPx activity increased, this enzyme is using GSH to detoxify the cells, also explaining the higher increase in GR activity observed.

Considering the increase in GST and GPx activity for EC20 associated with TG content decrease, this must reflect a severe fall in GSH levels, since it's been mobilized by both enzymes. As to EC80, the increase in GST activity and TG levels seems to be a consequence of the conversion of GSH into GSSG. Regarding the higher TG levels (plus the increase in GST and GR activities), we propose two hypotheses/mechanisms for Ag⁺ scavenger: 1. The endogenous GSH was mobilized to scavenger Ag⁺ and/or 2. The increase in MT levels to scavenge Ag⁺ occurred between 4-6d followed by a decrease at day 7. A similar pattern was reported for *Folsomia candida* (EC50 of Cu and Cd, 0-10 days exposure), where an induction in MT levels was measured after 6 days followed by a decrease (Maria et al., 2014). It is known that Ag has a strong affinity to MT and, since the used method detects unbound MT, MT could had been bound to Ag⁺ before day 3, hence earlier than for AgNP and not detected in the present design. In summary, despite the activated antioxidant mechanisms by *E. crypticus* to avoid oxidative damage, this was not enough to prevent LPO for AgNO₃_EC50_3d. On the other hand, the mechanism to protect the cells from LPO was more efficient for EC20 and EC80 during the test period.

Ag NPs mechanisms

For the AgNP exposed organisms, the early decline in CAT and GPx activities could have led to an accumulation of H₂O₂ in the cells and contributed to an antioxidant system imbalance seen as enzyme “deactivation/lost” through denaturation process by the ROS build-up inside the cell, i.e. AgNP-induced oxidative damage. Nevertheless, CAT and GPx activities increased after 7d, although for different exposure concentration, which indicates the induction of protein biosynthesis and further activation of other antioxidant enzymes, e.g. GST and GR as observed here, but also an increase in cellular GSH contents which also counteract the ROS action and in this way prevent denaturation of proteins (e.g. enzymes). An increase in GST activity was also observed in *E. fetida* (20-500 mg AgNP/kg, 14 d exposure) (Hu et al., 2012) and in *Chironomus riparius* at the mRNA level (0.2–1 AgNP mg/L, 24 hour exposure) (Nair et al., 2013). The increase pattern in GST

activity is similar between AgNP and Ag salt and could be due to Ag⁺ ions, i.e. that AgNP is either dissolved in the media or inside the worm. However, there is no clear knowledge of the possible degree of dissolution for Ag NM300K in soils, e.g. van der Ploeg et al. (2014) report lower Ag in soil pore-water following AgNP exposure compared to AgNO₃ (without specifying whether this is ions or nanomaterial). In the same study, the AgNP were attached to the worms, with bioaccumulation factors being lower for AgNP exposed worms compared to Ag salt exposed worms. Schlich et al. (2013) used Diffusion Gradient Thin-films (DGT) and detected equivalent amount of Ag in pore water (it is presently unclear how much AgNP will diffuse into the DGT, as particulate matter is known to enter DGTs (Van Leeuwen, 2011). Considering that a possible detoxification route of Ag⁺ ions involves elimination via conjugation to GSH in a reaction catalysed by GST, this could explain the increase in its activity. Also, it could be acting in response to CAT and GPx failure, which suggest a later action of Ag NPs.

While GR activity was induced, GST maintained unaltered after the initial activation for EC50 exposure, maybe due to a mobilization of GSH as non-enzymatic antioxidant substrate, functioning by quenching intracellular ROS, albeit it was not sufficient to neutralize them since inhibition in CAT and GPx activities were observed. Consequently, a robust increase in the ratio GSH /GSSG content (TG increased) was observed possibly due to the presence of GSH. Higher GSH levels were also reported in *E. fetida* (Hu et al., 2012). The decrease in TG for EC50_7d may be related to the GPx and GST increased activities that generated GSSG through GSH oxidation in the cells.

The potential release of Ag⁺ does not seem to be linked to the increase in MT for AgNP_7d given the observations of much lower values for AgNO₃. An increase in MT mRNA expression was also observed in exposure to AgNP in zebrafish (Choi et al., 2010) and in *E. fetida* (Hayashi et al., 2013; Tsyusko et al., 2012). The increase of MT must be linked to the observed TG decrease despite the increase in GST and GR activities. Hence, we consider that the decrease in the ratio GSH/GSSG (implying less available GSH) triggered an increase in the levels of MT (another thiol substrate) in order to reduce the oxidant Ag⁺ action. However, despite these mechanisms, LPO still occurred after 7d.

Comparison of Ag Nano and Ag Salt Mechanisms

As seen above, results show different biomarker response-patterns for organisms exposed to AgNP and AgNO₃, both across all time-points and within each time-point. For AgNO₃ oxidative stress is associated by an initial activation of enzymes like CAT, GR and

GPx, and causing LPO, followed by a decreased importance of GR and GPx at day 7. For AgNP oxidative stress is associated with the increased activities/levels of e.g., GPx, GST, TG but especially CAT from 0–7 d, although the activated mechanisms are not sufficient to avoid LPO as measured at EC20_7d. The lower LPO at EC50 and EC80 was possibly related with earlier induction of antioxidant enzymes for these concentrations, however this didn't occur in AgNO₃ exposed animals, resulting in higher LPO levels.

It is known that oxidative stress can be directly induced by the active surface of Ag NPs (He et al., 2012). An alternative, may be a combined possibility, is that the present study reflects a delay in the effects of AgNP compared to AgNO₃ due to the release of Ag⁺ ions from the particles either externally (e.g., in soil) or internally (e.g., in lysosomes), although this is presently impossible to verify for NM300K; it would probably require a soil Bio Ligand Model (BLM) kind of approach to the possible ratio between dissolution and uptake rates. The degree of toxicity caused by the soluble fraction (Ag⁺) and the particulate fraction is unclear and likely vary from experiment to experiment depending on conditions, see e.g., Baalousha et al. (2009) who argued that not all toxicity is caused by the soluble part. In a research covering the immunological effects of AgNP in human monocytes it was proposed that the release of Ag⁺ generates the production of hydroxyl radicals in acidic endo/lysosomes (Yang et al., 2012). Moreover, Ag NPs can exert their toxicity by entering the cells and releasing large amounts of Ag⁺, a Trojan-horse type mechanism (Autrup et al., 2012; Park et al., 2010). Hence, the observed effect can partly be due to slower Ag⁺ release from AgNP (outside or inside the organism), which also leads to a change in the order of cascade of events and hence potentiates different effects.

Figure 3 shows a schematic representation of the events. As can be seen, there are some common features between AgNP and AgNO₃ in terms of activated enzymes. Variation is observed in terms of time of activation, which by itself can create a different cascade of events. Moreover, the variation can be observed in terms of the induced levels per concentration and per material. Particular differences include e.g., for AgNP the increased CAT and MT.

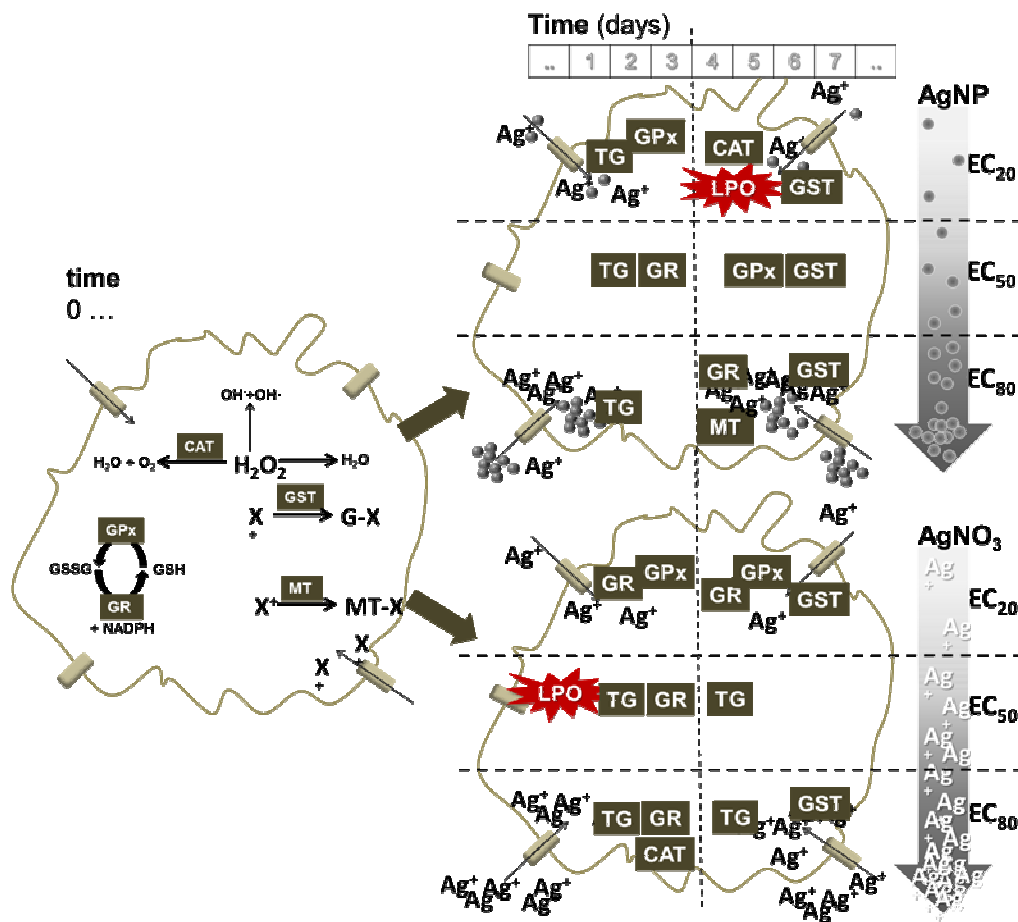


Figure 3: Schematic representation of the redox events in the cell when exposed to AgNP and AgNO₃ (variation in concentration is signalled in the arrows from low to high (EC₂₀-50-80), top to bottom respectively) and along various time periods (0-3-7 days). Cell at time 0 (left) indicates the general set of existing reactions that occur involving the measured markers in the present study. CAT: Catalase, GPx: Glutathione Peroxidase, GST: Glutathione S-Transferase, GR: Glutathione Reductase, TG: Total Glutathione, MT: Metallothionein, LPO: Lipid Peroxidation.

CONCLUSIONS

Comparison between exposure to AgNP and AgNO₃ in *E. crypticus* showed dissimilar oxidative stress responses, e.g., a delayed increase in the antioxidant enzymes responses (CAT, GST, GPx) for Ag NPs exposure (7 d) compared to AgNO₃ (3 d), initial LPO damage for AgNO₃ followed by stabilization, whereas for AgNP LPO occurred after 7 d, MT increased only in organisms exposed to Ag NPs. The present can partly reflect a delay in effects of AgNP compared to AgNO₃ due to the slower release of Ag⁺ ions from

the Ag particles, i.e., AgNP acts as a continuous source of Ag⁺ to the soil pore-water although this possible dissolution is still unclear.

ACKNOWLEDGEMENTS

The present study was supported by the European Commission by EU FP7-project MARINA (ref. 263215) and SUN (ref. 604305) and by FEDER through COMPETE e Operational Program for Competitiveness Factors (Programa Operacional Factores de Competitividade) and by National funding through FCT-Fundação para a Ciência e Tecnologia, within the research project NANOkA (PTDC/BIA-BEC/103716/2008), within CESAM by PEst-C/MAR/LA0017/2013, through an FCT PhD grant to Maria J. Ribeiro (SFRH/BD/95027/2013) and a Post-Doctoral grant to Vera L. Maria (SFRH/BPD/95093/2013).

AUTHOR CONTRIBUTIONS

Maria J. Ribeiro, Vera L. Maria performed the experiments. Maria J. Ribeiro, Vera L. Maria, Janeck J. Scott-Fordsmand and Mónica J. B. Amorim conceived and designed the experiment, analysed the data and wrote the paper.

CONFLICTS OF INTEREST

The authors declare no conflict of interest.

REFERENCES

Ahamed, M., Posgai, R., Gorey, T.J., Nielsen, M., Hussain, S.M., Rowe, J.J., 2010. Silver nanoparticles induced heat shock protein 70, oxidative stress and apoptosis in *Drosophila melanogaster*. *Toxicol. Appl. Pharmacol.* 242, 263–269. doi:10.1016/j.taap.2009.10.016

Ahn, J.-M., Eom, H.-J., Yang, X., Meyer, J.N., Choi, J., 2014. Comparative toxicity of silver nanoparticles on oxidative stress and DNA damage in the nematode, *Caenorhabditis elegans*. *Chemosphere* 108, 343–52. doi:10.1016/j.chemosphere.2014.01.078

Arora, S., Jain, J., Rajwade, J.M., Paknikar, K.M., 2008. Cellular responses induced by silver nanoparticles: In vitro studies. *Toxicol. Lett.* 179, 93–100. doi:10.1016/j.toxlet.2008.04.009

Autrup, H., Sutherland, D.S., Scott-fordsmand, J., 2012. Earthworms and Humans in Vitro: Characterizing Evolutionarily Conserved Stress and Immune Responses to Silver Nanoparticles.

Baalousha, M., Lead, J.R., von der Kammer, F., Hofmann, T., 2009. Natural colloids and nanoparticles in aquatic and terrestrial environments. *Environ. Hum. Heal. Impacts Nanotechnol.* 109–161.

Baker, M.A., Cerniglia, G.J., Zaman, A., 1990. Microtiter plate assay for the measurement of glutathione and glutathione disulfide in large numbers of biological samples. *Anal. Biochem.* 190, 360–365.

Baud, O., Greene, A.E., Li, J., Wang, H., Volpe, J.J., Rosenberg, P. a, 2004. Glutathione peroxidase-catalase cooperativity is required for resistance to hydrogen peroxide by mature rat oligodendrocytes. *J. Neurosci.* 24, 1531–40. doi:10.1523/JNEUROSCI.3989-03.2004

Bird, R.P., Draper, H.H., 1984. Comparative studies on different methods of malonaldehyde determination. *Methods Enzymol.* 105, 299.

Bradford, M.M., 1976. A rapid and sensitive method for the quantitation of microgram quantities of protein utilizing the principle of protein-dye binding. *Anal. Biochem.* 72, 248–254.

Braydich-Stolle, L., Hussain, S., Schlager, J.J., Hofmann, M.-C., 2005. In vitro cytotoxicity of nanoparticles in mammalian germline stem cells. *Toxicol. Sci.* 88, 412–9. doi:10.1093/toxsci/kfi256

Calabrese, E.J., 2008. Hormesis: principles and applications for pharmacology and toxicology. *Am. J. Pharmacol. Toxicol.* 3, 59.

Carlberg, I., Mannervik, B., 1975. Purification and characterization of the flavoenzyme glutathione reductase from rat liver. *J. Biol. Chem.* 250, 5475–5480.

Castro-Ferreira, M.P., Roelofs, D., van Gestel, C. a M., Verweij, R. a, Soares, A.M.V.M., Amorim, M.J.B., 2012. *Enchytraeus crypticus* as model species in soil ecotoxicology. *Chemosphere* 87, 1222–7. doi:10.1016/j.chemosphere.2012.01.021

Choi, J.E., Kim, S., Ahn, J.H., Youn, P., Kang, J.S., Park, K., Yi, J., Ryu, D.-Y., 2010. Induction of oxidative stress and apoptosis by silver nanoparticles in the liver of adult zebrafish. *Aquat. Toxicol.* 100, 151–9. doi:10.1016/j.aquatox.2009.12.012

Clairborne, A., 1985. Catalase activity, in: Greenwald, R. (Ed.), *Handbook of Methods in Oxygen Radical Research*. CRC Press, Boca Raton.

Ghosh, M., J. M., Sinha, S., Chakraborty, A., Mallick, S.K., Bandyopadhyay, M., Mukherjee, A., 2012. In vitro and in vivo genotoxicity of silver nanoparticles. *Mutat. Res.* 749, 60–9. doi:10.1016/j.mrgentox.2012.08.007

Giri, U., Iqbal, M., Athar, M., 1996. Porphyrin-mediated photosensitization has a weak tumor promoting activity in mouse skin: possible role of in situ-generated reactive oxygen species. *Carcinogenesis* 17, 2023–2028.

Gomes, S.I.L., Hansen, D., Scott-Fordsmand, J.J., Amorim, M.J.B., 2015. Effects of silver nanoparticles to soil invertebrates: Oxidative stress biomarkers in *Eisenia fetida*. *Environ. Pollut.* 199, 49–55. doi:10.1016/j.envpol.2015.01.012

Gomes, S.I.L., Novais, S.C., Scott-Fordsmand, J.J., De Coen, W., Soares, A.M.V.M., Amorim, M.J.B., 2012. Effect of Cu-nanoparticles versus Cu-salt in *Enchytraeus albidus* (Oligochaeta): Differential gene expression through microarray analysis. *Comp. Biochem. Physiol. - C Toxicol. Pharmacol.* 155, 219–227. doi:10.1016/j.cbpc.2011.08.008

Gomes, S.I.L., Soares, A.M.V.M., Scott-Fordsmand, J.J., Amorim, M.J.B., 2013. Mechanisms of response to silver nanoparticles on *Enchytraeus albidus* (Oligochaeta): survival, reproduction and gene expression profile. *J. Hazard. Mater.* 254–255, 336–44. doi:10.1016/j.jhazmat.2013.04.005

Habig, W.H., Pabst, M.J., Jakoby, W.B., 1974. Glutathione S-transferases the first enzymatic step in mercapturic acid formation. *J. Biol. Chem.* 249, 7130–7139.

Hayashi, Y., Engelmann, P., Foldbjerg, R., Szabó, M., Somogyi, I., Pollák, E., Molnár, L., Autrup, H., Sutherland, D.S., Scott-Fordsmand, J., Heckmann, L.-H., 2012. Earthworms and humans in vitro: characterizing evolutionarily conserved stress and immune responses to silver nanoparticles. *Environ. Sci. Technol.* 46, 4166–73. doi:10.1021/es3000905

Hayashi, Y., Heckmann, L.-H., Simonsen, V., Scott-Fordsmand, J.J., 2013. Time-course profiling of molecular stress responses to silver nanoparticles in the earthworm *Eisenia fetida*. *Ecotoxicol. Environ. Saf.* 98, 219–26. doi:10.1016/j.ecoenv.2013.08.017

He, W., Zhou, Y.-T., Wamer, W.G., Boudreau, M.D., Yin, J.-J., 2012. Mechanisms of the pH dependent generation of hydroxyl radicals and oxygen induced by Ag nanoparticles. *Biomaterials* 33, 7547–55. doi:10.1016/j.biomaterials.2012.06.076

Hu, C., Li, M., Wang, W., Cui, Y., Chen, J., Yang, L., 2012. Ecotoxicity of silver nanoparticles on earthworm *Eisenia fetida*: responses of the antioxidant system, acid phosphatase and ATPase. *Toxicol. Environ. Chem.* 94, 732–741. doi:10.1080/02772248.2012.668020

ISO, I.O. for S.S.Q., 2005. Effects of pollutants on Enchytraeidae (*Enchytraeus* sp.). Determination of effects on reproduction and survival. Guideline 16387. Geneva, Switzerland.

Kawata, K., Osawa, M., Okabe, S., 2009. In vitro toxicity of silver nanoparticles at noncytotoxic doses to HepG2 human hepatoma cells. *Environ. Sci. Technol.* 43, 6046–51.

Klein, C.L., Comero, S., Locoro, G., Gawlik, B.M., Linsinger, T., Stahlmecke, B., Romazanov, J., Kuhlbusch, T.A.J., Van Doren, E., De Temmerman, P.J., 2011. NM-Series of Representative Manufactured Nanomaterials NM-300 Silver Characterisation. Stability, Homog. JRC 60709.

Kwak, J. Il, Lee, W.-M., Kim, S.W., An, Y.-J., 2014. Interaction of citrate-coated silver nanoparticles with earthworm coelomic fluid and related cytotoxicity in *Eisenia andrei*. *J. Appl. Toxicol.* 34, 1145–1154. doi:10.1002/jat.2993

Maria, V.L., Ribeiro, M.J., Amorim, M.J.B., 2014. Oxidative stress biomarkers and metallothionein in *Folsomia candida* - responses to Cu and Cd. *Environ. Res.* 133C, 164–169. doi:10.1016/j.envres.2014.05.027

Massarsky, A., Dupuis, L., Taylor, J., Eisa-Beygi, S., Strek, L., Trudeau, V.L., Moon, T.W., 2013. Assessment of nanosilver toxicity during zebrafish (*Danio rerio*) development. *Chemosphere* 92, 59–66. doi:10.1016/j.chemosphere.2013.02.060

Nair, P.M.G., Park, S.Y., Choi, J., 2013. Evaluation of the effect of silver nanoparticles and silver ions using stress responsive gene expression in *Chironomus riparius*. *Chemosphere* 92, 592–9. doi:10.1016/j.chemosphere.2013.03.060

OECD, 2004. Guidelines for the testing of chemicals No. 220. Enchytraeid Reproduction Test. Organization for Economic Co-Operation and Development, Paris, France.

Ohkawa, H., Ohishi, N., Yagi, K., 1979. Assay for Lipid Peroxides in Animal Tissues Thiobarbituric Acid Reaction 358, 351–358.

Park, E.-J., Yi, J., Kim, Y., Choi, K., Park, K., 2010. Silver nanoparticles induce cytotoxicity by a Trojan-horse type mechanism. *Toxicol. In Vitro* 24, 872–8. doi:10.1016/j.tiv.2009.12.001

SAS Enterprise Guide 5.1, 2012. SAS Institute Inc., Cary, NC, USA.

Schlich, K., Klawonn, T., Terytze, K., Hund-Rinke, K., 2013. Effects of silver nanoparticles and silver nitrate in the earthworm reproduction test. *Environ. Toxicol. Chem.* 32, 181–8. doi:10.1002/etc.2030

SigmaPlot, 1997. Statistical Package for the Social Sciences, 11.0. Systat Software, Inc., Chicago, IL, USA.

Tietze, F., 1969. Enzymic method for quantitative determination of nanogram amounts of total and oxidized glutathione: applications to mammalian blood and other tissues. *Anal. Biochem.* 27, 502–522.

Tsyusko, O. V., Hardas, S.S., Shoults-Wilson, W.A., Starnes, C.P., Joice, G., Butterfield, D.A., Unrine, J.M., 2012. Short-term molecular-level effects of silver nanoparticle exposure on the earthworm, *Eisenia fetida*. *Environ. Pollut.* 171, 249–55. doi:10.1016/j.envpol.2012.08.003

van der Ploeg, M.J.C., Handy, R.D., Waalewijn-Kool, P.L., van den Berg, J.H.J., Herrera Rivera, Z.E., Bovenschen, J., Molleman, B., Baveco, J.M., Tromp, P., Peters, R.J.B., Koopmans, G.F., Rietjens, I.M.C.M., van den Brink, N.W., 2014. Effects of silver nanoparticles (NM-300K) on *Lumbricus rubellus* earthworms and particle characterization in relevant test matrices including soil. *Environ. Toxicol. Chem.* 33, 743–52. doi:10.1002/etc.2487

Van Leeuwen, H.P., 2011. Steady-state DGT fluxes of nanoparticulate metal complexes A. *Environ. Chem.* 8, 525–528. doi:10.1071/EN11022

Viarengo, A., Ponzano, E., Donderob, F., Fabbri, R., 1997. A Simple Spectrophotometric Method for Metallothionein Evaluation in Marine Organisms: an Application to Mediterranean and Antarctic Molluscs. *Mar. Environ. Res.* 44, 69–84..

Wang, W., Ballatori, N., 1998. Endogenous glutathione conjugates: occurrence and biological functions. *Pharmacol. Rev.* 50, 335–356.

Wilhelm Filho, D., Tribess, T., Gaspari, C., Claudio, F.D., Torres, M.A., Magalhaes, A.R.M., 2001. Seasonal changes in antioxidant defenses of the digestive gland of the brown mussel (*Perna perna*). *Aquaculture* 203, 149–158.

Xiu, Z., Zhang, Q., Puppala, H.L., Colvin, V.L., Alvarez, P.J.J., 2012. Negligible Particle-Specific Antibacterial Activity of Silver Nanoparticles. *Nano Lett.* 12, 4271–4275..

Yang, E.-J., Kim, S., Kim, J.S., Choi, I.-H., 2012. Inflammasome formation and IL-1 β release by human blood monocytes in response to silver nanoparticles. *Biomaterials* 33, 6858–67. doi:10.1016/j.biomaterials.2012.06.016

Yang, X., Gondikas, A.P., Marinakos, S.M., Auffan, M., Liu, J., Hsu-Kim, H., Meyer, J.N., 2012. Mechanism of silver nanoparticle toxicity is dependent on dissolved silver and surface coating in *Caenorhabditis elegans*. *Environ. Sci. Technol.* 46, 1119–27. doi:10.1021/es202417t

CHAPTER II

Silver (nano)materials cause genotoxicity in *Enchytraeus crypticus* – as determined by the comet assay

Vera L. Maria ^{1,*}, Maria J. Ribeiro ¹, Sofia Guilherme¹, Amadeu M.V.M. Soares¹, Janeck J. Scott-Fordsmand ² and Mónica J. B. Amorim ¹

¹Department of Biology & CESAM (Centre for Environmental and Marine Studies), University of Aveiro, 3810-193 Aveiro, Portugal ² Department of Bioscience, Aarhus University, Vejlsovej 25, DK-8600 Silkeborg, Denmark.

Environmental Toxicology and Chemistry 37(1) (2018) 184-191.

DOI: 10.1002/etc.3944

ABSTRACT

Enchytraeids have been used in standard ecotoxicity testing for approximately 20 yr. Since adopting the standard test for survival and reproduction, a number of additional tools have been developed, including transcriptomics and enzymatic biomarkers. So far, a genotoxicity tool and endpoint have not been used; hence, the goals of the present study included optimization of the *in vivo* alkaline comet assay in *Enchytraeus crypticus*. Further, the effect of silver nanomaterial (Ag NM300K, dispersed, 15 nm) was tested and compared with silver nitrate. Hydrogen peroxide was used as a positive control. The various steps were optimized. The fully detailed standard operating procedure is presented. Silver materials caused genotoxicity, this being differentiated for the nano and non-nano forms. Silver nitrate caused genotoxicity after 3 d of exposure in a dose-related manner, although after 7 d the effects were either reduced or repaired. Ag NM300K caused higher genotoxicity after 7 d for the lowest concentration, highlighting a potential nonmonotonic dose–response effect. Overall, the comet assay showed the power to discriminate effects between materials and also toxicity at low relevant doses.

Keywords: single cell gel electrophoresis (SCGE); genetic damage indicator (GDI); metallic nanoparticle; soil invertebrate

INTRODUCTION

Injuries to DNA can be caused either by direct interaction of the toxicant and/or its metabolites with the DNA or by secondary interaction (e.g., toxicant-induced reactive oxygen species [ROS] generation leading to DNA adducts) (Ahmad et al., 2006; Kermanizadeh et al., 2015). Such genotoxicity may be mitigated through an increase of DNA repair, antioxidant counteraction, and cell renewal (Kermanizadeh et al., 2015). Although genotoxicity has been reported for various biota (Fontanetti et al., 2011) on exposure to contaminants, it has not been described in enchytraeids. Enchytraeids represent many key species for soil ecosystems, which is also why some of these species are used as standard organisms in soil toxicology. For these organisms, a wide range of tools is available at the organism level, for example, the reproduction test and the full–life cycle test, including endpoints like hatching and growth (Bicho et al., 2016; Castro-Ferreira et al., 2012; Gomes et al., 2013). Moreover, biochemical/molecular level tools that describe the mechanism of toxicity are also available, including endpoints like cellular

energy allocation (Gomes et al., 2015c), oxidative stress (Ribeiro et al., 2015), and transcriptomics (Castro-Ferreira et al., 2014; Gomes et al., 2013). Hence, the addition of a genotoxicity tool (such as the comet assay) will be valuable for a better understanding of the mechanisms of toxicity, from starting events to later full-organism effects, through adverse outcome pathways.

Genotoxicity evaluation *via* the comet assay was described in a range of other terrestrial invertebrates, including nematodes and earthworms. For the earthworm *Eisenia fetida* these studies include genotoxicity caused, for example, by metals (e.g., Lourenço et al. (2011)). A few soil animal studies have dealt with the genotoxic effects of nanomaterials, like (*in vitro* and *in vivo*) studies with *E. fetida* exposed to TiO₂ (Hu et al., 2010), ZnO (Gupta et al., 2014; Hu et al., 2010), and CdSe/ZnS quantum dots (Saez et al., 2015) as well as *in vitro* studies on the nematode *Caenorhabditis elegans* exposed to silver (Ag) (Chatterjee et al., 2014b, 2014a; Hunt et al., 2013).

In the present study we aimed to implement, optimize, and use the comet assay in *Enchytraeus crypticus*. For the assay we used Ag exposure because it is well known to cause DNA damage (Asharani et al., 2009b). We compared the comet induction between free Ag (following exposure to an Ag salt) to that of an Ag-based nanomaterial (Ag NM300K, a referential type nanomaterial from the Joint Research Centre). We have ample additional experience with the effects of Ag nanomaterial in enchytraeids, namely transcriptomics (Gomes et al., 2017), cellular energy allocation (Gomes et al., 2015), and oxidative stress (Ribeiro et al., 2015).

Enchytraeus crypticus were exposed for a range of days (0, 3, and 7 d, based on previous cell studies (Ribeiro et al., 2015)) using the same reproduction effect concentrations (ECs) for silver nitrate (AgNO₃) and Ag NM300K (i.e., 20, 50, and 80% reproduction ECs [EC20, EC50, EC80, respectively]) (Bicho et al., 2016). The hypotheses tested were as follows: 1) Ag materials cause genotoxicity in the tested sublethal range, and 2) an exposure time of 3 to 7 d is sufficient to assess the comet effects.

MATERIALS AND METHODS

Test organisms

The test species *E. crypticus* (Oligochaeta: Enchytraeidae) was used. Cultures were kept in agar plates, consisting of Bacti-Agar medium (Oxoid; Agar No. 1) and a sterilized mixture of 4 different salt solutions at final concentrations of 2 mM $\text{CaCl}_2 \cdot 2\text{H}_2\text{O}$, 1 mM MgSO_4 , 0.08 mM KCl, and 0.75 mM NaHCO_3 . Organisms were fed *ad libitum* with ground autoclaved oatmeal twice per week and maintained in the laboratory under controlled conditions (at 19 °C and a 16:8-h light:dark photoperiod). Adults with visible clitellum and similar size were selected for the experiments.

Test soil

Standard LUFA 2.2 natural soil (Speyer) was used. The main characteristics can be described as follows: pH (0.01 M CaCl_2) 5.5, organic matter = 1.77%, cation exchange capacity = 10.1 meq/100 g, maximum water holding capacity = 41.8 %, and grain size distribution of 7.3% clay (<0.002 mm), 13.8% silt (0.002–0.05 mm), and 78.9% sand (0.05–2.0 mm).

Test materials and spiking

The reference Ag nanomaterial (Ag NM300K) and AgNO_3 (>99% purity; Sigma-Aldrich) were used. The Ag NM300K, from the European Commission Joint Research Centre, was fully characterized (Klein et al., 2011). In short, Ag NM300K particles were spherical and consisted of a colloidal dispersion with a nominal Ag content of 10.2% w/w, dispersed in 4% w/w of polyoxyethylene glycerol trioleate and polyoxyethylene (20) sorbitan monolaurate (Tween 20), having >99% of particles with a nominal size of approximately 15 nm, with no coating. Transmission electron microscopy (TEM) indicated a size of 17 ± 8 nm. Smaller nanoparticles of approximately 5 nm were also present. The dispersant (as dispersant control) was also tested alone.

Test concentrations were selected based on the reproduction EC_x values, as summarized in Table 1. Test chemicals were spiked onto premoistened soil as aqueous solution. Stock aqueous solution was prepared and serially diluted. For AgNO_3 soil batches per

concentration were homogeneously mixed and divided over replicates. Spiking of Ag NM300K was done per individual replicate. The dispersant control was made by adding the same volume of dispersant to soil as used with the highest concentration of Ag NM300K. Soil was allowed to equilibrate for 3 d prior to test start. Soil moisture content was adjusted to 50% of the maximum water holding capacity.

Table 1: Selected test concentrations (milligrams of Ag per kilogram dry wt of soil LUFA 2.2)^a

Test materials	EC20	EC50	EC80
AgNO ₃	45	60	96
Ag NM300K	60	170	225

^aEffect concentrations for *Enchytraeus crypticus* exposure based on Bicho et al., (2016). EC20, EC50 and EC80 = effect concentration reduced *E. crypticus* reproductive output by 20, 50 and 80 %, respectively, within 95 % confidence intervals.

Test procedures

Pretest optimization steps. Five aspects were considered for the optimization process: 1) number of test organisms tested in pools of 20 and 40, 3 replicates performed; 2) disaggregation methods, enchytraeids were disaggregated using either scissor or the Ultra-Turrax device (Ystral; model X-1020); 3) matrix fractionation method, the cellular suspension was dispersed by applying the “gravity” method, centrifugation (150 g for 4 min, 4 °C) keeping the supernatant, or the pellet (“gravity” term means waiting for 10 s after chopping for settling of big fragments in the microtube); 4) *in vitro* positive control, hydrogen peroxide (H₂O₂) 75 μM (15 and 30 min of exposure) was used to test the suitability as positive control genotoxicity in *E. crypticus* cellular suspension; and 5) effect of soil particles, sampling the enchytraeids from the test vessels (with soil) was done including washing 5 times with cold distilled water with maintenance for 20–30 min on ice and directly from the soil without washing, prior transference to cold phosphate-buffered saline (PBS). Details can be found in the Supporting Information as standard operating procedure.

The comet assay was performed according to Collins (2004) and Guilherme et al. (2010). At this point (i.e., after having the data from the pretest optimization), it was decided that the best experimental approach was to find at least 100 nonoverlapping nucleoids per gel.

To ensure cell viability, as needed to proceed for comet analysis, we followed Collins's (2004) recommendation, in which the control cells must present comets with a background (low) level of breaks (i.e., mostly class 0, or ~ 10% of DNA in the tail). Although not used in the present study, the trypan blue test can check cell viability. Cells with permeable/damaged membranes, which are considered trypan blue test–positive, may recover and survive, being in fact false trypan blue test–positive (Collins, 2004) and hence not recommended.

In vivo exposure. The procedures followed the standard guidelines (ISO, 2014; OECD, 2004a) with adaptations. In short, 40 adult enchytraeids collected from cultures were selected and introduced in each test vessel containing 20 g of moist soil and food supply. Tests were performed at 19 ± 1 °C (standard error [SE]; n = 7) and a 16:8-h light:dark photoperiod. Four replicates per treatment were used. Sampling was done at days 0, 3, and 7. Enchytraeids were carefully collected from the soil, rinsed (5 times) in a Petri dish with cold deionized water, maintained for 20 to 30 min, and transferred to 200 μ L of cold PBS (on ice). Afterward, enchytraeids were chopped (scissors), 10 to 15 times; resuspended once in PBS; and left (10 s) for the larger fragments to deposit/settle in the microtube. Cellular suspension preparation and the next procedure (comet assay) were performed under dimmed light condition to prevent additional DNA damage.

Genotoxicity evaluation—Comet assay. An alkaline version of the comet assay was used (Collins, 2004; Guilherme et al., 2010) with minor modifications, allowing the separation of strand breaks (single-strand and double-strand breaks of the supercoiled DNA) to migrate out of the nucleus during electrophoresis. Briefly, 40 μ L of cold cell suspension was mixed with 140 μ L of 1% low–melting point agarose at 37 °C. The final low–melting point agarose content was 0.6%. Immediately, 2 gel replicates of 70 μ L each were placed on one glass microscope slide precoated with 1% normal–melting point agarose. Slides used as *in vitro* positive controls (organisms from culture) were made with H₂O₂ 75 μ M. Then, slides were immersed in a lysis solution, placed in a tank with electrophoresis buffer for alkaline treatment (20 min), neutralized (using PBS), and washed (using distillate water). After air-drying, gels were stained for further visualization. Lastly, one slide with 2 replicate gels

(100 nucleoids/gel were scored) was observed for each pool (4 biological replicates/condition). The detailed standard operating procedure is included as Supporting Information.

Data analysis

A visual classification of nucleoids was performed to evaluate the DNA damage considering 5 comet classes, according to the tail intensity and length, from 0 (no tail) to 4 (almost all DNA in tail) (Collins, 2004) (Figure 1). The total score expressed as a genetic damage indicator was calculated multiplying the mean percentage of nucleoids in each class by the corresponding factor as follows:

Genetic damage indicator (arbitrary units) = (%nucleoids class 0 x 0) + (%nucleoids class 1) + (%nucleoids class 2 x 2) + (%nucleoids class 3 x 3) + (%nucleoids class 4 x 4)

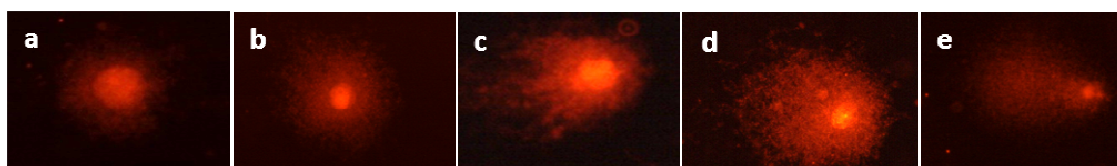


Figure 1: The DNA damage classes from *Enchytraeus crypticus* nucleoids (x400 magnification): (a) class 0, no damage; (b) class 1; (c) class 2; (d) class 3; and (e) class 4.

Results were expressed as arbitrary units because they can be associated with the relative tail intensity that is a function of break frequency, on a scale of 0 to 400 per 100 scored nucleoids (as average value for the 2 gels observed per pool). Besides the genetic damage indicator, the frequency of nucleoids observed in each comet class was expressed (Azqueta et al., 2009), and the subtotal frequency of nucleoids with medium (class 2), high (class 3), and complete (class 4) damaged DNA was also calculated (2 + 3 + 4) (Çavaş and Könen, 2007; Palus et al., 1999).

Statistical analysis used SigmaPlot Ver 11.0 software. Data were tested for normality and homogeneity of variance using the Kolmogorov-Smirnov and the Levene tests, respectively. One-way analysis of variance followed by Dunnett's post hoc test ($p < 0.05$) was used to compare the treatments (Ag NM300K and AgNO₃) with the controls (control

or dispersant), within the same exposure period. To compare different concentrations (EC20, EC50, and EC80) within the same exposure duration, Tukey's test was used.

RESULTS AND DISCUSSION

Optimization

Results from the tested enchytraeid cell extraction methods are reported in Table 2. These data are related to the first 3 points that were considered for the pretest optimization process (number, disaggregation, and matrix fractionation methods).

Table 2: Nucleoids number during the optimization procedure ^a

No.	Ultra-Turrax ^{b,d}			Scissor ^{c,d}			
	organisms	i. 1 st Sp ^e	ii. 2 nd Sp ^f	iii. Pellet ^g	i. 1 st Sp ^e	ii. 2 nd Sp ^f	iii. Pellet ^g
20		0.0±0.0	0.0±0.0	0.0±0.0	64±36.9	2±0.9	83±47.8
40		0.3±0.19	0.0±0.0	0.0±0.0	216±124.7	11±6.3	277±159.9

^a Optimizing process in whole *Enchytraeus crypticus*.

^b Disaggregated method: ultra-turrax.

^c Disaggregated method : scissor.

^d Values are expressed as average ± standard error (SE) [n=3 slides, two gels/pool/slide].

^{e, f, g} Fractions: **i.** 1st Sp- first supernatant (by gravity) ^e, **ii.** 2nd Sp- second supernatant (by centrifugation) ^f and **iii.** Pellet (at 150 g, 4 min at 4 °C) ^g.

No.= number.

All cell categories were present in the suspension because whole organisms were used for extraction. Hence, the selected method required a pool of 40 organisms cut by scissor, where nucleoids were visible and in sufficient number. Moreover, the design fits well in studies on biochemical effects using *E. crypticus* (Ribeiro et al., 2015), where 40 organisms provided sufficient levels of total protein for oxidative stress measurements.

The Ultra-Turrax method caused more cell injuries than scissors and exposed the nuclear material to the endonuclease action. This resulted in deteriorated DNA during the fragmentation process, explaining the absence of nucleoids (Table 2). Thus, the scissor method was preferred and caused less cell destruction (e.g., nuclear membrane disruption) before the lysis step.

More than 100 nucleoids, the required minimum number for the genetic damage indicator, were observed at the combinations using pools of 40 organisms, manually chopped with scissors. The cellular suspension was obtained by gravity and using the pellet (Table 2). Despite a high number (average of 216) of nucleoids, these were not densely packed in the gel (i.e., tails were not imbricated), allowing us to choose randomly nonoverlapping comets. On the contrary, the background noise observed in the pellet as colored granules and disrupted membranes did not allow the counting of nucleoids (although in a higher number). Indeed, a higher occurrence of orange ovoid structures was observed when compared with the first supernatant (Figure 2). These colored granules (orange) may be related to coelomocytes (Franchini and Marchetti, 2006), which appear in the coelomic cavity of *E. crypticus* (Hess, 1970; Schmelz et al., 2000). Also, the observed color suggested absorption of the dye ethidium bromide. Without the dye, using fresh cell suspensions (absence of low-melting point agarose), the cells (only eleocytes, granulocytes) were light green, which may be a result of the autofluorescence of internal granules (Cholewa et al., 2006).

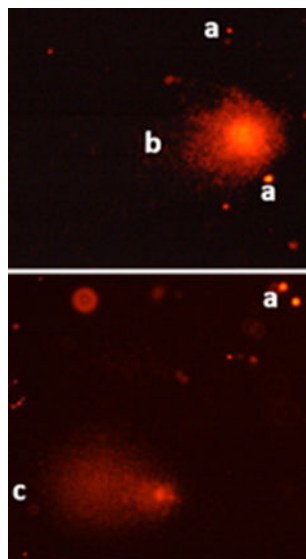


Figure 2: Visualization (x400 magnification) of colored granules (a) and comets (b, class 2; c, class 4) from *Enchytraeus crypticus* agarose slides prepared by the pellet obtained using scissor as the disaggregation tool and by centrifuging at 1500 g for 4 min at 4 °C as the matrix fractionation process.

In addition, the second supernatant had the lowest nucleoid number, probably because the cells in this fraction were settled in the pellet.

Overall, based on the optimization process, fresh cell preparations were made using a pool of 40 whole organisms chopped and the first supernatant. In the present study the achieved baselines, 152 arbitrary units (as genetic damage indicator) were in the same range as the ones found in the liver of *Anguilla anguilla* (Marques et al., 2014) using the same method (scissor). In addition, DNA damage in coelomocytes of *E. fetida* (control/unexposed) was found in the same range as in the present study (≈ 175 arbitrary units) (Lourenço et al., 2011). Also, according to Collins (2004), we saw that control cells presented comets with a background (low) level of breaks.

As shown for controls, genetic damage indicator values were the same for organisms collected from culture (agar) plates and from test vessels with soil, 152 and 156 nucleoids respectively; hence, these matrix properties (agar vs soil) did not cause variation for DNA damage.

Despite the occurrence of colored granules (dyed by ethidium bromide) in organisms from both agar and soil, ovoid structures resembling coccus were only found for soil (Figure 3). However, this aspect did not prevent the counting of nucleoids because sites where they occurred were ignored and only clear fields of “cocoid” structures were used (100 per gel).



Figure 3: Visualization ($\times 100$ magnification) of background noise represented by the filamentous (a) or dispersed (b) structures (ovoid) from *Enchytraeus crypticus* agarose slides prepared by the scissor method and the first supernatant (by gravity).

The genetic damage indicator values for H_2O_2 75 μM exposure (positive control) were significantly higher compared to 0 min ($p < 0.05$), confirming this concentration as an effective positive control for the comet assay. In addition, no differences were found

between 15 and 30 min of *in vitro* exposure ($p > 0.05$). This typical DNA damage–inducing agent has been applied as a positive control by several authors (Benhusein et al., 2010; Guilherme et al., 2012). Specifically, 75 μM H_2O_2 was reported in studies on coelomocytes, hemocytes, and cell lines (Cheung et al., 2006; Fuchs et al., 2011). The present data showed that using the present positive control, the DNA damage ranged from 150 (± 90 ; SE) genetic damage indicator at time 0 (not exposed) to 281 (± 162 ; SE), and 258 (± 149 ; SE) genetic damage indicators at 15 and 30 min, respectively ($p < 0.05$ vs time 0) for 3 replicates/condition. However, a study using HepG2 cells (Benhusein et al., 2010) reported an increase in DNA damage with increasing time of incubation, 5 and 60 min to H_2O_2 75 μM . Moreover, higher H_2O_2 concentrations (0.01–0.05–0.1–0.5–1 mM) compared to 75 μM were not lethal in thyroid cells (Driessens et al., 2009). A study with extruded coelomocytes of *E. fetida* also used H_2O_2 as a positive control for DNA fragmentation (e.g., H_2O_2 200 μM , 60 min) (Lourenço et al., 2011).

Genotoxicity evaluation—Comet assay

Exposure of *E. crypticus* to the selected ECs caused no mortality (survival $\geq 98\%$) regardless of the period (3 or 7 d).

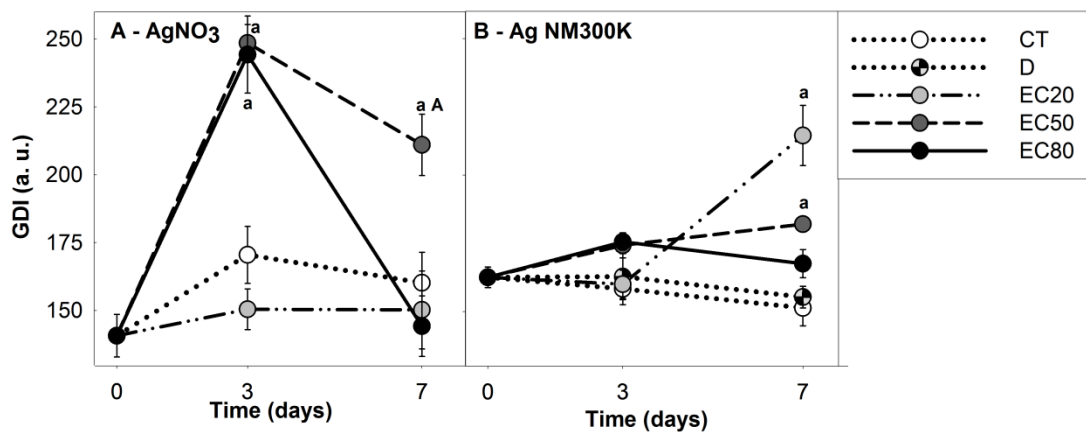


Figure 4: The DNA damage measured as genetic damage indicator (arbitrary units) after standard (alkaline) comet assay (average_ standard error) in whole *Enchytraeus crypticus* exposed to AgNO₃ (A) and Ag NM300K (B), (EC20, EC50, and EC80) for 0, 3, and 7 d. Statistically different ($p < 0.05$): (a) versus control or dispersant control within the same exposure duration; (A) versus same treated group along time exposures. a.u. = arbitrary

units; CT = control; D = dispersant control; ECx = x% effect concentration; GDI = genetic damage indicator.

Results regarding AgNO₃ and Ag NM300K genotoxicity can be seen in Figure 4. Control and dispersant control did not differ ($p > 0.05$). Thus, further comparisons were done versus control. Control values were stable along the entire test duration (Figure 4A,B). The genotoxic potential of AgNO₃ (Figure 4A) was shown after 3 d as observed by an increase in DNA damage for the EC50 and EC80. After 7 d, there was a decrease, and only EC50 was still high, although also reduced, compared to 3 d ($p < 0.05$; Figure 4A). Moreover, an early DNA damage (2 + 3 + 4) increment was observed for both EC50 and EC80 of AgNO₃ (Figure 5A). Particularly, on day 3, the most frequent class of damage for EC50 and EC80 was 2 and 4, respectively. The highest degree of nucleoid damage (as enlarged comet tail) for the highest EC (Figure 5A) was shown, although both ECs caused a similar intensity in DNA damage (as genetic damage indicator values; Figure 4A). At the end of exposure (7 d), a reduction in damage may be seen through the most frequent type of nucleoid damage, that is, class 1, concomitantly with a decrease in genetic damage indicator values for EC50 and EC80 (Figure 4A). In particular, the predominant classes of damage frequency were classes 1 for EC20, 2 for EC50, and 1 and 4 for EC80 after 3-d exposure (Figure 5A). Hence, the observed time-related reduction of DNA damage in AgNO₃ EC80 (7 d; i.e., class 1 is predominant) suggests the occurrence of DNA repair and/or catabolism of damaged cells.

Exposure to Ag NM300K caused a genotoxic effect only after 7 d for the EC20 and EC50 (Figure 4A). Moreover, DNA damage was the highest for the EC20 exposure compared with EC50 and EC80. The present data suggest the possibility of early activation of detoxifying mechanisms in the organisms exposed to higher doses. In particular, it is known from a previous study (Ribeiro et al., 2015) with the same nanomaterials that metallothionein levels were increased in *E. crypticus* exposed to EC80 (7 d). Besides, there was a generally higher antioxidant enzymatic response to higher ECs (EC50 and EC80, 7 d) (Ribeiro et al., 2015). A similar relationship between concentration and damage was also reported by Asharani et al. (2008) in embryos of zebrafish (*Danio rerio*) where apoptosis and necrosis were associated with lower Ag nanomaterial concentration. Conversely, there are also examples of increasing damage with increasing Ag nanomaterial as observed either in *Lumbricus terrestris* (as apoptosis) (Lapied et al., 2010) or in *Nereis diversicolor* (as tail moment and intensities) (Cong et al., 2014, 2011).

In these specific cases, the Ag nanomaterial properties (e.g., size, morphology, coatings) and the biological entities may be the source of varying results.

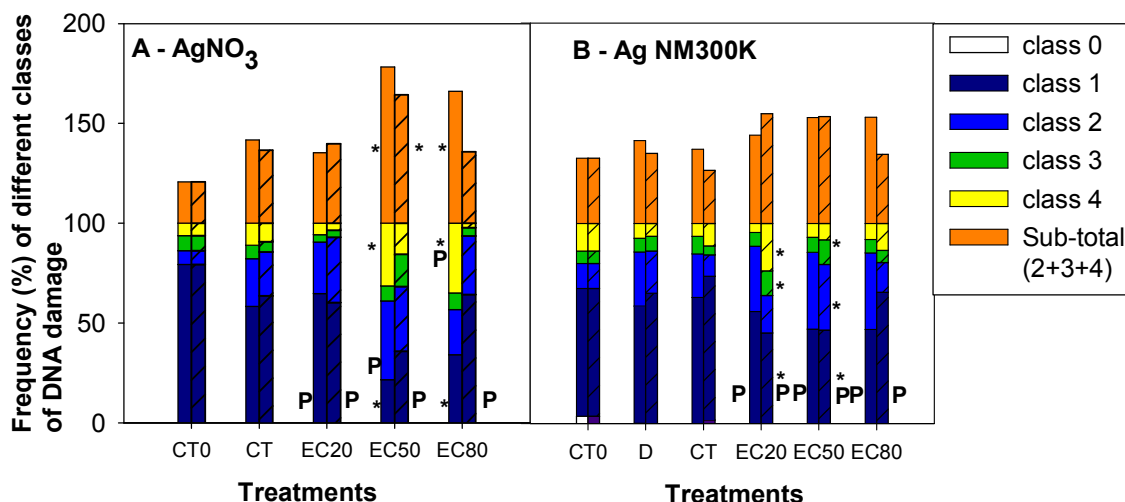


Figure 5: Mean frequencies of each DNA damage class and subtotal of damaged nucleoids, measured by comet assay in whole *Enchytraeus crypticus* exposed to AgNO₃ (A) and Ag NM300K (B), (EC20, EC50, and EC80), dispersant control, and deionized water (control) for 3 and 7 d (bars with dashed lines). Statistically different ($p < 0.05$) versus control within the same exposure duration. P = predominant class for genotoxicity; CT = control (CT0 = organisms from agar culture); D = dispersant control; ECx = x% effect concentration.

As shown in Figure 5B, nucleoids from class 1 were the most represented (i.e., predominant) in each Ag NM300K group (EC20, EC50, and EC80) for 3- and 7-d exposure. Regarding the frequency of individual classes of DNA damage, only after 7 d did they significantly change. Thus, class 1 decreased ($p < 0.05$) in EC50 and EC80, whereas an increase ($p < 0.05$) in the frequencies of classes 2 and 3 was observed in EC50. Furthermore, for EC20, class 3 and 4 frequencies were also augmented ($p < 0.05$), suggesting some repair capacity patent in the EC50 and EC80 exposures (based on classes of damage analysis). Despite the differences in damage classes of both ECs (20 and 50), their subtotal values were higher ($p < 0.05$; Figure 5B).

Differences of genotoxicity between Ag materials are likely related to either a higher dissolution rate of salt (compared with nanomaterial) or a lower bioavailability of agglomerated nanomaterial, at higher concentrations. As shown in Bicho et al. (2016),

there was a nonmonotonic dose response for Ag NM300K, with a much higher effect caused at 20 mg/kg. This is corroborated in the present results (7 d).

Overall, genotoxicity effects of Ag nanomaterial and Ag salt have been reported in aquatic invertebrates (Cong et al., 2014, 2011; Park and Choi, 2010), vertebrate embryos (Asharani et al., 2008; Bar-Ilan et al., 2009), and cell lines (Asharani et al., 2009a, 2009b; Lim et al., 2012; Park et al., 2011), being absent for soil invertebrates. These studies reported that DNA damage potency variations may depend on the organism, physical and chemical Ag nanomaterial properties, doses, and time/route of exposures. Cong et al. (2014, 2011) showed increased genotoxicity with increased Ag salt and Ag nanomaterial concentrations for *N. diversicolor* coelomocytes, where Ag nanomaterial had the higher genotoxic effect. On the other hand, Asharani et al. (2008, 2009a) showed that Ag nanomaterial internalization in the mitochondria and nucleus may lead to ROS generation (by mitochondrial chain disruption) and, consequently, DNA damage.

A previous study with *E. crypticus* (Ribeiro et al., 2015) showed lipid peroxidation after 7-d exposure to Ag NM300K (EC20), whereas this response occurred earlier for AgNO₃ (EC50) after 3 d. Thus, Ag⁺ can induce oxidative stress (Asharani et al., 2009a, 2009b) via the interaction with sulfhydryl groups of enzymes, and probably these ions can interact with DNA by either covalent binding to DNA [(Hossain and Huq, 2002) or cell division and DNA synthesis inhibition (Hidalgo and Dominguez, 1998; Singh et al., 2009) causing damage.

CONCLUSIONS

An *in vivo* comet assay was optimized and tested in *E. crypticus* for the first time. A genotoxic effect was confirmed for Ag materials, being different for the nano and non-nano forms. Genotoxicity was caused by AgNO₃ after 3 d of exposure for the EC50 and EC80 levels (after 7 d, effects were repaired), whereas effects of Ag NM300K were apparent after 7 d for the EC20. In summary, the comet assay demonstrated different genotoxicity for ECs below those showing effects on *E. crypticus* reproduction, namely the EC50 (AgNO₃) and EC20 (Ag NM300K).

SUPPORTING INFORMATION

The supporting information are available on the Wiley Online Library at DOI: 3944.

ACKNOWLEDGMENTS

The present study was funded by the European Commission FP7 MARINA (G.A. no. 263215), by FEDER through COMPETE Programa Operacional Factores de Competitividade, and by national funding through FCT–Fundação para a Ciência e Tecnologia, with cofunding by FEDER within the PT2020 Partnership Agreement and Compete 2020 within the research project NM_OREO (POCI-01-0145-FEDER-016771, PTDC/AAG-MAA/4084/2014) and to CESAM (UID/AMB/50017). The FCT grants were to V.L. Maria (SFRH/BPD/95093/2013), M.J. Ribeiro (SFRH/BD/95027/2013), and S. Guilherme (SFRH/BPD/88947/2012).

REFERENCES

- Ahmad, I., Maria, V.L., Oliveira, M., Pacheco, M., Santos, M.A., 2006. Oxidative stress and genotoxic effects in gill and kidney of *Anguilla anguilla* L. exposed to chromium with or without pre-exposure to β -naphthoflavone. *Mutat. Res. - Genet. Toxicol. Environ. Mutagen.* 608, 1, 16–28. doi:10.1016/j.mrgentox.2006.04.020
- Asharani, P. V, Hande, M.P., Valiyaveetil, S., 2009a. Anti-proliferative activity of silver nanoparticles. *BMC Cell Biol.* 10, 65.
- Asharani, P. V, Lian Wu, Y., Gong, Z., Valiyaveetil, S., 2008. Toxicity of silver nanoparticles in zebrafish models. *Nanotechnology* 19, 255102. doi:10.1088/0957-4484/19/25/255102
- Asharani, P. V, Low, G., Mun, K., Hande, M.P., Valiyaveetil, S., 2009b. Cytotoxicity and Genotoxicity of Silver in Human cells 3, 279–290.
- Azqueta, A., Shaposhnikov, S., Collins, A.R., 2009. DNA oxidation: investigating its key role in environmental mutagenesis with the comet assay. *Mutat. Res. Toxicol. Environ. Mutagen.* 674, 101–108.
- Bar-Ilan, O., Albrecht, R.M., Fako, V.E., Furgeson, D.Y., 2009. Toxicity assessments of multisized gold and silver nanoparticles in zebrafish embryos. *Small* 5, 1897–1910.

Benhusein, G., Mutch, E., Aburawi, S., Williams, F., 2010. Genotoxic effect induced by hydrogen peroxide in human hepatoma cells using comet assay. *Libyan J. Med.* 5, 4637.

Bicho, R.C., Ribeiro, T., Rodrigues, N.P., Scott-Fordsmand, J.J., Amorim, M.J.B., 2016. Effects of Ag nanomaterials (NM300K) and Ag salt (AgNO₃) can be discriminated in a full life cycle long term test with *Enchytraeus crypticus*. *J. Hazard. Mater.* 318, 608–614. doi:10.1016/j.jhazmat.2016.07.040

Castro-Ferreira, M.P., de Boer, T.E., Colbourne, J.K., Vooijs, R., van Gestel, C.A.M., van Straalen, N.M., Soares, A.M.V.M., Amorim, M.J.B., Roelofs, D., 2014. Transcriptome assembly and microarray construction for *Enchytraeus crypticus*, a model oligochaete to assess stress response mechanisms derived from soil conditions. *BMC Genomics* 15. doi:10.1186/1471-2164-15-302

Castro-Ferreira, M.P., Roelofs, D., van Gestel, C. a M., Verweij, R. a, Soares, A.M.V.M., Amorim, M.J.B., 2012. *Enchytraeus crypticus* as model species in soil ecotoxicology. *Chemosphere* 87, 1222–7. doi:10.1016/j.chemosphere.2012.01.021

Çavaş, T., Könen, S., 2007. Detection of cytogenetic and DNA damage in peripheral erythrocytes of goldfish (*Carassius auratus*) exposed to a glyphosate formulation using the micronucleus test and the comet assay. *Mutagenesis* 22, 263–268.

Chatterjee, N., Eom, H.J., Choi, J., 2014a. Effects of silver nanoparticles on oxidative DNA damage–repair as a function of p38 MAPK status: A comparative approach using human Jurkat T cells and the nematode *Caenorhabditis elegans*. *Environ. Mol. Mutagen.* 55, 122–133.

Chatterjee, N., Yang, J., Kim, H.-M., Jo, E., Kim, P.-J., Choi, K., Choi, J., 2014b. Potential toxicity of differential functionalized multiwalled carbon nanotubes (MWCNT) in human cell line (BEAS2B) and *Caenorhabditis elegans*. *J. Toxicol. Environ. Heal. Part A* 77, 1399–1408.

Cheung, V. V, Depledge, M.H., Jha, A.N., 2006. An evaluation of the relative sensitivity of two marine bivalve mollusc species using the Comet assay. *Mar. Environ. Res.* 62, S301–S305.

- Cholewa, J., Feeney, G.P., O'Reilly, M., StÄżrzenbaum, S.R., Morgan, A.J., Płytycz, B., 2006. Autofluorescence in eleocytes of some earthworm species. *Folia Histochem. Cytobiol.* 44, 65–71.
- Collins, A.R., 2004. The comet assay for DNA damage and repair. *Mol. Biotechnol.* 26, 249.
- Cong, Y., Banta, G.T., Selck, H., Berhanu, D., Valsami-Jones, E., Forbes, V.E., 2014. Toxicity and bioaccumulation of sediment-associated silver nanoparticles in the estuarine polychaete, *Nereis (Hediste) diversicolor*. *Aquat. Toxicol.* 156, 106–115.
- Cong, Y., Banta, G.T., Selck, H., Berhanu, D., Valsami-Jones, E., Forbes, V.E., 2011. Toxic effects and bioaccumulation of nano-, micron- and ionic-Ag in the polychaete, *Nereis diversicolor*. *Aquat. Toxicol.* 105, 403–411.
- Driessens, N., Versteyhe, S., Ghaddhab, C., Burniat, A., De Deken, X., Van Sande, J., Dumont, J.-E., Miot, F., Corvilain, B., 2009. Hydrogen peroxide induces DNA single- and double-strand breaks in thyroid cells and is therefore a potential mutagen for this organ. *Endocr. Relat. Cancer* 16, 845–856.
- Fontanetti, C.S., Nogarol, L.R., de Souza, R.B., Perez, D.G., Maziviero, G.T., 2011. Bioindicators and biomarkers in the assessment of soil toxicity, in: *Soil Contamination. InTech.* 143-168
- Franchini, A., Marchetti, M., 2006. The effects of okadaic acid on *Enchytraeus crypticus* (Annelida: Oligochaeta). *Invertebr. Surviv. J* 3, 111–117.
- Fuchs, J., Piola, L., González, E.P., Oneto, M.L., Basack, S., Kesten, E., Casabé, N., 2011. Coelomocyte biomarkers in the earthworm *Eisenia fetida* exposed to 2, 4, 6-trinitrotoluene (TNT). *Environ. Monit. Assess.* 175, 127–137.
- Gomes, S.I.L., Roca, C.P., Scott-Fordsmand, J.J., Amorim, M.J.B., 2017. High-throughput transcriptomics reveals uniquely affected pathways: AgNPs, PVP-coated AgNPs and Ag NM300K case studies. *Environ. Sci. Nano* 4, 929–937.

Gomes, S.I.L., Scott-Fordsmand, J.J., Amorim, M.J.B., 2015. Cellular energy allocation to assess the impact of nanomaterials on soil invertebrates (Enchytraeids): the effect of Cu and Ag. *Int. J. Environ. Res. Public Health* 12, 6858–6878.

Gomes, S.I.L., Soares, A.M.V.M., Amorim, M.J.B., 2015. Changes in cellular energy allocation in *Enchytraeus crypticus* exposed to copper and silver—linkage to effects at higher level (reproduction). *Environ. Sci. Pollut. Res.* 22, 14241–14247. doi:10.1007/s11356-015-4630-4

Gomes, S.I.L., Soares, A.M.V.M., Scott-Fordsmand, J.J., Amorim, M.J.B., 2013. Mechanisms of response to silver nanoparticles on *Enchytraeus albidus* (Oligochaeta): survival, reproduction and gene expression profile. *J. Hazard. Mater.* 254–255, 336–44. doi:10.1016/j.jhazmat.2013.04.005

Guilherme, S., Gaivão, I., Santos, M.A., Pacheco, M., 2010. European eel (*Anguilla anguilla*) genotoxic and pro-oxidant responses following short-term exposure to Roundup®—a glyphosate-based herbicide. *Mutagenesis* 25, 523–530.

Guilherme, S., Santos, M.A., Barroso, C., Gaivão, I., Pacheco, M., 2012. Differential genotoxicity of Roundup® formulation and its constituents in blood cells of fish (*Anguilla anguilla*): considerations on chemical interactions and DNA damaging mechanisms. *Ecotoxicology* 21, 1381–1390.

Gupta, S., Kushwah, T., Yadav, S., 2014. Earthworm coelomocytes as nanoscavenger of ZnO NPs. *Nanoscale Res. Lett.* 9, 259. doi:10.1186/1556-276X-9-259

Hess, R.T., 1970. The fine structure of coelomocytes in the annelid *Enchytraeus fragmentosus*. *J. Morphol.* 132, 335–351.

Hidalgo, E., Dominguez, C., 1998. Study of cytotoxicity mechanisms of silver nitrate in human dermal fibroblasts. *Toxicol. Lett.* 98, 169–179.

Hossain, Z., Huq, F., 2002. Studies on the interaction between Ag⁺ and DNA. *J. Inorg. Biochem.* 91, 398–404.

Hu, C.W., Li, M., Cui, Y.B., Li, D.S., Chen, J., Yang, L.Y., 2010. Toxicological effects of TiO₂ and ZnO nanoparticles in soil on earthworm *Eisenia fetida*. *Soil Biol. Biochem.* 42, 586–591. doi:10.1016/j.soilbio.2009.12.007

Hunt, P.R., Marquis, B.J., Tyner, K.M., Conklin, S., Olejnik, N., Nelson, B.C., Sprando, R.L., 2013. Nanosilver suppresses growth and induces oxidative damage to DNA in *Caenorhabditis elegans*. *J. Appl. Toxicol.* 33, 1131–1142.

ISO, I.O. for S.S.Q., 2014. Soil quality—Effects of contaminants on Enchytraeidae (*Enchytraeus* sp.)—Determination of effects on reproduction. ISO 16387.

Kermanizadeh, A., Chauché, C., Brown, D.M., Loft, S., Møller, P., 2015. The role of intracellular redox imbalance in nanomaterial induced cellular damage and genotoxicity: A review. *Environ. Mol. Mutagen.* 56, 111–124. doi:10.1002/em.21926

Klein, C.L., Comero, S., Locoro, G., Gawlik, B.M., Linsinger, T., Stahlmecke, B., Romazanov, J., Kuhlbusch, T.A.J., Van Doren, E., De Temmerman, P.J., 2011. NM-Series of Representative Manufactured Nanomaterials NM-300 Silver Characterisation. Stability, Homog. JRC 60709.

Lapied, E., Moudilou, E., Exbrayat, J., Oughton, D.H., Joner, E.J., 2010. Silver nanoparticle exposure causes apoptotic response in the earthworm *Lumbricus terrestris* (*Oligochaeta*). *Nanomedicine* 5, 975–984.

Lim, H.K., Asharani, P. V, Hande, M.P., 2012. Enhanced genotoxicity of silver nanoparticles in DNA repair deficient mammalian cells. *Front. Genet.* 3, 104.

Lourenço, J.I., Pereira, R.O., Silva, A.C., Morgado, J.M., Carvalho, F.P., Oliveira, J.M., Malta, M.P., Paiva, A.A., Mendo, S.A., Gonçalves, F.J., 2011. Genotoxic endpoints in the earthworms sub-lethal assay to evaluate natural soils contaminated by metals and radionuclides. *J. Hazard. Mater.* 186, 788–795. doi:10.1016/j.jhazmat.2010.11.073

Marques, A., Custódio, M., Guilherme, S., Gaivão, I., Santos, M.A., Pacheco, M., 2014. Assessment of chromosomal damage induced by a deltamethrin-based insecticide in fish

(*Anguilla anguilla* L.)—A follow-up study upon exposure and post-exposure periods. Pestic. Biochem. Physiol. 113, 40–46.

OECD, 2004. Guidelines for the testing of chemicals No. 220. Enchytraeid Reproduction Test. Organization for Economic Co-Operation and Development, Paris, France

Palus, J., Dziubałtowska, E., Rydzyński, K., 1999. DNA damage detected by the comet assay in the white blood cells of workers in a wooden furniture plant. Mutat. Res. Toxicol. Environ. Mutagen. 444, 61–74.

Park, M.V.D.Z., Neigh, A.M., Vermeulen, J.P., de la Fonteyne, L.J.J., Verharen, H.W., Briedé, J.J., van Loveren, H., de Jong, W.H., 2011. The effect of particle size on the cytotoxicity, inflammation, developmental toxicity and genotoxicity of silver nanoparticles. Biomaterials 32, 9810–7. doi:10.1016/j.biomaterials.2011.08.085

Park, S.-Y., Choi, J.-H., 2010. Geno- and Ecotoxicity Evaluation of Silver Nanoparticles in Freshwater Crustacean *Daphnia magna*. Environ. Eng. Res. 15, 23–27. doi:10.4491/eer.2010.15.1.428

Ribeiro, M., Maria, V., Scott-Fordsmand, J., Amorim, M., 2015. Oxidative Stress Mechanisms Caused by Ag Nanoparticles (NM300K) are Different from Those of AgNO₃: Effects in the Soil Invertebrate *Enchytraeus Crypticus*. Int. J. Environ. Res. Public Health 12, 9589–9602. doi:10.3390/ijerph120809589

Saez, G., Aye, M., Meo, M., Aimé, A., Bestel, I., Barthélémy, P., Giorgio, C., 2015. Genotoxic and oxidative responses in coelomocytes of *Eisenia fetida* and *Hediste diversicolor* exposed to lipid-coated CdSe/ZnS quantum dots and CdCl₂. Environ. Toxicol. 30, 918–926.

Schmelz, R.M., Collado, R., Myohara, M., 2000. A taxonomic study of *Enchytraeus japonensis* (Enchytraeidae, Oligochaeta): morphological and biochemical comparisons with *E. bigeminus*. Zoolog. Sci. 17, 505–516.

Singh, N., Manshian, B., Jenkins, G.J.S., Griffiths, S.M., Williams, P.M., Maffei, T.G.G., Wright, C.J., Doak, S.H., 2009. NanoGenotoxicology: The DNA damaging potential of

engineered nanomaterials. *Biomaterials* 30, 3891–3914.
doi:10.1016/j.biomaterials.2009.04.009

SUPPORTING INFORMATION


Standard operating procedure (SOP)

- Comet assay for *Enchytraeus crypticus*: endpoint genotoxicity.


MATERIALS

1. Preparation of solutions

- Phosphate-buffered saline – PBS 1X, pH 7.4: Sodium chloride (NaCl) 0.137M, Potassium chloride (KCl) 0.0027 M, di-Sodium hydrogen phosphate (Na_2HPO_4) 10 mM, Potassium dihydrogen phosphate (KH_2PO_4) 1.8 mM in ultra-pure (u. p) water. Adjust pH at 7.4. Keep solution at 4 °C for one month.
- Lysis solution (base solution), pH 10: Sodium chloride (NaCl) 2.5M, ethylenediaminetetraacetic acid (EDTA) 0.1 M and tris(hydroxymethyl)aminomethane (Tris) 10 mM. Adjust pH at 10. Keep at 4 °C protected from light for one month.
- Lysis solution (fresh solution), pH >13: 20 mL Dimethylsulfoxide (DMSO), 2 mL Triton – X100 and 180 mL lysis solution (base solution). Keep at 4 °C protected from the light.

 **NOTE** Prepare on the experiment day.

- Denaturation and electrophoresis solution: Sodium hydroxide (NaOH) 8M and EDTA 0.1 M in cold ultra-pure (u.p.) water. Keep at 4°C protected from light.

 **NOTE** Prepare on the experiment day.

- Normal melting point agarose (NMPA) 1 %: Solution for slide pre-coating. Dissolve in u.p. water at 80 °C. Let it to cold (65-70 °C) and immediately spread into slides (frosted-end microscope slides) and dry-air during 12 h.


 **NOTE** Slides can be prepared and stored with desiccant.

- Low melting point agarose (LMPA) 1 %: Solution for slide coating. Dissolve in u.p. water at 80 °C. Distribute aliquots of 750 µL into microtubes. Keep at 4 °C protected from the light.


 **NOTE**: LMPA can be prepared and stored at 4 °C.

- Ethidium bromide: EtBr 10 mg/ mL (stock solution) (in u.p. water). Keep at 4 °C protected from the light. Diluted (1: 500) in order to get 20 µg / mL at the moment of slide staining.

 **CAUTION** EtBr is carcinogenic!

 **NOTE** Stock solution can be prepared and stored at 4 °C.

Hydrogen peroxide (H₂O₂) 75 µM in PBS 1X.

 **NOTE** Prepared on the experiment day.


2. Equipment

- Disposable plastic microtubes (1.5 mL).
- Thermo-block (dry bath) for melting agarose at 90 °C and maintaining agarose at 37 °C.
- Frosted-end microscope slides (25 mm × 75 mm).
- Glass coverslips (18 mm x 18 mm).
- Covered glass containers for slide lysis and wash.
- Covered plastic container for slide storage.
- Horizontal gel electrophoresis chamber and power supply.
- Epifluorescence microscope with 25× objective and filter set for blue-green excitation if using ethidium bromide to stain DNA [excitation (absorption) at 482 nm and emission at 616 nm (red-orange)].

PROCEDURE

1. Sample preparation

- I. Collect live and intact *Enchytraeus crypticus* organisms (pool of 40) from the exposure in soil (ISO, 2014; OECD, 2016)] and wash five times with cold deionised water. Leave them at deionised water for 20 to 30 min.

 **NOTE** Enchytraeids collection must be performed gently to ensure the well-being of organisms and the washing step is important to remove attached soil particles and other.

- II. Place the pool into a microtube with 200 µL cold PBS 1X (on ice) and chop with a scissor 10 to 15 times, re-suspending once with a micropipette and leave 10 s for the larger fragments to deposit/settle in the microtube.

NOTE This cell suspension must be maintained on ice until its use in the comet assay. These steps and the next (comet assay) must be performed under dimmed light condition to prevent additional DNA damage.

2. Comet assay

III. Collect 40 μL of cold cell suspension mixing with 140 μL of 1% LMPA at 37 $^{\circ}\text{C}$.

NOTE Few seconds prior the collection of the 40 μL , do the resuspension (1 time) again, wait 10 s and collect an aliquot of cell suspension. The microtube containing LMPA must be on thermo-block (37 $^{\circ}\text{C}$). LMP temperature is very important, since an elevation of one more degree can directly damage the cells.

IV. Proceed immediately, in order to avoid agarose solidification, placing two gel replicates of 70 μL each on one glass microscope slide pre-coated with 1 % NMPA. A glass coverslip is placed on each gel, and slides were kept in the fridge at 4 $^{\circ}\text{C}$ (5 min).

V. At this stage, slides to use as in vitro positive controls can be made. Cellular suspension is obtained from control group and prepared in accordance of previous point (2. III and IV). After this, add 25 μL H_2O_2 75 μM , place the glass coverslip and expose for 15 min at 4 $^{\circ}\text{C}$.

NOTE Control slides (as negative control) are also made in a similar way, but without the addition of the pro-oxidant (H_2O_2).

VI. Remove the coverslip (gently) and immerse slides in cold freshly prepared lysis solution at 4 $^{\circ}\text{C}$, for 1 up to 24 h.

VII. Immerse slides in an electrophoresis tank in a proper cold and new electrophoresis buffer to alkaline treatment (20 min). Perform electrophoresis step using same buffer during 15 min at voltage of 25 V and a current of 300 mA.

NOTE The tank is placed on a tray containing ice to ensure cold temperature for suitable denaturation and electrophoresis processes. This process and next (e.g., slide staining and analyses) must occur at dimmed light condition.

VIII. Neutralize slides in cold PBS 1X (10 min at 4 $^{\circ}\text{C}$) and wash with cold distillate water (10 min at 4 $^{\circ}\text{C}$).

IX. Air-dry slides, place them in a vertical position (20 ± 1 $^{\circ}\text{C}$ in dark, overnight).

3. Slide staining

- X. Stain gels adding 25 μL of EtBr (20 $\mu\text{g}/\text{mL}$) directly onto the slide, place a small glass cover for immediate visualization.

NOTE Slides maintain a good fluorescent image for at least 3 - 4 d when kept in dark conditions, 4 $^{\circ}\text{C}$ and 40-50 % of humidity.

4. Slide analysis

- XI. Observe one slide with two replicate gels (100 nucleoids / gel were scored) for each pool (e.g., 4 biological replicates / condition) through fluorescence microscope ($\times 400$ magnification).
- XII. Perform a visual classification of nucleoids to evaluate the DNA damage into five comet classes, according to the tail intensity and length, from 0 (no tail) to 4 (almost all DNA in tail) (Figure 1) (Collins, 2004; García et al., 2004).

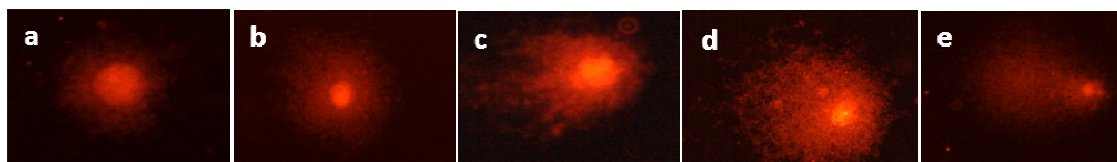


Fig. 1. Nucleoids classification: a) class 0 (no damage); b) class 1; c) class 2, d) class 3 and e) class 4 (Collins, 2004; García et al., 2004) ($\times 400$ magnification).

REFERENCES

Collins, A.R., 2004. The comet assay for DNA damage and repair. *Mol. Biotechnol.* 26, 249.

García, O., Mandina, T., Lamadrid, A.I., Diaz, A., Remigio, A., Gonzalez, Y., Piloto, J., Gonzalez, J.E., Alvarez, A., 2004. Sensitivity and variability of visual scoring in the comet assay: results of an inter-laboratory scoring exercise with the use of silver staining. *Mutat. Res. Mol. Mech. Mutagen.* 556, 25–34.

ISO, I.O. for S.S.Q., 2014. Soil quality—Effects of contaminants on Enchytraeidae (Enchytraeus sp.)—Determination of effects on reproduction. ISO 16387.

OECD, 2016. Test No. 220: Enchytraeid Reproduction Test / Organisation for Economic Co-operation and Development, OECD Guidelines for the Testing of Chemicals, Section 2,. Paris: OECD Publishing.

CHAPTER III

Fate and effect of nano tungsten carbide cobalt (WCCo) in the soil environment: observing a nanoparticle specific toxicity in *Enchytraeus crypticus*

Maria J. Ribeiro¹, Vera L. Maria ¹, Amadeu M.V.M. Soares¹, Janeck J. Scott-Fordsmand²
and Mónica J.B. Amorim¹

¹Department of Biology & CESAM (Centre for Environmental and Marine Studies), University of Aveiro, 3810-193 Aveiro, Portugal ² Department of Bioscience, Aarhus University, Vejlsovej 25, DK-8600 Silkeborg, Denmark.

Published in Environmental Science and Technology 52 (19) (2018) 11394-11401.

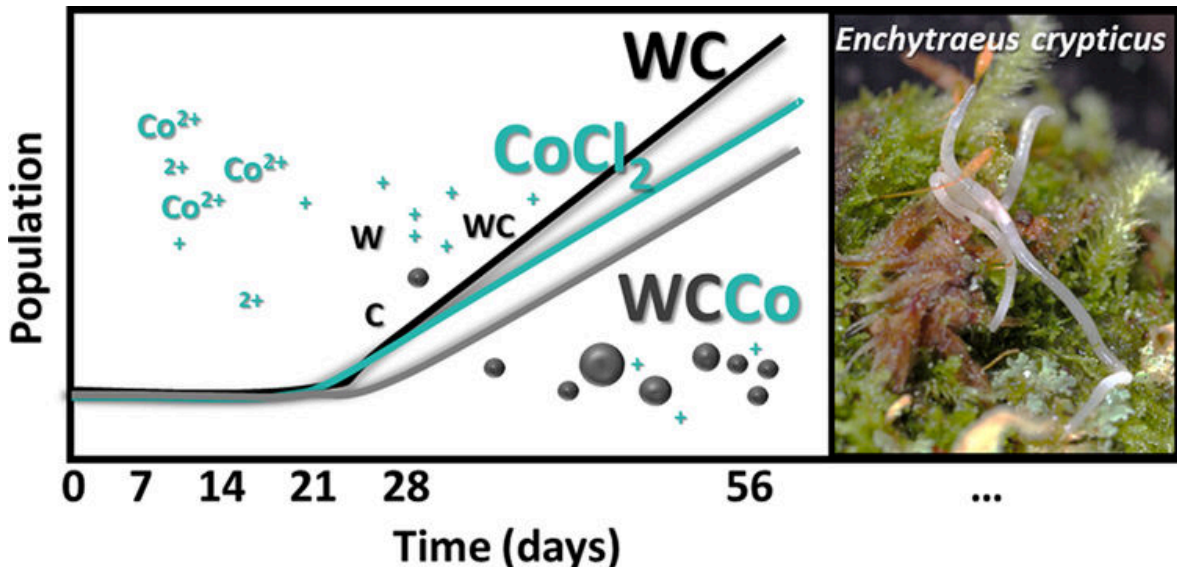
DOI: 10.1021/acs.est.8b02537

ABSTRACT

Tungsten carbide cobalt (WCCo) nanoparticles (NPs) are widely used in hard metal industries. Pulmonary diseases and risk of cancer are associated with occupational exposure, but knowledge about the environmental fate and effects is virtually absent. In this study, the fate and effects of crystalline WCCo NPs, WC, and Co^{2+} were assessed in the soil model *Enchytraeus crypticus*, following the standard Enchytraeid Reproduction Test (ERT). An additional 28 day exposure period compared to the ERT (i.e., a total of 56 days) was performed to assess longer-term effects. WCCo NPs affected reproduction at a concentration higher than the corresponding Co based ($\text{EC}_{50} = 1500 \text{ mg WCCo/kg}$, equivalent to 128 mg Co/kg). WC showed no negative effect up to 1000 mg W/kg . Maximum uptake of Co was 10-fold higher for CoCl_2 compared to WCCo exposed organisms. Overall toxicity seems to be due to a combined effect between WC and Co. This is supported by the soil bioavailable fraction and biological tissue measurements. Last, results highlight the need to consider longer exposure period of NPs for comparable methods standardized for conventional chemicals.

Keywords: Nanotoxicology; invertebrates; hard metals; long-term exposure; soil

TOC



INTRODUCTION

Tungsten carbide cobalt (WCCo) is a hard composite metal which has mechanical properties of great interest to the mining and drilling industries (Prakash, 1995), among others. Its properties increase hardness, durability and wear resistance of materials, improving the lifetime of industrial machinery (Yao et al., 1998). During production and usage, release (e.g., aerosolization) of WCCo can result in high levels of tungsten carbide and cobalt of varying sizes in, for example, the production facilities (Day et al., 2009; Stefaniak et al., 2009) and the surrounding areas due to emission (Abraham and Hunt, 1995; Sheppard et al., 2007). WCCo containing products may also, due to general decomposition (e.g., wear and tear), release particles into the environment.

It is known that WCCo can be toxic, for example, WCCo occupational exposure has been associated with pulmonary toxicity and increased risk of cancer, being classified as “probably carcinogenic to humans” (group 2A) by the International Agency for Research on Cancer (IARC) (IARC, 2006). General toxicity of WCCo particles is attributed to production of activated oxygen species (AOS) due to oxidation of cobalt (Co) catalyzed at the surface of tungsten carbide (WC) (Lison et al., 1995), which can damage proteins, lipids and DNA in the cell.

As the name indicates, the technically important part of WCCo particles is the W (tungsten) in the form of WC (tungsten carbide) and Co (cobalt) content.

Ecotoxicological studies showed that W is toxic to fish (Strigul et al., 2010), plants (Adamakis et al., 2011; Kennedy et al., 2012), soil invertebrates, (*Eisenia fetida* (Inouye et al., 2006; Strigul et al., 2009), *Otala lactea* (Kennedy et al., 2012)) and marine invertebrates (*Daphnia magna* (Strigul et al., 2009)). The mechanism of action is still unclear but it has been proposed that, even though W is not carcinogenic per se, it is able to potentiate tumorigenic effects of other compounds by disrupting phosphate-dependent cell signaling pathways (Johnson et al., 2010). Also W in the form of WC was found to negatively affect cell viability (Kühnel et al., 2009), interfere with voltage gated sodium channels in neurons (Shan et al., 2013, 2012), induce apoptosis (Lombaert et al., 2004) and inflammation (Huaux et al., 1995). Conversely, some studies revealed absent or mild toxicity of W or WC compounds, being difficult to establish an accurate toxicological profile. For instance, no impact on different cell lines' viability was found by Bastian et al. (2009) with nano-WC or W (as $\text{Na}_2\text{WO}_4 \cdot 2\text{H}_2\text{O}$), whereas mild cytotoxicity was found with W exposure in rat liver cells (BRL 3A) (Hussain et al., 2005). *In vivo* instillation of μm -WC

had no effect on the production of the inflammatory mediators (Huaux et al., 1995), nor on the acute pulmonary responses of rats (Lasfargues et al., 1992).

Cobalt (Co) is an essential component of the vitamin B12 necessary in biological processes such as DNA synthesis (Schrauzer, 1968; Stutzenberger, 1974). However, mammalian models show that when in excess, Co induces oxidative stress (Moorhouse et al., 1985; Zou et al., 2001), genotoxicity (Anard et al., 1997), inhibition of the DNA repair system (Hartwig et al., 1991), apoptosis (Zou et al., 2001) and upregulation of hypoxia-inducible factor HIF-1 α (Yuan et al., 2003).

Besides the fact that WC and Co are able to cause toxicity on their own, it is reported that, when combined, toxicity is potentiated (Busch et al., 2010; Kühnel et al., 2009; Lombaert et al., 2013). Studies with WCCo (Lison and Lauwerys, 1992) and WCCo nanoparticles (NPs) (Bastian et al., 2009) showed that the increased toxicity of WCCo could not be explained by available Co present in WCCo, since the particle led to a markedly higher toxicity than observed with a combined WC and Co²⁺ exposure. Further, Busch et al. (2010) studied the expression profile of human keratinocytes exposed to WCCo NPs, WC and Co, and found no differences in transcription, indicating combinatory effects of WC and Co. Studies on the mammalian toxicity of WCCo NPs are scarce and mostly focused in *in vitro* models, and they are virtually absent for environmental species. In cell lines, cytotoxicity was observed with WCCo NP concentrations from 8 $\mu\text{g}/\text{mL}$ (Bastian et al., 2009) with the occurrence of apoptosis at higher concentrations, such as 1000 $\mu\text{g}/\text{mL}$ (Armstead et al., 2014) or 40 – 100 $\mu\text{g}/\text{cm}^2$ (Zhao et al., 2013). Lower (sub-lethal) concentrations were observed to cause increased inflammation (1 – 100 $\mu\text{g}/\text{mL}$ (Armstead and Li, 2016), and genotoxicity (60 - 120 $\mu\text{g}/\text{mL}$, 5 – 75 $\mu\text{g}/\text{mL}$ (Paget et al., 2015)).

No acute local pulmonary and systemic inflammation in Sprague-Dawley rats was reported, after a 24-hour intra-tracheal instillation of 0-500 μg WCCo NP/rat (Armstead et al., 2015) .

For *Folsomia candida* no effects were observed for WCCo NP in terms of survival or reproduction after 28 days of exposure up to 6400 mg WCCo/kg soil DW (Noordhoek et al., 2018) although the authors highlighted the importance of exploring longer exposure times. Implementation of long-term effect studies has been previously described as a major concern regarding the hazard assessment of NPs (Amorim et al., 2016; Baalousha et al., 2016), which is not covered by the current testing paradigm.

Hence, the present study aimed to assess the effects of crystalline WCCo NPs in the environment, using the standard and ecologically relevant soil model *Enchytraeus crypticus*. The Co salt CoCl_2 was also tested to infer about the effects that are due to the

Co fraction in WCCo, as well as WC alone. The survival and reproduction are determined after 28 days as in the standard guideline (OECD, 2004a) and an additional 28 days exposure period was tested to assess longer term effects in the population.

MATERIALS AND METHODS

Test organism

The test species *Enchytraeus crypticus* (Oligochaeta: Enchytraeidae) was used. Cultures have been kept in agar plates for several years at the University of Aveiro. For details please see Bicho et al. (2015). Synchronized cultures were prepared, briefly, mature adults (well-developed clitellum) are transferred to fresh agar plates to lay cocoons, being removed after 2 days. Synchronized juveniles with 17-19 days old were used.

Test soil

The standard LUFA 2.2 natural soil (Speyer, Germany) was used. The main characteristics are: pH (0.01 M CaCl₂) of 5.5, 1.78% organic matter, 10 mequiv/100 g CEC (cation exchange capacity), 43.3% WHC (water holding capacity), 7.9% clay, 16.3% silt, and 75.8% sand regarding grain size distribution.

Test materials and spiking

Nanostructured Tungsten Carbide Cobalt powder (WCCo NP), cobalt chloride (CoCl₂·6H₂O, 98% purity, Sigma-Aldrich) and Tungsten (IV) Carbide (WC, 2 μm powder, 99% purity, Sigma-Aldrich) were used. Full characterisation was performed, for details see Table 1.

For WCCo NPs, tested concentrations were 0–200–400–800–1200–1600 mg WCCo/kg soil dry weight (DW), and 0–48–96–192–240–288 mg Co/kg soil (DW) for CoCl₂, selected to correspond to the equivalent concentration of Co in the WCCo NPs (according to producers' MSDS). Quantification and revised information showed that WCCo has ca. 8% Co (and not 12%), hence 0–200–400–800–1200–1600 mg WCCo/kg soil DW corresponds to 0–17–33–66–100–133 mg Co/kg soil DW of the WCCo. For WC, tested concentrations were 0–30–100–300–1000 mg W/kg soil DW.

WCCo NPs and WC was directly mixed with the dried soil following the recommended for dry powder nondispersible nanomaterials (OECD, 2012). Moisture was adjusted to 50% of the maximum water holding capacity (maxWHC). The spiking of the soil was done per individual replicate to ensure total raw amounts per replicate. The test chemical CoCl_2 was prepared as stock aqueous solution, serially diluted and spiked onto the premoistened soil. The total amount of soil *per* concentration were homogeneously mixed and split onto replicates. Soil equilibrated for 1 day prior test start for both materials. Soil was sampled to quantify Co at days 0, 1, 7, 14, 21, and 28 days and stored at $-20\text{ }^\circ\text{C}$ until further analysis. Additional time points for CoCl_2 included 0.13 (8 h) and 3 days, due to the expected faster oxidation compared to the NPs.

Test procedures

The standard guideline (ISO, 2014; OECD, 2004a) was followed, with some adaptations as described in Bicho et al. (2015). Briefly, 10 synchronized age organisms were introduced in each test container ($\varnothing 4\text{ cm}$) with 20 g of moist soil and food supply ($24 \pm 1\text{ mg}$, autoclaved rolled oats). Test ran during 28 days at $20\text{ }^\circ\text{C}$ and 16:8h photoperiod. Food ($12 \pm 1\text{ mg}$) and water were replenished every week. Four replicates *per* treatment were used, plus one without organisms for abiotic factors measurement (e.g., pH, materials characterization). At test end, to extract organisms from soil and counting, replicates were fixated with 96% ethanol and Bengal rose (1% solution in ethanol). Samples were sieved through three meshes (0.6, 0.2, 0.1 mm) to separate individuals from most of the soil and facilitate counting using a stereo microscope. End points included survival and reproduction (number of adults and juveniles, respectively). Additionally, 1 replicate was performed for control and higher concentrations (0–1600 mg WCCo/kg and 0–288 mg Co/kg, and for all concentrations of WC), to monitor days 7, 14, and 21. For the 56 days exposure, four extra replicates were done (0–1600 mg WCCo/kg and 0–192 mg Co/kg), and hence, larger test containers ($\varnothing 5.5\text{ cm}$) were used with 40 g of soil *per* replicate because of the expected higher density of organisms. For these replicates, at day 28, adults were carefully removed from the soil, after which the soil was left, replenishing water and food weekly. Adult organisms were sampled for analysis of Co content after 28 days of exposure, being carefully retrieved from the soil, depurated in reconstituted ISO water (OECD, 2004b) (for 24 h), snap-frozen in liquid nitrogen and stored at $-80\text{ }^\circ\text{C}$ until further analysis.

Exposure characterization

Materials were fully characterized as produced, for details see Table 1. Cobalt concentration in the experiment samples in soil, soil:water extracts, and organisms' body was measured using Atomic Absorption Spectrometer (AAS, PerkinElmer 4100, Ueberlingen, Germany). The soil (1 g dry weight) was digested using 65% HNO₃ and heated up to 120 °C until all brown fumes were gone (Scott-Fordsmand et al., 2000).

The soil:water extract was the supernatant of a (1:5) soil:water solution, mixed for 5 min at 250 rpm (lab shaker) and then let settle for 2 h. One mL of the solution was digested following the same procedure as used for soil. The exposed organisms were dried at 80 °C and weighed. The digestion followed the same procedure. Before analysis, all samples were resuspended in 2% HNO₃. A biological standard reference sample (standard lobster tissue TORT-1, Marine Analytical Chemistry Standards Program, Division of Chemistry, National Research Council Canada), and a soil standard reference sample (Loam soil C74-06, Laboratory of the Government Chemist, United Kingdom) were used.

Data analysis

One-way analysis of variance (ANOVA) followed by Dunnett's comparison posthoc test ($p < 0.05$) was used to evaluate differences between effects in controls and treatments (SigmaPlot, 1997). Effect concentrations (EC_x) were estimated modelling data to logistic or threshold sigmoid 2 parameters regression models, as indicated in Table 2, using the Toxicity Relationship Analysis Program (TRAP v1.22) software.

RESULTS

Exposure characterization

Nanomaterials were fully characterized as synthesized using a suite of instruments (Table 1).

Table 1: Characterisation of WCCo NPs as synthesised. ICP-MS: Inductively Coupled Plasma Mass Spectrometry (Perkin Elmer NexION 300D; Perkin Elmer Optima 2100); TEM: Transmission Electron Microscope (FEI Tecnai 12 G2); XRD: X-ray Diffraction (Philips PW 1830); IEP: IsoElectric Point; DLS: Dynamic Light Scattering (Malvern Zsizer

Nano); BET: Brunauer–Emmett–Teller (Quantachrome Autosorb iQ); ELS: Electrophoretic Light Scattering (Malvern Zsizer Nano); FT-IR: Fourier- Transform Infrared Spectroscopy (Spectrum One Perkin Elmer (Waltham, MA, USA)); RAMAN (Xantus-1); XPS: Xray Photoelectron Spectroscopy (Perkin Elmer 5600ci).

characteristics	WCCo NP	instrument
Source	NBM Nanomaterialia, Italy	
Composition (%)	Tungsten carbide (WC<88% Wt., CAS 12070-12-1)	ICP - MS
	Cobalt (Co=8.32% Wt., CAS 744-48-4)	
Primary Size distribution [nm]	170 (23-1446)	
Average (Min-Max)		TEM
Mode [nm] (1 st and 3 rd quartile)	48 (69; 280)	
Crystalline size (Average) [nm]	15.4	XRD
IEP	<2	pH
Dispersability in water: D50 [nm];	182.8 ± 21.5; 31	DLS
Average Agglomeration Number (AAN)		
Specific Surface Area [m ² .g ⁻¹]	6.6±0.4	BET
Z-potential [mV]	7.1±0.5	ELS
Structure	O-W-O	FTIR
		and/or RAMAN
Pore size [nm]	Non-porous	BET
	Co=0.08±0.01	
Surface Chemistry [atomic fraction]	W=0.05±0.01	XPS
	O=0.31±0.03	
	C=0.56±0.05	

Measurements of total Co after soil spiking showed a recovery of 67–115% Co for both CoCl₂ and WCCo NP compared to the nominal concentrations.

The soil:water extracts–soil solution–measurements along the time series (Figure 1A) showed an increase of Co immediately after spiking and up to 7 days, after which it tended to decrease and stabilize.

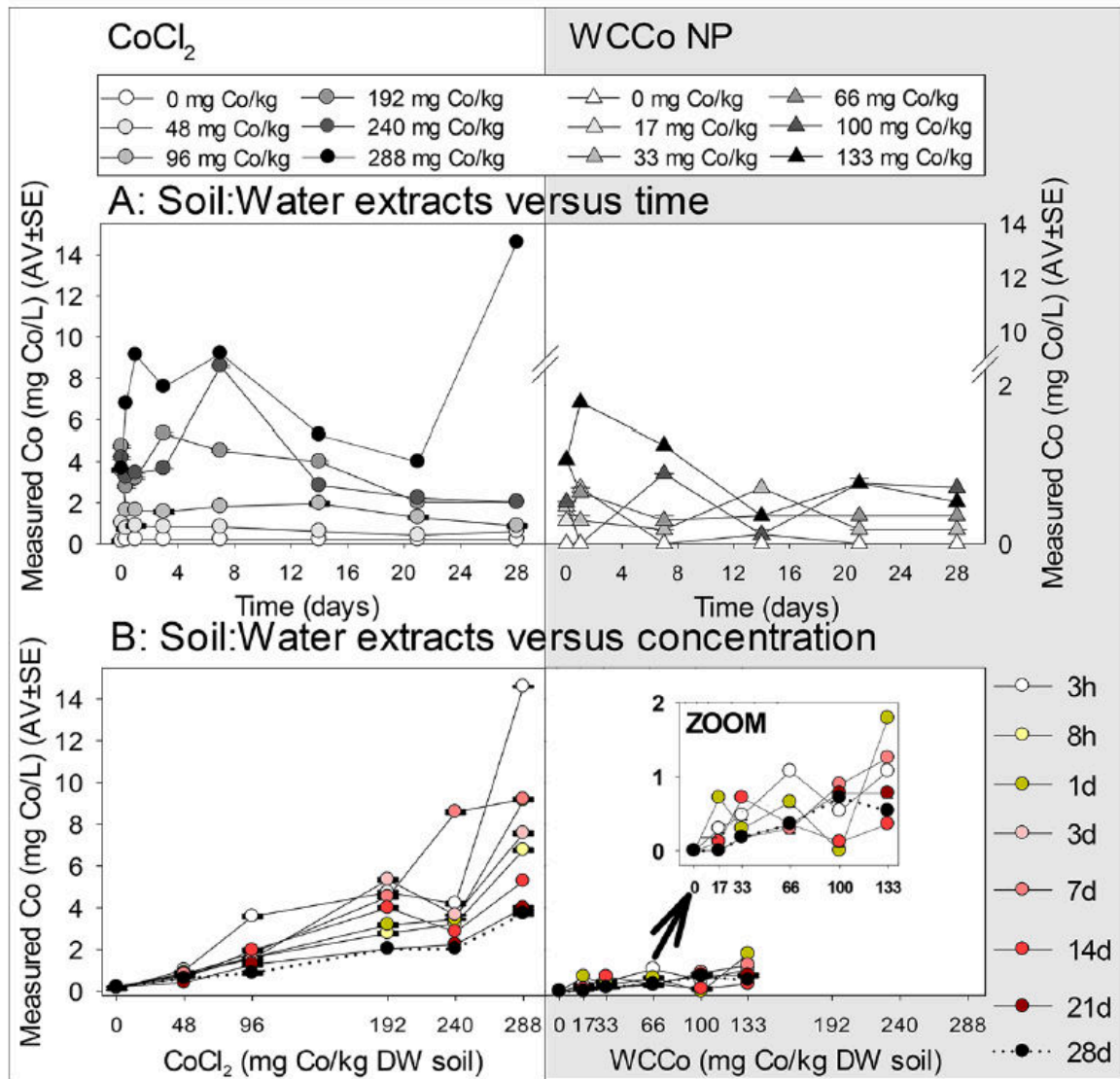


Figure 1: Total cobalt in soil solution, obtained from the enchytraeid reproduction test experiment performed in LUFA 2.2 soil spiked with CoCl₂ and WCCo NP (mg Co/kg soil DW). A: as a function of time (sample days 0, 1, 7, 14, 21, and 28 days, with additional time points for CoCl₂: 0.13 (8 h) and 3 days). B: as a function of concentrations 0–48–96–192–240–288 mg Co/kg DW for CoCl₂, and 0–17–33–66–100–133 mg Co/kg DW for WCCo NP. Values are expressed as average ± standard error (AV ± SE).

The results for CoCl_2 (Figure 1B) indicated a dependence of the concentration, that is, there was relatively higher Co in solution in higher concentration, that is, more than the relative difference between concentrations.

Biological characterisation

Results of the Enchytraeid Reproduction Test (ERT) can be observed in Figure 2.

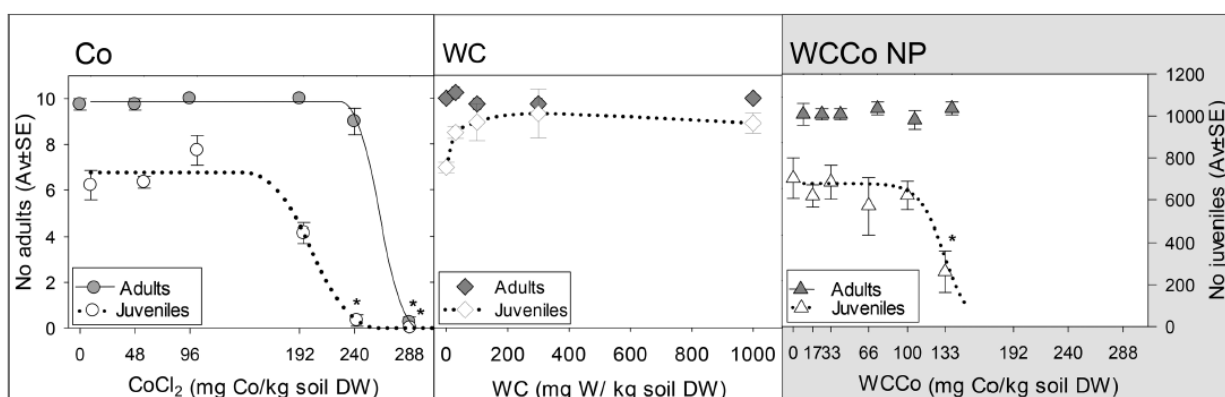


Figure 2: Survival and reproduction of *Enchytraeus crypticus* exposed in LUFA 2.2 soil to Co (mg Co/kg soil DW of CoCl_2), WC (mg W/kg soil DW) and WCCo NP (results expressed as mg Co/kg soil DW for comparability). Values are expressed as average \pm standard error (AV \pm SE). The lines represent the model fit to data. * $p < 0.05$, Dunnett's test.

The validity criteria were fulfilled according to the OECD 220 guideline (OECD, 2004a), that is, in control adults' mortality was $<20\%$, the number of juveniles was >50 , and coefficient of variation $<50\%$. For CoCl_2 , the pH decreased with concentration, from 6.4 to 5.8 for 0- 288 mg CoCl_2 /kg soil DW respectively; for WCCo pH was ca. 5.5. pH variation between test start and test end was below ± 0.5 for both materials.

Exposure to CoCl_2 showed a concentration-dependent response, with significant impact on both reproduction and survival. Exposure to WCCo NP caused no effect in survival and a significant decrease in reproduction with 1600 mg WCCo/kg ($p < 0.05$), this being ca. EC₅₀. Considering that WCCo NP has 8.3% Co, the toxicity was higher if the corresponding Co content is compared, that is, if EC_x would be estimated based on the Co in WCCo. Exposure to WC caused a positive effect with ca. 20% increase in

reproduction from 100 mg WC/kg soil DW. The Effect Concentration (EC_x) estimates are presented in Table 2.

Table 2. Summary of the effect concentrations (EC) for *Enchytraeus crypticus* when exposed to WCCo NPs and CoCl₂ in LUFA 2.2 soil.^a

test material	endpoint	EC10	EC20	EC50	EC80	model and parameters
CoCl ₂ (mg Co/ kg soil DW)	Survival	241 (235-246)	250 (243-252)	260 (256-265)	270 (259-280)	Thresh sig 2 par S: 0.0282; Y0: 9.9
	Reproduction	166 (119-213)	177 (159-195)	200 (159-195)	215 (195-235)	Log 2 par S: 0.0017; Y0: 737.4
WC (mg W/kg soil DW)	Survival	n.e.	n.e.	n.e.	n.e.	
	Reproduction	n.e.	n.e.	n.e.	n.e.	
WCCo NP (mg WCCo/ kg soil DW)	Survival	n.e.	n.e.	n.e.	n.e.	
	Reproduction	1200 (863-1607)	1300 (1084-1609)	1500 (1412-1661)	1700 (1517-1936)	Log 2 par S: 0.0023; Y0: 639.8
WCCo NP (mg Co/ kg soil DW)	Reproduction	104 (70 – 139)	113 (89 – 137)	128 (117 – 139)	143 (124 – 162)	Log 2 par S: 0.01; Y0: 668.7

^aResults show estimates for survival and reproduction, with the corresponding 95% confidence intervals (in brackets). Model and parameters include the values for slope (S) and interception (Y0). n.e.: no effect.

Internal measurements of Co in *E. crypticus* after exposure for 28 days (Figure 3) showed that the body concentration increased up to a maximum of ca. 600 µg/g body DW for exposure to 192 mg Co/kg soil DW of CoCl₂, with higher variation here than for other concentrations.

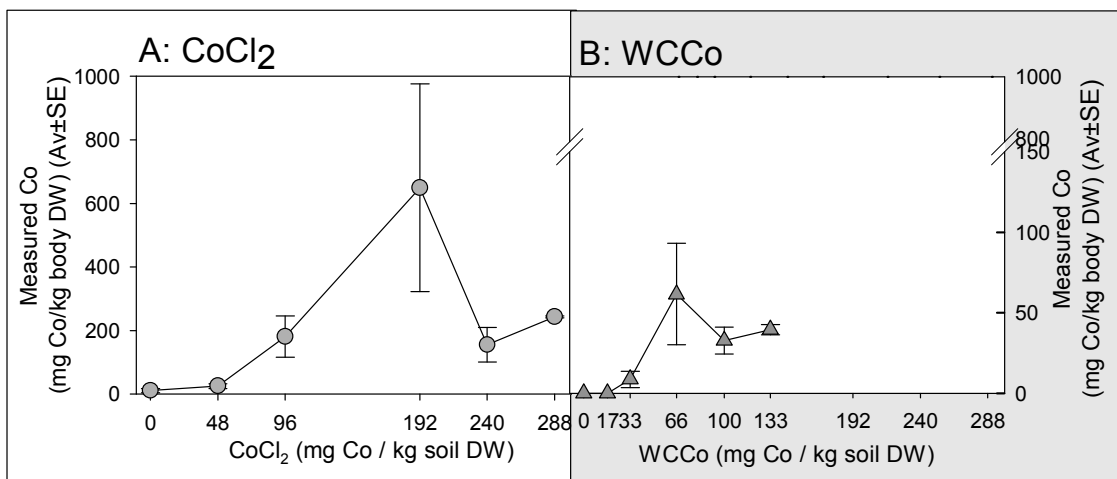


Figure 3: Total cobalt in *Enchytraeus crypticus*, obtained from the enchytraeid reproduction test experiment performed in LUFA 2.2 soil spiked with (A) CoCl₂ and (B) WCCo NP (mg Co/kg soil DW) after 28 days. Values are expressed as average ± standard error (AV ± SE).

The results from the monitoring along time can be seen in Figure 4.

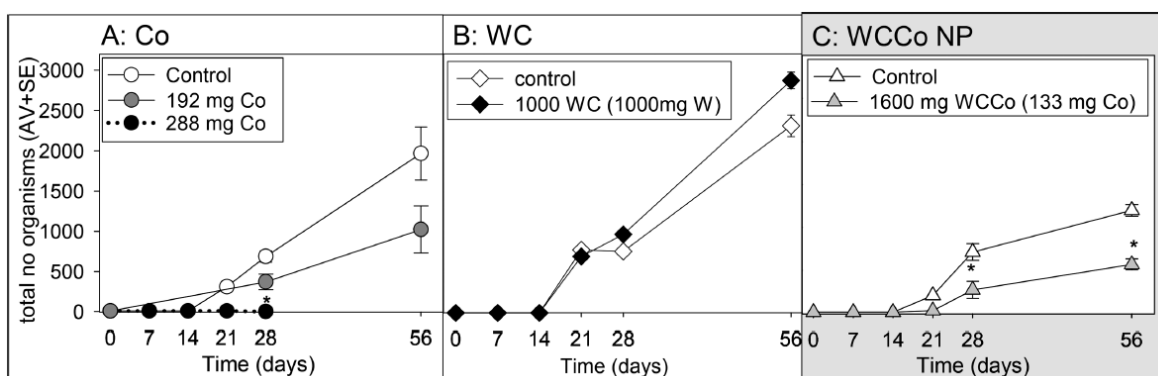


Figure 4: Results of the exposure monitoring of *Enchytraeus crypticus* in LUFA 2.2 soil in terms of total number of individuals at days 0, 7, 14, 21, 28, and 56 to (A) 0–192–288 mg Co/kg soil DW of CoCl₂, (B) 0–30–100–300–1000 mg W/kg soil DW and (C) 0–1600 mg WCCo NP/kg soil DW. Values are expressed as average ± standard error (AV ± SE). * p < 0.05 (between control and treatment).

For the tested concentrations (ca. EC50) the “population growth curve” was similar between CoCl₂ and WCCo NP (28 days) although the impact was relatively higher after 56 days for WCCo NPs. There was an indication of a delay in development as apparent from results on day 21, where the control organisms already reproduced but not the WCCo NP (or CoCl₂) exposed. Testing of WC showed an increase of population growth compared to control at day 28 which became more pronounced at day 56. Details on the full dose-range exposure can be found in SI Figure S2.

DISCUSSION

For both CoCl₂ and WCCo NPs reproduction was affected while 100% survival was observed for the adults, indicating a specific reproductive effect. Considering the concentration of Co and associated toxicity, WCCo NP was relatively more toxic than CoCl₂ (the highest concentration tested of 1600 mg WCCo NP/kg soil DW equivalent to 133 mg Co/kg soil DW, was ca. EC50). Tested alone WC did not show any negative effect on reproduction or mortality up to 1000 mg W/kg soil DW, in fact there was approximately 20% increase in the reproductive output. Similarly, other studies with W confirmed low toxicity (Bamford et al., 2011, Inouye et al., 2006, Strigul et al. 2009). Hence, this shows that there must be some additional (synergistic) effect for Co when in WCCo, for example, that Co was more available when present in WCCo or that there is a NP specific effect.

Previous studies on CoCl₂ with *Enchytraeus albidus* (Lock et al., 2006) in a 14 day exposure for acute effects showed a similar LC50 (LC50 = 227 mg Co/kg). For the springtail *Folsomia candida* (Lock et al., 2004; Noordhoek et al., 2018), the EC50 for reproduction was ca. 450 mg Co/kg soil DW (LC50 of 620 mg Co/kg soil DW, that is, 2 fold higher than for *E. crypticus*). No effects on survival and reproduction with WCCo NP were reported in *F. candida*, even for concentrations up to 6400 mg WCCo/kg soil DW (Noordhoek et al., 2018). Cobalt is known to be an oxidative stress inducing agent, hence, the observed effects in both survival and reproduction in *E. crypticus* could be the result of irreversible impairment of the antioxidant strategies, this for concentrations above 192 mg Co/kg.

The CoCl₂ selected concentrations in our study represent a (although lower) range of Co in WCCo NP, and show that the toxicity of WCCo NP is not fully explained by Co. Our results suggest that the combination with WC in particles significantly potentiated Co toxicity, or changed speciation and/or availability, or that there is a NP specific effect. The NP effect may be both an enhancement of the Co effect or a direct NP effect. Both

Soil:Water concentration and internal organisms' Co measurements indicate that Co was less available and less taken up in WCCo exposure than in CoCl₂ (much higher internal uptake), hence does not support the increased availability of Co for the WCCo (see also SI). Noordhoek et al. (2018) found lower Co values in the pore-water from WCCo NP spiked soil which could indicate Co is more strongly bound in WCCo, hence the toxicity must be caused by a combined effect within the WCCo compound/NPs. As the soil water concentration fluctuate over the experiments, it is difficult to calculate a single soil:water based EC_x (i.e., what soil*water concentration to choose). We estimated the exposure in two different ways, that is, using the average soil:water concentration over time (i.e., for each total exposure concentration) and the integrated soil:water concentration (i.e., area under the curve, (Westlake, 1973), see SI Figure S1 for details). Both soil:water exposure methods showed the EC₅₀ for CoCl₂ 4 times higher than WCCo, for example, the EC₅₀ was 98 mg Co/L.d for CoCl₂ and 24 mg Co/L.d for WCCo, hence again indicating that toxicity is not explained by soil:water concentration/content. Other studies have reported that doping WC with Co has resulted in increased toxicity compared to W, WC or Co alone, both at nano scale (Bastian et al., 2009; Kühnel et al., 2009) and micro scale (Anard et al., 1997; Lison et al., 1995). Moreover, WC tested together with Co in a nonparticulate form (WC with added Co²⁺) seems to elicit a reduced toxic response compared to that observed for the particulate form, for example, cell viability (Bastian et al., 2009; Lison and Lauwerys, 1992) or genotoxicity (Anard et al., 1997), meaning that the presence of WCCo as a particle is necessary for the combinatorial toxic effect. This is in contrast to studies with metallic nanoparticles (e.g., Ag, Ni, Cu) which often show similar or higher toxicity of the salt compared to the nanoform (Bicho et al., 2017; Gomes et al., 2013; Santos et al., 2017). Additional analysis in terms of local distribution of W and Co would be of interest, for example, nanotomography coupled with X-ray fluorescence imaging (Cagno et. al, 2017), as it could provide additional evidence of the combined effect and target organs.

It has been argued that longer exposure periods may be required for nanoparticles exposure for an equivalent comparison to conventional chemicals, and this has been reported (Gonçalves et al., 2017). Although it is commonly agreed that longer exposure period may be required, there is at present no recommendation for the best or standard way to approach the challenge. There are several implications in terms of practical feasibility, for example, a simple extension of the exposure time of the standard tests will not do, let alone that the time required is more, but unclear how much more is enough for a worst case scenario. Detailed dose and time series samplings would be required to

assess longer-term effects. The results on the time scan monitoring here performed (even if for a reduced number of treatments and replicates) showed relatively similar trends for population growth exposed to both materials. We could argue that the time-period of 56 days was perhaps not long enough. Another practical problem is due to the fact that the test design here implemented yields the total number of organisms. This means, in this case, that the number includes more than one reproductive cycle (multigenerational) and a combination of adults and juveniles of various sizes. To overcome this issue, the multigenerational effect should be targeted in a dedicated design to be able to discriminate effects. For instance, in the present results at 56 days, we can also speculate that a selection of the most resistant organisms can occur and perhaps lead to higher reproduction rates because there was no control in the starting number of juveniles at day 28. For example, for *E. crypticus*, the use of a full life cycle test is a good improvement to the standard method as it provides longer exposure (46 instead of 21–28 days), many additional end points (hatching, growth, maturation, besides survival and reproduction) and the organisms are exposed from an earlier life stage (cocoons instead of adults), hence increased sensitivity stages are targeted. Full life cycle studies have been implemented for Ag (Bicho et al., 2016), Cu (Bicho et al., 2017) or Ni (Santos et al., 2017) and delivered considerable more in-depth understanding on the mechanisms or elements deriving toxicity.

CONCLUSIONS

To conclude, the present study showed that WCCo NPs caused toxicity in *E. crypticus*, (EC₅₀ = 1500 mg WCCo/kg soil DW) being more toxic than the equivalent toxicity of Co alone (*via* CoCl₂) or WC alone, and hence toxicity must be due to a nanospecific effect or a combined effect of WC and Co. Results highlight the need to consider longer exposure period of NPs for comparable methods standardized for conventional chemicals.

FUNDING

This study was supported by funds of the European Commission Project: SUN-Sustainable Nanotechnologies (FP7-NMP-2013-LARGE-7, GA No. 604305), and CESAM (UID/AMB/50017 - POCI-01-0145-FEDER-007638), by FCT/MCTES through national funds (PIDDAC), and the cofunding by the FEDER, within the PT2020 Partnership Agreement and Compete 2020, and through the individual PhD grant to Maria J. Ribeiro (SFRH/BD/95027/2013). We further acknowledge the pristine materials full

characterization work (please see Table 1, and Figure S3) made within the SUN consortium partners (Work Package 2).

REFERENCES

Abraham, J.L., Hunt, A., 1995. Environmental contamination by cobalt in the vicinity of a cemented tungsten carbide tool grinding plant. *Environ. Res.* 69, 67–74.

Adamakis, I.D.S., Panteris, E., Eleftheriou, E.P., 2011. The fatal effect of tungsten on *Pisum sativum* L. root cells: Indications for endoplasmic reticulum stress-induced programmed cell death. *Planta* 234, 21–34. doi:10.1007/s00425-011-1372-5

Amorim, M.J.B., Roca, C.P., Scott-Fordsmand, J.J., 2016. Effect assessment of engineered nanoparticles in solid media - Current insight and the way forward. *Environ. Pollut.* 218, 1370–1375. doi:10.1016/j.envpol.2015.08.048

Anard, D., Kirsch-Volders, M., Elhajouji, A., Belpaeme, K., Lison, D., 1997. *In vitro* genotoxic effects of hard metal particles assessed by alkaline single cell gel and elution assays. *Carcinogenesis* 18, 177–184. doi:10.1093/carcin/18.1.177

Armstead, A.L., Arena, C.B., Li, B., 2014. Exploring the potential role of tungsten carbide cobalt (WC-Co) nanoparticle internalization in observed toxicity toward lung epithelial cells *in vitro*. *Toxicol. Appl. Pharmacol.* 278, 1–8. doi:10.1016/j.taap.2014.04.008

Armstead, A.L., Li, B., 2016. *In vitro* inflammatory effects of hard metal (WC-Co) nanoparticle exposure. *Int. J. Nanomedicine* 11, 6195–6206. doi:10.2147/IJN.S121141

Armstead, A.L., Minarchick, V.C., Porter, D.W., Nurkiewicz, T.R., Biomaterials, B.L., 2015. Acute inflammatory responses of nanoparticles in an intra-tracheal instillation rat model. *PLoS One* 10. doi:10.1371/journal.pone.0118778

Baalousha, M., Cornelis, G., Kuhlbusch, T.A.J., Lynch, I., Nickel, C., Peijnenburg, W., van den Brink, N.W., 2016. Modeling nanomaterial fate and uptake in the environment: current knowledge and future trends. *Environ. Sci. Nano* 3, 323–345. doi:10.1039/C5EN00207A

Bamford, J.E., Butler, A.D., Heim, K.E., Pittinger, C.A., Lemus, R., Staveley, J.P., Lee, K.B., Venezia, C., Pardus, M.J., 2011. Toxicity of sodium tungstate to earthworm, oat, radish, and lettuce. *Environ. Toxicol. Chem.* 30, 2312–2318. doi:10.1002/etc.635

Bastian, S., Busch, W., Kühnel, D., Springer, A., Meißner, T., Holke, R., Scholz, S., Iwe, M., Pompe, W., Gelinsky, M., Potthoff, A., Richter, V., Ikonomidou, C., Schirmer, K., 2009. Toxicity of tungsten carbide and cobalt-doped tungsten carbide nanoparticles in mammalian cells *in vitro*. *Environ. Health Perspect.* 117, 530–535. doi:10.1289/ehp.0800121

Bicho, R.C., Ribeiro, T., Rodrigues, N.P., Scott-Fordsmand, J.J., Amorim, M.J.B., 2016. Effects of Ag nanomaterials (NM300K) and Ag salt (AgNO₃) can be discriminated in a full life cycle long term test with *Enchytraeus crypticus*. *J. Hazard. Mater.* 318, 608–614. doi:10.1016/j.jhazmat.2016.07.040

Bicho, R.C., Santos, F.C.F., Gonçalves, M.F.M., Soares, A.M.V.M., Amorim, M.J.B., 2015. Enchytraeid Reproduction TestPLUS: hatching, growth and full life cycle test-an optional multi-endpoint test with *Enchytraeus crypticus*. *Ecotoxicology* 24, 1053–1063. doi:10.1007/s10646-015-1445-5

Bicho, R.C., Santos, F.C.F., Scott-Fordsmand, J.J., Amorim, M.J.B., 2017. Effects of copper oxide nanomaterials (CuONMs) are life stage dependent - full life cycle in *Enchytraeus crypticus*. *Environ. Pollut.* 224, 117–124. doi:10.1016/j.envpol.2017.01.067

Busch, W., Kühnel, D., Schirmer, K., Scholz, S., 2010. Tungsten carbide cobalt nanoparticles exert hypoxia-like effects on the gene expression level in human keratinocytes. *BMC Genomics* 11, 65.

Cagno, S., Brede, D.A., Nuyts, G., Vanmeert, F., Pacureanu, A., Tucoulou, R., Cloetens, P., Falkenberg, G., Janssens, K., Salbu, B., Lind, O.C., 2017. Combined computed Nanotomography and Nanoscopic X-ray fluorescence imaging of cobalt nanoparticles in *Caenorhabditis elegans*. *Anal. Chem.* 89, 11435-11442

Day, G. a, Virji, M.A., Stefaniak, A.B., 2009. Characterization of exposures among cemented tungsten carbide workers. Part II: Assessment of surface contamination and

skin exposures to cobalt, chromium and nickel. *J. Expo. Sci. Environ. Epidemiol.* 19, 423–34. doi:10.1038/jes.2008.33

Gomes, S.I.L., Soares, A.M.V.M., Scott-Fordsmand, J.J., Amorim, M.J.B., 2013. Mechanisms of response to silver nanoparticles on *Enchytraeus albidus* (Oligochaeta): survival, reproduction and gene expression profile. *J. Hazard. Mater.* 254–255, 336–44. doi:10.1016/j.jhazmat.2013.04.005

Gonçalves, M.F.M., Gomes, S.I.L., Scott-Fordsmand, J.J., Amorim, M.J.B., 2017. Shorter lifetime of a soil invertebrate species when exposed to copper oxide nanoparticles in a full lifespan exposure test. *Sci. Rep.* 7, 1–8. doi:10.1038/s41598-017-01507-8

Hartwig, A., Snyder, R.D., Schlepegrell, R., Beyersmann, D., 1991. Modulation by Co (II) of UV-induced DNA-repair, mutagenesis and sister-chromatid exchanges in mammalian cells. *Mutat. Res. Mol. Mech. Mutagen.* 248, 177–185.

Huax, F., Lasfargues, G., Lauwerys, R., Lison, D., 1995. Lung toxicity of hard metal particles and production of interleukin-1, tumor necrosis factor-alpha, fibronectin, and cystatin-c by lung phagocytes. *Toxicol. Appl. Pharmacol.* 132, 23-62 doi:10.1006/taap.1995.1086

Hussain, S.M., Hess, K.L., Gearhart, J.M., Geiss, K.T., Schlager, J.J., 2005. *In vitro* toxicity of nanoparticles in BRL 3A rat liver cells. *Toxicol. In Vitro* 19, 975–83. doi:10.1016/j.tiv.2005.06.034

IARC, 2006. Cobalt in hard metals and cobalt sulfate, gallium arsenide, indium phosphide and vanadium pentoxide. *IARC Monogr. Eval. Carcinog. risks to humans* 86, 1.

Inouye, L.S., Jones, R.P., Bednar, A.J., 2006. Tungsten effects on survival, growth, and reproduction in the earthworm, *Eisenia fetida*. *Env. Toxicol Chem* 25, 763–768. doi:10.1897/04-578R.1

ISO, I.O. for S.S.Q., 2014. Soil quality—Effects of contaminants on Enchytraeidae (*Enchytraeus* sp.)—Determination of effects on reproduction. ISO 16387.

Johnson, D.R., Ang, C., Bednar, A.J., Inouye, L.S., 2010. Tungsten effects on phosphate-dependent biochemical pathways are species and liver cell line dependent. *Toxicol. Sci.* 116, 523–532. doi:10.1093/toxsci/kfq124

Kennedy, A.J., Johnson, D.R., Seiter, J.M., Lindsay, J.H., Boyd, R.E., Bednar, A.J., Allison, P.G., 2012. Tungsten toxicity, bioaccumulation, and compartmentalization into organisms representing two trophic levels. *Environ. Sci. Technol.* 46, 9646–9652. doi:10.1021/es300606x

Kühnel, D., Busch, W., Meißner, T., Springer, A., Potthoff, A., Richter, V., Gelinsky, M., Scholz, S., Schirmer, K., 2009. Agglomeration of tungsten carbide nanoparticles in exposure medium does not prevent uptake and toxicity toward a rainbow trout gill cell line. *Aquat. Toxicol.* 93, 91–99. doi:10.1016/j.aquatox.2009.04.003

Lasfargues, G., Lison, D., Maldague, P., Lauwerys, R., 1992. Comparative study of the acute lung toxicity of pure cobalt powder and cobalt-tungsten carbide mixture in rat. *Toxicol. Appl. Pharmacol.* 112, 41–50. doi:10.1016/0041-008X(92)90277-Y

Lison, D., Carbonnelle, P., Mollo, L., Lauwerys, R., Fubini, B., 1995. Physicochemical mechanism of the interaction between cobalt metal and carbide particles to generate toxic activated oxygen species. *Chem. Res. Toxicol.* 8, 600–606.

Lison, D., Lauwerys, R., 1992. Study of the mechanism responsible for the elective toxicity of tungsten carbide-cobalt powder toward macrophages. *Toxicol. Lett.* 60, 203–210. doi:10.1016/0378-4274(92)90275-O

Lock, K., Becaus, S., Criel, P., Van Eeckhout, H., Janssen, C.R., 2004. Ecotoxicity of cobalt to the springtail *Folsomia candida*. *Comp. Biochem. Physiol. - C Toxicol. Pharmacol.* 139, 195–199. doi:10.1016/j.cca.2004.10.002

Lock, K., De Schampelaere, K.A.C., Becaus, S., Criel, P., Van Eeckhout, H., Janssen, C.R., 2006. Development and validation of an acute biotic ligand model (BLM) predicting cobalt toxicity in soil to the potworm *Enchytraeus albidus*. *Soil Biol. Biochem.* 38, 1924–1932. doi:10.1016/j.soilbio.2005.12.014

Lombaert, N., Boeck, M. De, Decordier, I., Cundari, E., Lison, D., Kirsch-Volders, M., 2004. Evaluation of the apoptogenic potential of hard metal dust (WC-Co), tungsten carbide and metallic cobalt. *Toxicol. Lett.* 154, 23–34. doi:10.1016/j.toxlet.2004.06.009

Lombaert, N., Castrucci, E., Decordier, I., Van Hummelen, P., Kirsch-Volders, M., Cundari, E., Lison, D., 2013. Hard-metal (WC-Co) particles trigger a signaling cascade involving p38 MAPK, HIF-1 α , HMOX1, and p53 activation in human PBMC. *Arch. Toxicol.* 87, 259–268. doi:10.1007/s00204-012-0943-y

Moorhouse, C.P., Halliwell, B., Grootveld, M., Gutteridge, J.M.C., 1985. Cobalt (II) ion as a promoter of hydroxyl radical and possible 'crypto-hydroxyl' radical formation under physiological conditions. Differential effects of hydroxyl radical scavengers. *Biochim. Biophys. Acta (BBA)-General Subj.* 843, 261–268.

Noordhoek, J.W., Verweij, R.A., van Gestel, C.A.M., van Straalen, N.M., Roelofs, D., 2018. No effect of selected engineered nanomaterials on reproduction and survival of the springtail *Folsomia candida*. *Environ. Sci. Nano.* doi:10.1039/C7EN00824D

OECD, 2012. Guidance on sample preparation and dosimetry for the safety testing of manufactured nanomaterials. Organization for Economic Co-Operation and Development, Paris, France

OECD, 2004a. Guidelines for the testing of chemicals No. 220. Enchytraeid Reproduction Test. Organization for Economic Co-Operation and Development, Paris, France.

OECD, 2004b. Test No. 202: *Daphnia* sp. Acute Immobilisation Test. Organization for Economic Co-Operation and Development, Paris, France Sect. 2 1–12. doi:10.1787/9789264069947-en

Paget, V., Moche, H., Kortulewski, T., Grall, R., Irbah, L., Nesslany, F., Chevillard, S., 2015. Human cell line-dependent WC-Co nanoparticle cytotoxicity and genotoxicity: A key role of ROS production. *Toxicol. Sci.* 143, 385–397. doi:10.1093/toxsci/kfu238

Prakash, L.J., 1995. Application of fine grained tungsten carbide based cemented carbides. *Int. J. Refract. Met. Hard Mater.* 13, 257–264. doi:10.1016/0263-4368(95)92672-7

Santos, F.C.F., Gomes, S.I.L., Scott-Fordsmand, J.J., Mónica J.B, V.F., 2017. Hazard assessment of nickel nanoparticles in soil – the use of a full life cycle test with *Enchytraeus crypticus*. *Environ. Toxicol. Chem.* doi:10.1002/etc.3853

Schrauzer, G., 1968. Organocobalt Chemistry of Vitamine B12 Model Compounds (Cobaloximes). *Acc. Chem. Res.* 1, 97–103. doi:10.1021/ar50004a001

Scott-Fordsmand, J.J., Weeks, J.M., Hopkin, S.P., 2000. Importance of contamination history for understanding toxicity of copper to earthworm *Eisenia fetida* (Oligochaeta: Annelida), using neutral-red retention assay. *Environ. Toxicol. Chem.* 19, 1774–1780. doi:10.1897/1551-5028(2000)019<1774:IOCHF>2.3.CO;2

Shan, D., Xie, Y., Ren, G., Yang, Z., 2013. Attenuated effect of tungsten carbide nanoparticles on voltage-gated sodium current of hippocampal CA1 pyramidal neurons. *Toxicol. Vitr.* 27, 299–304.

Shan, D., Xie, Y., Ren, G., Yang, Z., 2012. Inhibitory effect of tungsten carbide nanoparticles on voltage-gated potassium currents of hippocampal CA1 neurons. *Toxicol. Lett.* 209, 129–135. doi:10.1016/j.toxlet.2011.12.001

Sheppard, P.R., Speakman, R.J., Ridenour, G., Witten, M.L., 2007. Temporal Variability of Tungsten and Cobalt in Fallon , Nevada 115, 715–719. doi:10.1289/ehp.9451

SigmaPlot, 1997. Statistical Package for the Social Sciences, 11.0. Systat Software, Inc., Chicago, IL, USA.

Stefaniak, A.B., Virji, M.A., Day, G.A., 2009. Characterization of exposures among cemented tungsten carbide workers. Part I: Size-fractionated exposures to airborne cobalt and tungsten particles. *J. Expo. Sci. Environ. Epidemiol.* 19, 475.

Strigul, N., Galdun, C., Vaccari, L., Ryan, T., Braida, W., Christodoulatos, C., 2009. Influence of speciation on tungsten toxicity. *Desalination* 248, 869–879. doi:10.1016/j.desal.2009.01.016

Strigul, N., Koutsospyros, A., Christodoulatos, C., 2010. Tungsten speciation and toxicity: Acute toxicity of mono- and poly-tungstates to fish. *Ecotoxicol. Environ. Saf.* 73, 164–171. doi:10.1016/j.ecoenv.2009.08.016

Stutzenberger, F., 1974. Ribonucleotide reductase of *Pithomyces chartarum*: Requirement for B12 coenzyme. *Microbiology* 81, 501–503.

Westlake, W.J., 1973. Use of statistical methods in evaluation of *in vivo* performance of dosage forms. *J. Pharm. Sci.* 62, 1579–1589. doi:10.1002/jps.2600621002

Yao, Z., Stiglich, J.J., Sudarshan, T., 1998. Nanosized WC-Co holds promise for the future. *Met. Powder Rep.* 53, 26–33.

Yuan, Y., Hilliard, G., Ferguson, T., Millhorn, D.E., 2003. Cobalt inhibits the interaction between hypoxia-inducible factor- α and von Hippel-Lindau protein by direct binding to hypoxia-inducible factor- α . *J. Biol. Chem.* 278, 15911–15916. doi:10.1074/jbc.M300463200

Zhao, J., Bowman, L., Magaye, R., Leonard, S.S., Castranova, V., Ding, M., 2013. Apoptosis induced by tungsten carbide-cobalt nanoparticles in JB6 cells involves ROS generation through both extrinsic and intrinsic apoptosis pathways. *Int. J. Oncol.* 42, 1349–1359. doi:10.3892/ijo.2013.1828

Zou, W., Yan, M., Xu, W., Huo, H., Sun, L., Zheng, Z., Liu, X., 2001. Cobalt chloride induces PC12 cells apoptosis through reactive oxygen species and accompanied by AP-1 activation. *J. Neurosci. Res.* 64, 646–653. doi:10.1002/jnr.1118

SUPPORTING INFORMATION

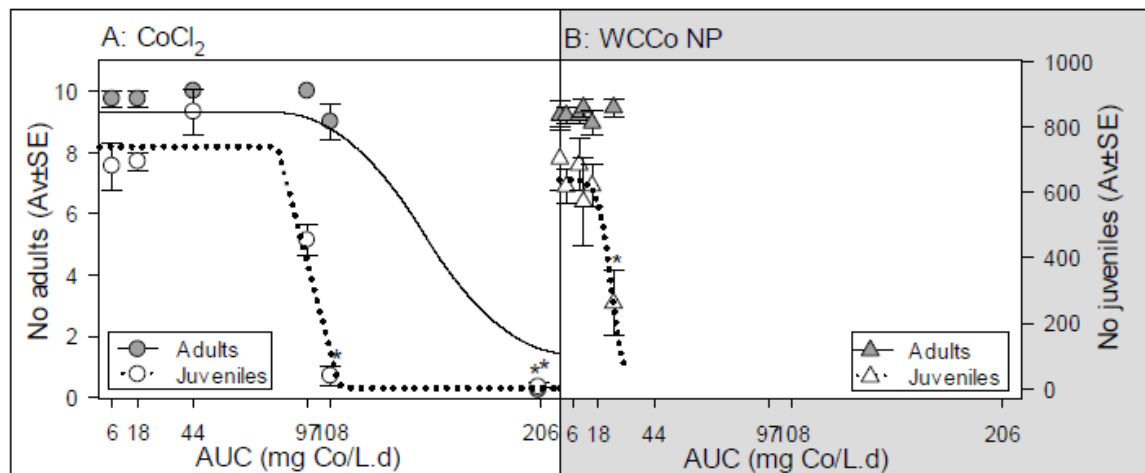


Figure S1: Survival and reproduction of *Enchytraeus crypticus* exposed in LUFA 2.2 soil to (A) CoCl_2 and (B) WCCo NP expressed as AUC - Area Under the Curve (values obtained from the area under the curve Measured Co in soil-water extract (mg Co/L) vs time (days)). Values are expressed as average \pm standard error (AV \pm SE). The lines represent the model fit to data. * $p < 0.05$, Dunnett's test.

To obtain a more complete measure of exposure in the soil water, the soil water concentration was cumulated over time. Accumulation over time was done by integrating the area under the curve (AUC) in Figure S1 i.e. 0-28 days [assuming a linear interpolation between the individual sampling times, i.e. the lines shown]. The AUC show that WCCo was 4-fold more toxic than CoCl_2 , when expressing both as Co concentrations.

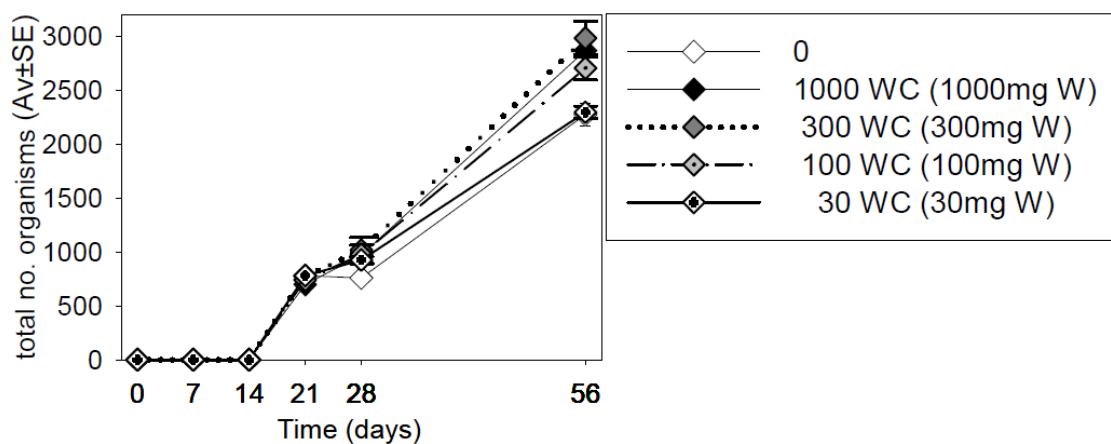


Figure S2: Results of the exposure monitoring of *Enchytraeus crypticus* in LUFA 2.2 soil in terms of total number of individuals at days 0, 7, 14, 21, 28 and 56 to 0-30-100-300-1000 mg W / kg soil DW. Values are expressed as average \pm standard error (AV \pm SE).

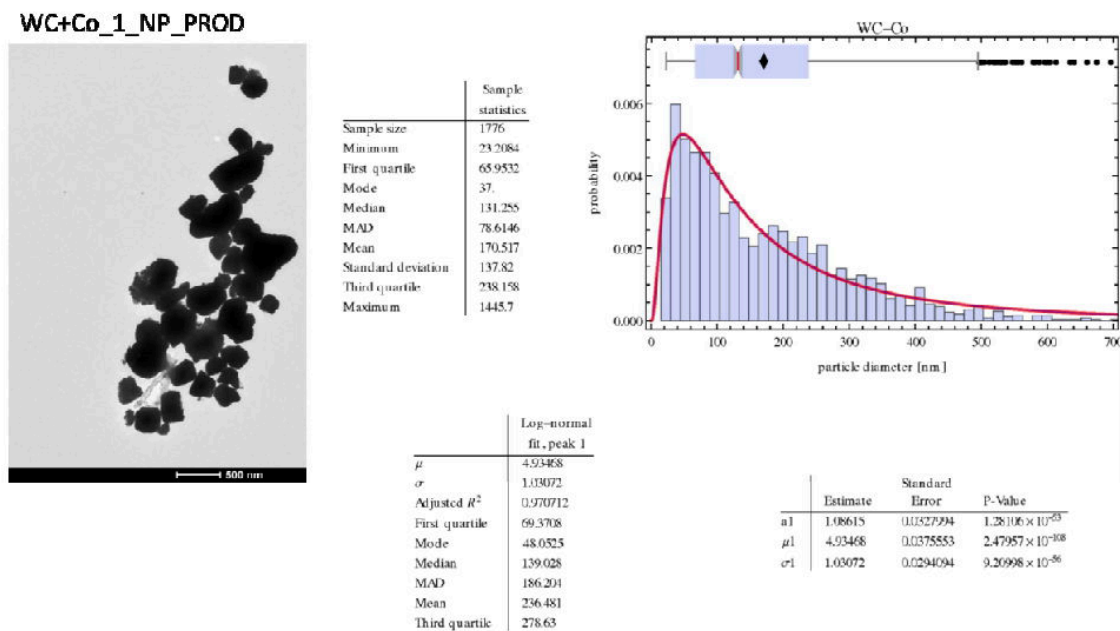


Figure S3: Representative TEM micrograph and measured particle size distributions for WCCo.

CHAPTER IV

**Multigenerational exposure to Cobalt (CoCl₂) and WCCo nanoparticles in
*Enchytraeus crypticus***

Maria J. Ribeiro¹, Janeck J. Scott-Fordsmand² and Mónica J.B. Amorim^{1*}

¹Department of Biology & CESAM (Centre for Environmental and Marine Studies), University of Aveiro, 3810-193 Aveiro, Portugal

²Department of Bioscience, Aarhus University, Vejlsvøvej 25, DK-8600 Silkeborg, Denmark

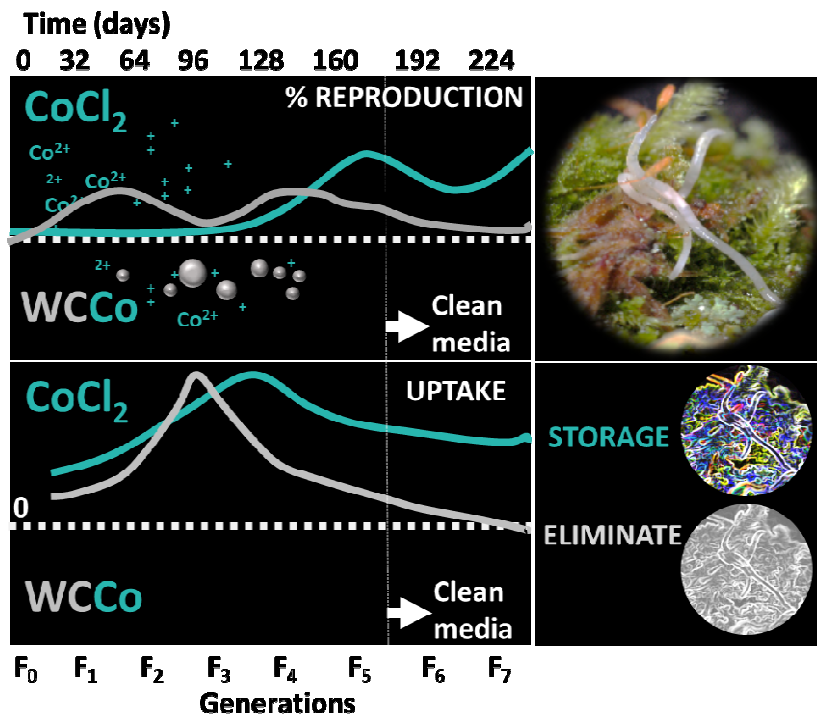
Submitted in Nanotoxicology (major revisions)

ABSTRACT

Cobalt and cobalt nanoparticles have many applications, e.g. in the hard metal industry and in tires. The assessment of long term effects is crucial, as these materials are persistent. For many organism groups, multigenerational (MG) exposure is a highly relevant scenario for persistent materials. In this study, the biological effect of CoCl_2 (salt) and Tungsten Carbide Cobalt nanoparticles (WCCo NPs) exposure was assessed in a MG test (4 generations in spiked + 2 generations in clean soil) using the OECD/ISO standard soil test species *Enchytraeus crypticus*. To ensure trans-generational survival, sub-lethal concentrations were used to assess the MG impact. Multigenerational exposure did not increase toxicity (survival, reproduction). There was an increase in reproduction at low concentrations of Co. Materials were characterised in the exposure media and the organisms in terms of Co content. Uptake of Co occurred from exposure to both CoCl_2 and WCCo, although without toxicity for WCCo. Cobalt from CoCl_2 exposure seemed to be stored, whereas for WCCo it was eliminated.

Keywords: Environmental toxicology, long-term exposure, transgenerational, uptake, terrestrial

TOC



INTRODUCTION

Cobalt (Co) and Co-based nanoparticles are used in the production of highly resistant alloys. For example, Tungsten Carbide Cobalt nanoparticles (WCCo NPs) are a class of cemented carbides used in various applications, e.g. in the hard metal industry (Yao et al., 1998), endowing the products with increased wear resistance (Upadhyaya, 1998). The release of WCCo NPs during production and wear and tear has been associated with pulmonary diseases and risk of cancer (Armstead and Li, 2016; Day et al., 2009; Stefaniak et al., 2009). *In vitro* studies have shown toxicity to be related to oxidative stress (Armstead et al., 2014; Liu et al., 2015) and other cellular effects, such as DNA damage (Paget et al., 2015) or apoptosis (Zhao et al., 2013). Results from *in vivo* exposures are limited, with some studies indicating no effect, e.g. no effect on survival and reproduction in the hard bodied soil invertebrate *Folsomia candida* (Collembola) exposed in one generation (soil concentrations up to 6400 mg WCCo NP/kg soil dryweight (DW)) (Noordhoek et al., 2018). Other studies show effect, e.g. in the soft bodied soil invertebrate *Enchytraeus crypticus*, where the reproduction EC50 was ca. 1600 mg WCCo NP/kg soil dry weight (DW) (Ribeiro et al., 2018). These studies mainly deal with standard exposure duration, i.e. according to OECD standards (21 days for Enchytraeids), but many organisms are exposed for multiple generations, mostly the species with short generation time or life cycle. This is an important, but less covered, aspect, in fact, among one of the challenges for the risk assessment of nanomaterials (NMs) is the implementation of realistic exposure scenarios (e.g. long term, low dose exposures) (Hu et al., 2016; van Gestel, 2012). To date, the only study covering multigenerational effects of NPs in soil organisms was performed using the model species *E. crypticus* exposed to CuO NPs and CuCl₂ (Bicho et al., 2017). Effects in reproduction differed between Cu forms, developing increased tolerance to CuCl₂ (with transgenerational toxicity) and increased effect with CuO NMs along generations. The toxicological mechanisms in a multigenerational exposure of persistent materials, such as many NMs, may involve physiological responses (acclimation), genetic change (adaptation) (Janssens et al., 2009) or epigenetics modifications (Mirbahai and Chipman, 2014). When such phenotypic changes occur, the tolerance can either have costs for the organism or be lost in the absence of the stressor (Marinković et al., 2012; Sun et al., 2014). Experimental MG designs should therefore include a transfer to clean media to assess transgenerational effects. For instance, in *Drosophila melanogaster* exposed to AgNPs, there was a recovery in fecundity over 10 generations, following an initial decrease in fecundity

(Panacek et al., 2011). As mentioned, transgenerational effects can occur when the organism is transferred to a stressor-free environment (Heard and Martienssen, 2014). The soil compartment is a sink where released NPs can accumulate, potentially affecting soil dwelling organisms (Cornelis et al., 2014). This highlights the importance of long term exposure testing and is a current gap for hazard prediction and risk assessment. Hence, we here studied the multigenerational exposure to WCCo NPs and CoCl₂ in *E. crypticus*, assessing survival and reproduction using a 4 + 2 design, i.e. 4 generations in spiked soil with a transfer to 2 generations into clean soil to evaluate recovery. Exposure media was characterized in terms of total and water extractable Co content and organisms for internal Co content in all generations.

MATERIALS AND METHODS

Test organisms

The test species *Enchytraeus crypticus* (Oligochaeta: Enchytraeidae) was used. Cultures had been kept for several years at the University of Aveiro. For details, please see Bicho et al. (2015). Synchronized cultures were prepared. Briefly, mature adults (well developed clitellum) were transferred to fresh agar plates to lay cocoons, being removed after 2 days. Synchronized juveniles with 17-19 days old were used.

Test soil

The standard LUFA 2.2 natural soil (Speyer, Germany) was used. Its main characteristics are presented in Table 1.

Table 1. Summary of the main characteristics of the test soil, including pH, organic carbon (OC), cation exchange capacity (CEC), maximum water holding capacity (maxWHC) and grain size distribution.

Soil	pH (0.01 M CaCl ₂)	OC (%)	CEC (meq/100g)	maxWHC (%)	Grain size distribution (mm)
LUFA 2.2	5.5	1.61	10.0	43.3	7.9 clay (<0.002) 16.3 silt (0.002-0.05) 75.8 sand (0.05-2.0)

Test materials and spiking

Nanostructured Tungsten Carbide Cobalt powder (WCCo NP) and cobalt chloride ($\text{CoCl}_2 \cdot 6\text{H}_2\text{O}$, 98% purity, Sigma-Aldrich) were used. Full characterisation was performed, for details see Table 2.

The test concentrations were 0-1200-1500 mg WCCo NPs/kg soil dry weight (DW) (0-100-120 mg Co/kg equivalent) and 0-110-180 mg Co/kg soil DW for CoCl_2 , selected among sub-lethal concentrations based on the reproduction EC10 and EC50 (Ribeiro et al., 2018).

WCCo NPs were directly mixed with the dried soil following the recommendation for dry powder non-dispersible nanomaterials (OECD, 2012). Moisture was adjusted to 50% of the maximum water holding capacity (maxWHC). The spiking of the soil was done per individual replicate to ensure total raw amounts per replicate. The test chemical CoCl_2 was prepared as stock aqueous solution, serially diluted and spiked onto the pre-moistened soil. The total amount of soil per concentration was homogeneously mixed and split onto replicates. Soil equilibrated for 1 day prior test start for both materials. Sampling of soil (and animals) was done to quantify Co at each sampling point and stored at -20°C until further analysis.

Exposure characterization

Cobalt concentration in soil and adult organisms was measured using Atomic Absorption Spectrometer (AAS, Perkin Elmer 4100, Ueberlingen, Germany). For the total Co in soil, the soil (1 g dry weight) was digested using 65% HNO_3 and heated up to 120°C until all brown fumes disappeared (Scott-Fordsmand et al., 2000).

For the bioavailable Co in soil, the soil:water extract was used, this being the supernatant of a (1:5) soil:water solution, mixed for 5 min at 250 rpm (lab shaker) and then let settle for 2h. One mL of the solution was digested following the same procedure as used for soil.

The exposed organisms were dried at 80°C and weighed. The digestion followed the same procedure. A biological standard reference sample (standard lobster tissue TORT-1, Marine Analytical Chemistry Standards Program, Division of Chemistry, National Research Council Canada) and a soil standard reference sample (Loam soil C74-06, Laboratory of the Government Chemist, United Kingdom) were used.

Test procedures

The standard guideline (ISO, 2014; OECD, 2016) was followed, with some adaptations as described in Bicho et al. (2017). Briefly, forty (40) juveniles (17-18 days' synchronized age) per replicate were used. Organisms were collected and introduced in the test vessels containing 40 g of moist soil and food supply. For each generation, the tests ran for a period of 32 days at 20 °C and 16:8 h photoperiod. In total, six generations were exposed to CoCl₂ and seven to WCCo NPs, hence, the total test duration was 224 (CoCl₂) and 256 (WCCo NPs) days, corresponding to 4 + 2 and 5 + 2 generations (spiked soil + clean soil) [5+2 was a technical error since the aim was 4+2]. Food and water were replenished weekly. Six replicates per treatment were used, except for the higher concentration, where 10 replicates were used to ensure enough numbers of organisms for next generation exposure and analysis. At the end of each generation, deionized water was added to each replicate and soil was left to deposit for 20 min; after this, organisms (adults and juveniles) were carefully transferred to freshly made reconstituted ISO water (OECD, 2004a) for depuration and stored after 1 day. From each replicate, adults (n = 20) and juveniles of large and medium size (n = 400) were sampled, snap-frozen in liquid nitrogen, and kept at -80 °C for further analysis. Juveniles of medium size (n = 40) were collected and transferred to freshly spiked or non-spiked soil for another generation and so forth. The replicates were fixated with 96 % ethanol and Bengal red (1 % solution in ethanol), and the organisms were sieved through 3 size meshes (0.6, 0.2, 0.1 mm) to separate organisms from most of the soil, providing three rough size classes: between 0.1 and 0.2 mm as small, between 0.2 and 0.6 as medium and larger than 0.6 as large. Counting was performed using a stereo microscope.

Data analysis

One-way analysis of variance (ANOVA) followed by Dunnett's comparison post-hoc test ($p \leq 0.05$) were used to assess differences between the control and the treatments in each generation, and for differences between F0 and Fx (SigmaPlot, 1997).

RESULTS

Exposure Characterization

Characterisation of the pristine materials, i.e. as synthesized, was performed using a suite of techniques for various aspects, for details please see Table 2.

Table 2: Characterisation of WCCo NPs (Source: FP7 SUN: Sustainable Nanotechnologies). TEM: Transmission Electron Microscope; XRD: X-Ray Diffraction; DLS: Dynamic Light Scattering; BET: Brunauer, Emmett and Teller; ELS: Electrophoretic Light Scattering; FTIR: Fourier-Transform Infrared Spectroscopy; XPS: X-ray Photoelectron Spectroscopy.

Characteristics	WCCo NP	Technique
Source	NBM Nanomaterialia, Italy	
Composition (%)	Tungsten carbide (WC<88% Wt., CAS 12070-12-1) Cobalt (Co=8.32% Wt., CAS 744-48-4)	ICP -MS
Primary Size distribution [nm] Average (Min-Max) Mode [nm] (1 st and 3 rd quartile)	170 (23-1446) 48 (69; 280)	TEM
Crystalline size (Average) [nm]	15.4	XRD
Iso Electric Point (pH)	<2	pH
Dispersability in water: D50 [nm]; Average Agglomeration Number (AAN)	182.8 ± 21.5; 31	DLS
Specific Surface Area [m ² .g ⁻¹]	6.6±0.4	BET
Z-potential [mV]	7.1±0.5	ELS
Structure	O-W-O	FTIR and/or RAMAN
Pore size [nm]	Non-porous	BET
Surface Chemistry [atomic fraction]	Co=0.08±0.01 W=0.05±0.01 O=0.31±0.03 C=0.56±0.05	XPS

The total Co measured in the soil showed good recovery between nominal and measured concentrations, this being ca. 110 ± 8% and 114 ± 4% of the nominal total added concentration for CoCl₂ and WCCo, respectively. There was no significant variation

between day 0 and 32 of each generation cycle. Soil:water extract Co measurements (fig. 1) showed Co solubilization shortly after spiking (first 3 days) with increase of Co ions in soil solution, followed by a stabilization and decrease. For similar added concentrations, there was more Co in soil solution for CoCl_2 .

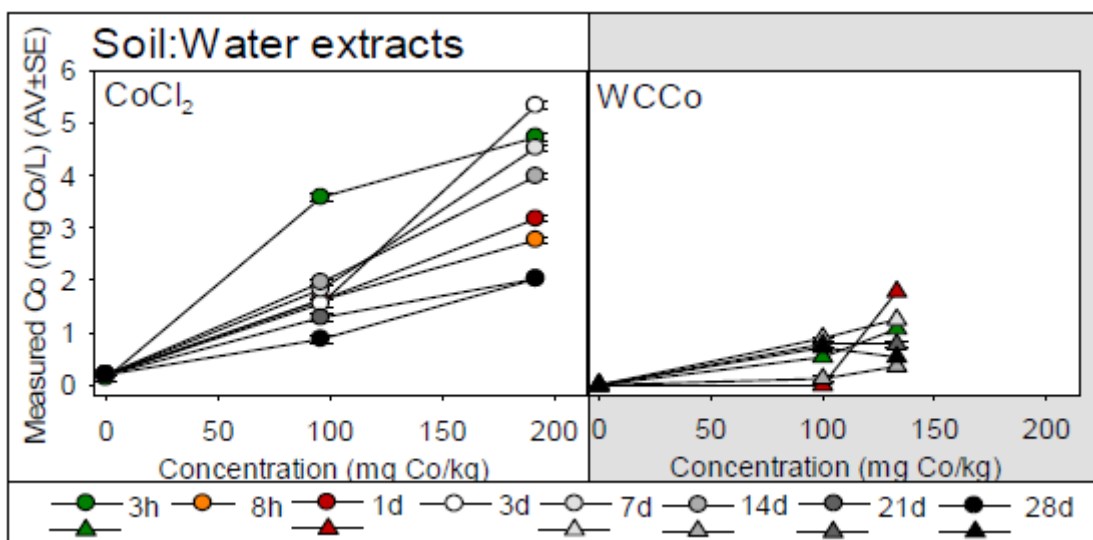


Figure 1: Total Cobalt in soil solution, obtained from the enchytraeid reproduction test experiment performed in LUFA 2.2 soil spiked with CoCl_2 (0-96-192 mg Co/kg soil DW) and WCCo NP (0-1200-1600 mg WCCo/kg soil DW) at sample days 0, 1, 7, 14, 21 and 28 days, with additional time points for CoCl_2 : 0.13 (8 hours) and 3 days. Values are expressed as average \pm standard error (AV \pm SE). Adapted from Ribeiro et al. (2018).

Effect characterisation

The validity criteria were fulfilled (for the comparable F0-F1 generation) according to the OECD 220 guideline (OECD, 2004b), i.e. for juveniles the coefficient of variation was < 20 %, the number of juveniles was ≥ 50 and adult mortality was ≤ 20 %. For CoCl_2 , the pH was ca. 6 and for WCCo ca. 6.3. Variation between test start and test end was below ± 0.3 for both materials.

Multigenerational effects of WCCo NP and CoCl_2 on survival and reproduction in *Enchytraeus crypticus* are depicted in figure 2.

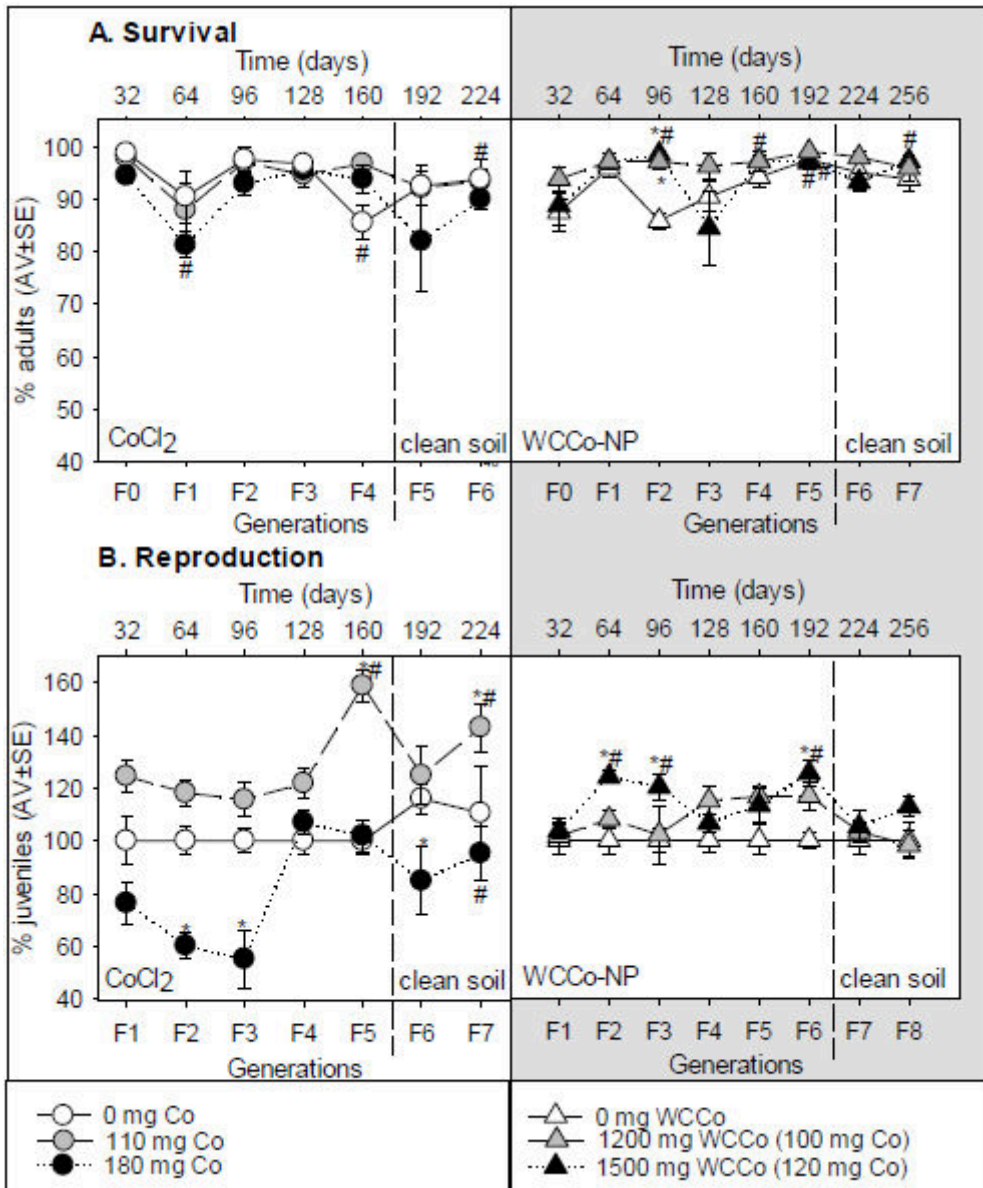


Figure 2: Multigenerational effects of WCCo NP (0-1200-1500 mg WCCo NP/kg, 0-100-120 mg Co/kg soil DW equivalent) and CoCl₂ (0-110-180 mg Co NP/kg soil DW) in *Enchytraeus crypticus* in terms of survival (A) and reproduction (B), in LUFA 2.2 soil. Values are expressed as % normalized to the control average ± standard error (AV±SE). *: p < 0.05 (between control and treatment); #: p < 0.05 (between F0 and Fx).

Adult survival was affected within the normal expected variation (<20%) for both test materials and was similar to controls. For CoCl₂, reproduction was affected negatively by 180 mg Co/kg soil DW from F1-F3, after which it increased to values similar to control. Exposure to 110 mg Co/kg soil DW caused an improvement in reproduction compared to control, significantly higher in F5.

For MG exposure to WCCo, reproduction was higher compared to control with both tested concentrations, also after transfer to clean soil.

Data in terms of size ranges (Fig. 3) seems to show a skewed distribution with relatively more large (and medium) than small organisms. In terms of Co effects, e.g. for CoCl_2 , 110 mg Co/kg exposure in F3, F4 and F7, there was tendency towards relatively more organisms of medium size compared to small and large. For WCCo, a similar impact occurred for 120 mg Co/kg exposure in F2, F3 and F5.

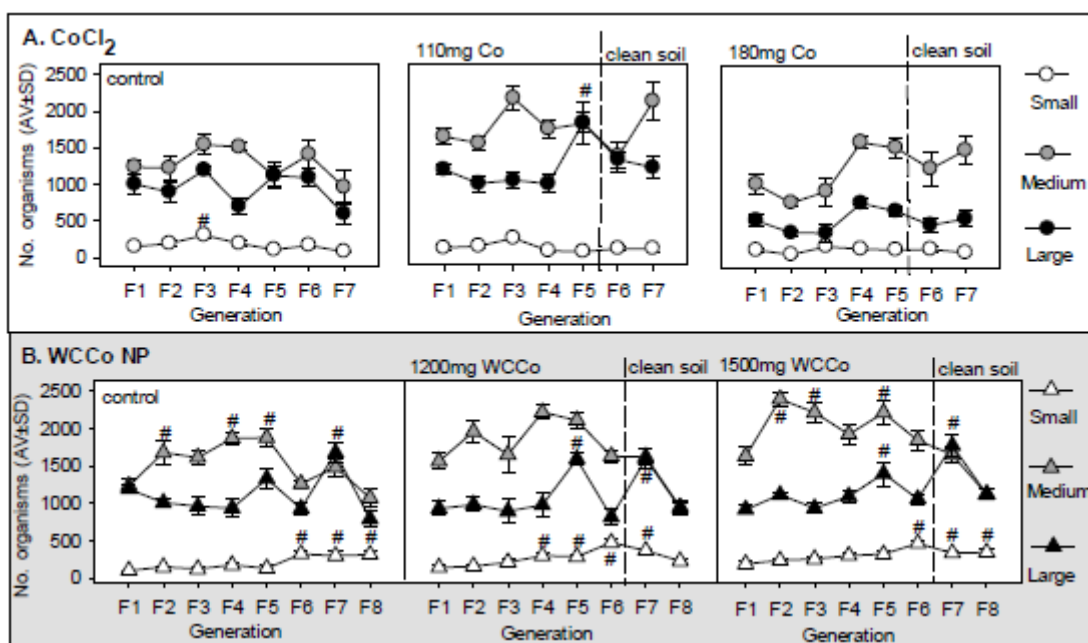


Figure 3: Multigenerational effects of WCCo NP (0-1200-1500 mg WCCo NP/kg, 0-100-120 mg Co/kg soil DW equivalent) and CoCl_2 (0-110-180 mg Co NP/kg soil DW) in *Enchytraeus crypticus* in terms of size: Small ≤ 0.1 mm; $0.1 \leq$ Medium ≤ 0.2 mm; $0.2 \leq$ Large ≤ 0.6 mm. Values are expressed as average \pm standard error (AV \pm SE). #: $p < 0.05$ (between F0 and Fx).

Internal Co body burdens in *E. crypticus*, as measured in all generations (fig. 4), showed that exposure to higher concentration had corresponding higher uptake. For CoCl_2 , Co levels were maintained throughout the MG exposure, although there was an increase of uptake to the lower concentration and a peak at F3 for 180 mg Co/kg soil. Transfer to clean soil for 2 generations did not decrease the prior levels. For WCCo, the Co uptake was relatively lower than for the similar CoCl_2 exposure. For WCCo, a major difference in the pattern was observed for the highest concentration (120 mg Co/kg soil equivalent, of

WCCo), where an increase occurred from F0 to F1-F2, after which there was a continuous decrease and complete elimination after transfer to clean media. MG exposure to ca. 100 mg Co/kg soil (of WCCo) caused a smaller increase followed by a decrease from F3 onwards.

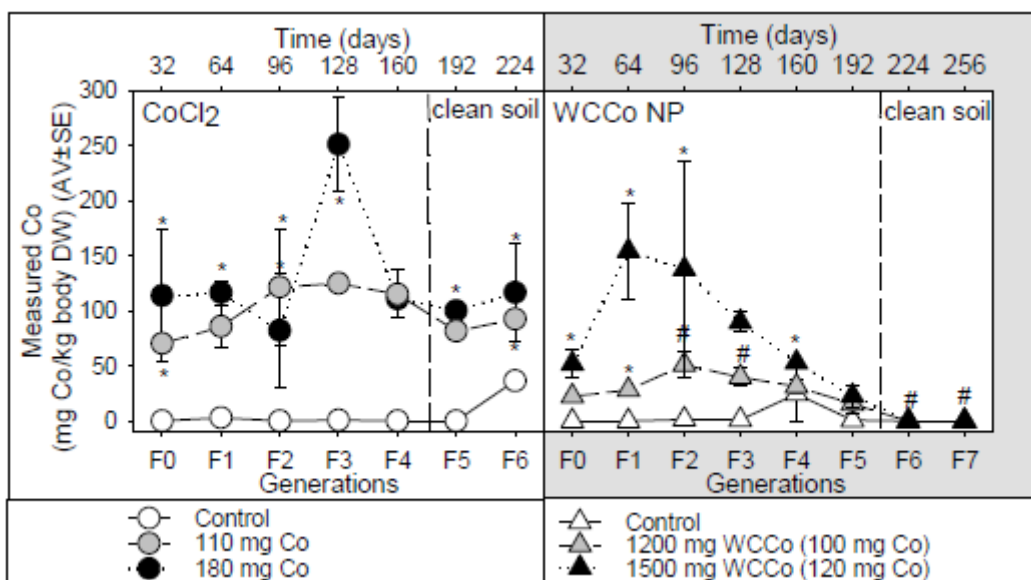


Figure 4: Cobalt quantification in *Enchytraeus crypticus* adults of each multigenerational exposure to CoCl₂ (0-110-180 mg/kg soil DW) and WCCo NP (0-1200-1500 mg WCCo/kg soil DW, 0-100-120 mg Co/kg soil equivalent). Values are expressed as average ± standard error (AV±SE). *: p < 0.05 (between control and treatment, (one-way ANOVA and Dunnett's post-hoc test); #: p < 0.05 (between F0 and Fx).

DISCUSSION

Multigenerational exposure to sub-lethal concentrations of CoCl₂ and WCCo NP did not affect long-term survival, which was not surprising since the dose was sub-lethal. On the other hand, the result could have been a cumulative effect along generations and multiple exposures.

Results from exposure to the estimated reproduction EC50 for CoCl₂ were in agreement with previous results, but for WCCo the EC50 showed lower effect than predicted (Ribeiro et al., 2018). The tested concentration (1600 mg WCCo/kg soil DW) caused ca. 50% reduction in the reproduction, whereas the concentration tested in this study (1500 mg WCCo/kg soil DW), i.e. 100 mg/kg lower, caused no impact on reproduction. This could be the reason that the shift between no effect and effect occurs between this

concentration range. Exposure was confirmed via the organisms' body burdens, as well the soil measurements and the increase between low to higher concentration in the soil. For CoCl_2 , for the exposure to 180 mg Co/kg soil DW the reproduction was negatively affected until F3, after which there was a recovery and organisms increased their reproduction to values similar to control levels. This is similar to what has been seen in multigenerational exposure to other nanoparticles, i.e. initial toxicity followed by the development of tolerance e.g. for *Caenorhabditis. elegans* to quantum dots (Contreras et al., 2013) and for *Drosophila melanogaster* to AgNPs (Panacek et al., 2011). Other studies showed no tolerance, e.g. for CuO NMs in *E. crypticus* (Bicho et al., 2017), TiO_2 NPs in *D. magna* (Jacobasch et al., 2014) or AuNPs in *C. elegans* (Moon et al., 2017). Since a peak in Co uptake was measured in F3 organisms (ca. 250 mg/kg body DW), this suggests that the higher accumulation triggered the activation of a Co detoxification response mechanism which then remained activated in the subsequent generations. The size data indicated a shift to a relatively higher number of medium and large size organisms (compared to small). Although this is a well-known population survival strategy, the detoxification mechanism did not seem related to changes in energy allocation between growth and reproduction (Calow, 1991). Further, the detoxification must have involved internal Co immobilization (and not its elimination) because Co body burdens showed that the internal Co concentration remained around 120 mg/kg body DW throughout the test, including when transferred to clean media. Detoxifying strategies, such as Co storage in metal-sequestering organelles of oligochaetes immune cells (chloragocytes) (Morgan et al., 2002), have been reported. For the 110 mg Co/kg soil exposure, there was a continuous higher reproductive output compared to the control, indicating a hormetic effect either through slight intoxication or because the organisms benefited from a slightly higher Co availability. The transfer of Co to generations in clean media seems rather peculiar, but may relate to an altered homeostatic requirement. Cobalt is known to be an essential element, e.g. as part of vitamin B12 and with a role in various biochemical reactions, hence, organisms have conserved mechanisms and biological reactions involving Co.

In contrast to what happened for the highest concentration CoCl_2 , but similar to the 110 mg Co/Kg exposure, the exposure to WCCo NPs caused an improvement in reproduction that was relatively stable throughout the generations. The Co body burdens showed that Co internal concentration increased from F0 to F2, up to ca. 150 mg Co/kg body DW, i.e. up to values of internal Co that caused 50% decrease reproduction in exposure to CoCl_2 . Hence, Co uptake did not seem to cause population effects. Soil water extract analysis

showed that there was comparatively more Co in soil solution for the CoCl₂ exposure than for WCCo NPs spiked soils at similar concentrations. Hence, internalized Co may come from different soil fractions, depending on whether it is CoCl₂ or WCCo, e.g. for CoCl₂ the uptake is from the soil solution, whereas for the NPs the Co maybe attached to the soil particles and ingested (either as attached ions or as attached NPs). In any case, even though *E. crypticus* was exposed to similar Co concentrations and had internalized Co, they appear to have a highly effective detoxifying mechanism towards WCCo that prevented Co to accumulate in the body along generations.

Although not analyzed, no typical epigenetic effect patterns were observed, i.e. toxicity in exposed generations being transferred to non-exposed generations (Heard and Martienssen, 2014). This was suggested to be the case e.g. for *Caenorhabditis elegans* MG exposure to silver (Schultz et al., 2016), although this was not confirmed. Enchytraeids have ca. 1.4% global methylation (Noordhoek et al., 2017) and, hence, this could be one of the epigenetics mechanisms.

CONCLUSIONS

Uptake of Co occurred from exposure to both CoCl₂ and WCCo, although without toxicity (reproduction decrease) for WCCo despite similar Co internal levels. Cobalt from CoCl₂ exposure must be stored, and possibly there is a higher physiological requirement induced, whereas for WCCo it was eliminated over generations and following transfer to clean media. The increase in reproduction with Co low doses shows evidence of the essentiality of the element. Multigenerational exposure to these sub-lethal concentrations did not increase toxicity (survival, reproduction), although we cannot exclude effects from other physiological endpoints.

ACKNOWLEDGEMENTS

This study was supported by funds of the European Commission Project: SUN SUstainable Nanotechnologies (FP7-NMP-2013-LARGE-7 No. 604305). Further support within CESAM (UID/AMB/50017-POCI-01-0145-FEDER-007638) via FCT/MCTES through national funds (PIDDAC) and the co-funding by the FEDER, within the PT2020 Partnership Agreement and Compete 2020), and by national funding through FCT-Fundação para a Ciência e Tecnologia via the individual PhD grant to Maria J. Ribeiro

(SFRH/BD/95027/2013). The authors acknowledge the laboratorial help provided by R. Bicho and V. Maria.

REFERENCES

Armstead, A.L., Arena, C.B., Li, B., 2014. Exploring the potential role of tungsten carbide cobalt (WC-Co) nanoparticle internalization in observed toxicity toward lung epithelial cells *in vitro*. *Toxicol. Appl. Pharmacol.* 278, 1–8. doi:10.1016/j.taap.2014.04.008

Armstead, A.L., Li, B., 2016. Nanotoxicity: Emerging concerns regarding nanomaterial safety and occupational hard metal (WC-Co) nanoparticle exposure. *Int. J. Nanomedicine* 11, 6421–6433. doi:10.2147/IJN.S121238

Bicho, R.C., Santos, F.C.F., Gonçalves, M.F.M., Soares, A.M.V.M., Amorim, M.J.B., 2015. Enchytraeid Reproduction TestPLUS: hatching, growth and full life cycle test-an optional multi-endpoint test with *Enchytraeus crypticus*. *Ecotoxicology* 24, 1053–1063. doi:10.1007/s10646-015-1445-5

Bicho, R.C., Santos, F.C.F., Scott-Fordsmand, J.J., Amorim, M.J.B., 2017. Multigenerational effects of copper nanomaterials (CuONMs) are different of those of CuCl₂: exposure in the soil invertebrate *Enchytraeus crypticus*. *Sci. Rep.* 7, 8457. doi:10.1038/s41598-017-08911-0

Calow, P., 1991. Physiological costs of combating chemical toxicants: Ecological implications. *Comp. Biochem. Physiol. Part C Comp. Pharmacol.* 100, 3–6. doi:http://dx.doi.org/10.1016/0742-8413(91)90110-F

Contreras, E.Q., Cho, M., Zhu, H., Puppala, H.L., Escalera, G., Zhong, W., Colvin, V.L., 2013. Toxicity of quantum dots and cadmium salt to *Caenorhabditis elegans* after multigenerational exposure. *Environ. Sci. Technol.* 47, 1148–1154. doi:10.1021/es3036785

Cornelis, G., Hund-Rinke, K., Kuhlbusch, T., van den Brink, N., Nickel, C., 2014. Fate and Bioavailability of Engineered Nanoparticles in Soils: A Review. *Crit. Rev. Environ. Sci. Technol.* 44, 2720–2764. doi:10.1080/10643389.2013.829767

Day, G. a, Virji, M.A., Stefaniak, A.B., 2009. Characterization of exposures among cemented tungsten carbide workers. Part II: Assessment of surface contamination and skin exposures to cobalt, chromium and nickel. *J. Expo. Sci. Environ. Epidemiol.* 19, 423–34. doi:10.1038/jes.2008.33

Heard, E., Martienssen, R.A., 2014. Transgenerational epigenetic inheritance: Myths and mechanisms. *Cell* 157, 95–109. doi:10.1016/j.cell.2014.02.045

Hu, X., Li, D., Gao, Y., Mu, L., Zhou, Q., 2016. Knowledge gaps between nanotoxicological research and nanomaterial safety. *Environ. Int.* 94, 8–23. doi:10.1016/j.envint.2016.05.001

ISO, I.O. for S.S.Q., 2014. Soil quality—Effects of contaminants on Enchytraeidae (Enchytraeus sp.)—Determination of effects on reproduction. ISO 16387.

Jacobasch, C., Völker, C., Giebner, S., Völker, J., Alsenz, H., Potouridis, T., Heidenreich, H., Kayser, G., Oehlmann, J., Oetken, M., 2014. Long-term effects of nanoscaled titanium dioxide on the cladoceran *Daphnia magna* over six generations. *Environ. Pollut.* 186, 180–186. doi:10.1016/j.envpol.2013.12.008

Janssens, T.K.S., Roelofs, D., Van Straalen, N.M., 2009. Molecular mechanisms of heavy metal tolerance and evolution in invertebrates. *Insect Sci.* 16, 3–18. doi:10.1111/j.1744-7917.2009.00249.x

Liu, L.Z., Ding, M., Zheng, J.Z., Zhu, Y., Fenderson, B.A., Li, B., Yu, J.J., Jiang, B.H., 2015. Tungsten Carbide-Cobalt Nanoparticles Induce Reactive Oxygen Species, AKT, ERK, AP-1, NF-κB, VEGF, and Angiogenesis. *Biol. Trace Elem. Res.* 166, 57–65. doi:10.1007/s12011-015-0331-6

Marinković, M., de Bruijn, K., Asselman, M., Bogaert, M., Jonker, M.J., Kraak, M.H.S., Admiraal, W., 2012. Response of the nonbiting midge *Chironomus riparius* to multigeneration toxicant exposure. *Environ. Sci. Technol.* 46, 12105–12111.

Mirbahai, L., Chipman, J.K., 2014. Epigenetic memory of environmental organisms: A reflection of lifetime stressor exposures. *Mutat. Res. - Genet. Toxicol. Environ. Mutagen.* 764–765, 10–17. doi:10.1016/j.mrgentox.2013.10.003

Moon, J., Kwak, J. II, Kim, S.W., An, Y.-J., 2017. Multigenerational effects of gold nanoparticles in *Caenorhabditis elegans*: Continuous versus intermittent exposures. *Environ. Pollut.* 220, 46–52. doi:10.1016/j.envpol.2016.09.021

Morgan, a. J., Turner, M.P., Morgan, J.E., 2002. Morphological plasticity in metal-sequestering earthworm chloragocytes: morphometric electron microscopy provides a biomarker. of exposure in field populations. *Environ. Toxicol. Chem.* 21, 610–618. doi:Doi 10.1897/1551-5028(2002)021<0610:Mpimse>2.0.Co;2

Noordhoek, J.W., Koning, J.T., Mariën, J., Kamstra, J.H., Amorim, M.J.B., van Gestel, C.A.M., van Straalen, N.M., Roelofs, D., 2017. Exploring DNA methylation patterns in copper exposed *Folsomia candida* and *Enchytraeus crypticus*. *Pedobiologia (Jena)*.

Noordhoek, J.W., Verweij, R.A., van Gestel, C.A.M., van Straalen, N.M., Roelofs, D., 2018. No effect of selected engineered nanomaterials on reproduction and survival of the springtail *Folsomia candida*. *Environ. Sci. Nano.* doi:10.1039/C7EN00824D

OECD, 2016. Test No. 220: Enchytraeid Reproduction Test / Organisation for Economic Co-operation and Development, OECD Guidelines for the Testing of Chemicals, Section 2,. Paris: OECD Publishing.

OECD, 2012. Guidance on sample preparation and dosimetry for the safety testing of manufactured nanomaterials. Organization for Economic Co-Operation and Development, Paris, France

OECD, 2004a. Test No. 202: Daphnia sp. Acute Immobilisation Test. Organization for Economic Co-Operation and Development, Paris, France. Sect. 2 1–12. doi:10.1787/9789264069947-en

Paget, V., Moche, H., Kortulewski, T., Grall, R., Irbah, L., Nesslany, F., Chevillard, S., 2015. Human cell line-dependent WC-Co nanoparticle cytotoxicity and genotoxicity: A key role of ROS production. *Toxicol. Sci.* 143, 385–397. doi:10.1093/toxsci/kfu238

Panacek, A., Pucek, R., Safarova, D., Dittrich, M., Richtrova, J., Benickova, K., Zboril, R., Kvitek, L., 2011. Acute and chronic toxicity effects of silver nanoparticles (NPs) on *Drosophila melanogaster*. *Environ. Sci. Technol.* 45, 4974–4979. doi:10.1021/es104216b

Ribeiro, M.J., Maria, V.L., Amorim, M.J.B., Scott-Fordsmand, J.J., 2018. Fate and effect of nano Tungsten Carbide Cobalt (WCCo) in the soil environment – observing a nanoparticle specific toxicity in *Enchytraeus crypticus*. *Environ. Sci. Technol.* 52, 11394–11401. doi: 10.1021/acs.est.8b02537

Schultz, C.L., Wamucho, A., Tsyusko, O. V., Unrine, J.M., Crossley, A., Svendsen, C., Spurgeon, D.J., 2016. Multigenerational exposure to silver ions and silver nanoparticles reveals heightened sensitivity and epigenetic memory in *Caenorhabditis elegans*. *Proc. R. Soc. B Biol. Sci.* 283, 20152911. doi:10.1098/rspb.2015.2911

Scott-Fordsmand, J.J., Weeks, J.M., Hopkin, S.P., 2000. Importance of contamination history for understanding toxicity of copper to earthworm *Eisenia fetida* (Oligochaeta: Annelida), using neutral-red retention assay. *Environ. Toxicol. Chem.* 19, 1774–1780. doi:10.1897/1551-5028(2000)019<1774:IOCHF>2.3.CO;2

SigmaPlot, 1997. Statistical Package for the Social Sciences, 11.0. Systat Software, Inc., Chicago, IL, USA.

Stefaniak, A.B., Virji, M.A., Day, G.A., 2009. Characterization of exposures among cemented tungsten carbide workers. Part I: Size-fractionated exposures to airborne cobalt and tungsten particles. *J. Expo. Sci. Environ. Epidemiol.* 19, 475.

Sun, P.Y., Foley, H.B., Handschumacher, L., Suzuki, A., Karamanukyan, T., Edmands, S., 2014. Acclimation and adaptation to common marine pollutants in the copepod *Tigriopus californicus*. *Chemosphere* 112, 465–471. doi:10.1016/j.chemosphere.2014.05.023

Upadhyaya, G.S., 1998. Cemented tungsten carbides: production, properties and testing. William Andrew.

van Gestel, C.A.M., 2012. Soil ecotoxicology: State of the art and future directions. Zookeys 176, 275–296. doi:10.3897/zookeys.176.2275

Yao, Z., Stiglich, J.J., Sudarshan, T., 1998. Nanosized WC-Co holds promise for the future. Met. Powder Rep. 53, 26–33.

Zhao, J., Bowman, L., Magaye, R., Leonard, S.S., Castranova, V., Ding, M., 2013. Apoptosis induced by tungsten carbide-cobalt nanoparticles in JB6 cells involves ROS generation through both extrinsic and intrinsic apoptosis pathways. Int. J. Oncol. 42, 1349–1359. doi:10.3892/ijo.2013.1828

CHAPTER V

Cell *in vitro* testing with soil invertebrates - challenges and opportunities to model the effect of nanomaterials – CuO surface modified case study

Maria J. Ribeiro¹, Mónica JB Amorim^{a*}, Janeck J Scott-Fordsmand^b

¹Department of Biology & CESAM (Centre for Environmental and Marine Studies), University of Aveiro, 3810-193 Aveiro, Portugal

²Department of Bioscience, Aarhus University, Vejlsøvej 25, DK-8600 Silkeborg, Denmark.

Submitted

ABSTRACT

Soil invertebrates (*in vivo*) have been widely used in ecotoxicology studies for decades, although their use as *in vitro* models, albeit promising, has not been pursued as much. The immune cells of earthworms (coelomocytes) and the coelomic fluid can be used and are a highly relevant *in vitro* system. Although it has been tested before, to cover the testing of nanomaterials (NMs) several challenges should be considered. NMs characteristics (dispersibility, agglomeration, etc.) can interfere with the common *in vitro* methodologies, not only during exposure, but also during the measurements. We have here assessed the effect of the CuO NMs case study, using surface modified particles, functionalized for safe-by-design strategies with ascorbate, citrate, polyethylenimine and polyvinylpyrrolidone, plus the pristine CuO NMs and copper chloride (CuCl₂) for comparison. *Eisenia fetida*'s coelomocytes were exposed for 24h via the coelomic fluid. Changes in cell viability were evaluated using flow cytometry, with 7-aminoactinomycin D (7-AAD) and propidium iodide (PI) dyes. CuCl₂ affected cell viability in a dose-related manner, although only observed with PI. No mortality was observed for any of the CuO NMs. Test materials interfere with the cell count characterization (e.g. it was not possible to discriminate between amoebocytes and eleocytes due to overlap with test materials), hence, effects can be underestimated. This preliminary screening showed the potential usage of the standard earthworm model as an *in vitro* standard. Further detailed *in vitro* studies are needed using other NMs towards the implementation and standardization. Additional cell endpoints can be assessed making it a high content tool for mechanistic understanding.

Keywords: earthworms; flow cytometry; coelomocytes; surface modification; safe by design; copper oxide nanoparticles

INTRODUCTION

Nanomaterials (NMs) display distinct physical-chemical properties with added value and have been increasingly used in a wide variety of fields (Liu, 2006; Pankhurst et al., 2003). The potential environmental risks of engineered NMs are still not fully clear, although research in nanotoxicology has developed significantly during recent decades. The current risk assessment (RA) framework for NMs still follows most of the standards previously established for conventional chemicals. It has been long argued that these

require adaptations that can reflect worst case scenarios for NMs (Kroll et al., 2009; Tiede et al., 2009). The dual nature of NMs, being a particle with physical properties and also a chemical, makes it difficult to relate observed toxicity and its cause and, hence, the associated risks. For instance, it is not always clear how many of the ions released from metal-based NMs are the source of toxicity and how much the NMs contribute and have a specific role themselves (Beer et al., 2012; Gomes et al., 2015). Often, researchers attempt to estimate the release by measuring the ion concentration in order to differentiate between chemical (ions) and particulate toxicity. However, the actual release and even the part that causes toxicity is this often very difficult to measure (Gomes et al., 2015). To get a better handle on some of the toxicity issues, a favorable approach would be to have a diverse biological set of methods, each highlighting certain topics. One approach is *in vitro* testing, which often is faster and more cost-effective than *in vivo* testing: *in vitro* further allows for simultaneous screening of different parameters by focusing on the individual cell pathways of toxicity (Niles et al., 2009). The majority of *in vitro* studies deal with cells from bacteria, fish, human or mouse-derived cellular models, and do not cover several other key organism groups. For instance, few studies deal with key terrestrial invertebrates, although they in the bigger cases are excellent candidates for *in vitro* testing (Hayashi et al. 2013). Many biological processes are conserved across mammals and invertebrates, e.g. the primary immune system, which also supports the use of invertebrates as surrogates for cross-species extrapolation to humans (Cooper and Roch, 2003; Lagadic and Caquet, 1998). Further, the fact that these are invertebrates, hence a 3R complying alternative model, makes them an even more important option.

Although few studies, earthworms have been shown useful in *in vitro* models. For example *via* exposure to Ag NMs, (Hayashi et al., 2012) illustrated that during *in vitro* exposure the biological response of *Eisenia fetida*'s coelomocytes was similar to that of human acute monocytic leukemia cell line cells (THP-1) in RPMI-1640 medium. They observed that the cytotoxicity (WST-8 assay), ROS occurrence (flow cytometry) and gene expression (qPCR) responses were conserved mechanisms (Hayashi et al. 2012). Other examples include the worm species, *Lumbricus terrestris* (Fugère et al., 1996), where metal-specific toxicity was observed for Hg, Cd, Zn and Pb using *in vitro* exposure, i.e. high decrease in viability and phagocytic activity (Hg), lower decrease in viability and high decrease in phagocytic activity (Zn, Cd), and no decrease in viability or phagocytic activity (Pb).

However, *in vitro* studies also have issues, e.g. the toxicology can be low on the ecological realism, especially when a variety of cell culture media are used that do not

reflect *in vivo* conditions. This can be an even more important issue for NM hazard assessment, given the high reactivity and interaction with the biomolecules present in the biological fluids and “corona” formation (Lynch et al., 2009; Monopoli et al., 2012). The use of native fluids for cell culture is a good approach for mimicking the real biological environment, but it is often difficult to obtain. However, the biomolecule composition will differ and so will the interactions with the NMs and the outcome (Maiorano et al., 2010). Surface modification has been widely used as a strategy to minimize NPs-biomolecule interactions in safe-by-design strategies for NMs stabilization (Tejamaya et al., 2012), but such changes will additionally influence the fate and effect of NMs (Javed et al., 2017; Meyer et al., 2010; Su et al., 2009). For instance, coatings that enable NMs with a positive surface charge are likely to improve biocompatibility with the negatively charged cellular membrane thus promoting cellular uptake with implications for cytotoxicity (Harush-Frenkel et al., 2007; Yue et al., 2011). However, predictive risk assessment is still hampered by contradictory results that show coating-independent toxicity (Bastos et al., 2017; Zhang et al., 2015). Hence, a shift in the current paradigm is necessary to cover the interactions of the NMs with the native biological fluid components allowing a correct prediction to *in vivo* effects.

Hence, in the present study we have assessed the cell viability of the standard earthworm test species *Eisenia fetida* (OECD, 2016) using the coelomocytes and the respective coelomic fluid. Copper oxide NMs were tested, including pristine and surface modified NMs (ascorbate, citrate, polyethylenimine and poly(vinylpyrrolidinone), as developed by (Ortelli et al., 2017) for safe by design strategy, plus a Cu salt (CuCl_2) for comparison.

MATERIALS AND METHODS

Test materials, spiking and characterization

Pristine copper oxide nanomaterials (PRI CuO NMs) (PlasmaChem GmbH, Germany), CuO NMs with four different surface modifications: citrate (CIT), ascorbate (ASC), polyvinylpyrrolidone (PVP) and polyethylenimine (PEI), were used plus copper (II) chloride dihydrate ($\text{CuCl}_2 \cdot 2\text{H}_2\text{O}$ > 99.9% purity, Sigma-Aldrich) for comparison. Coated CuO NPs were synthesized from commercial CuO nanopowder (PlasmaChem GmbH, Germany) and prepared according to Ortelli et al. (2017). Morphological characterization of pristine CuO NMs by STEM analysis showed that CuO NMs were spherical and mono-dispersed

with a primary nanoparticle average diameter of 12 ± 8 nm (N=50) (for full characterization details see table S1). Stock working solutions of 10 mg Cu/L in phosphate buffered-saline (PBS: 0.01 M phosphate buffer, 0.0027 M potassium chloride and 0.137 M sodium chloride, pH 7.4; Sigma-Aldrich, Cat. No. P4417) were used. Characterization in different media (Table 1) is provided.

Table 1: Characterization of pristine and surface modified CuO NMs samples dispersed in Milli-Q water (pH = 6.5), Phosphate Buffered Saline (PBS) (pH = 7.4) and biological media DMEM – (Dulbecco's Modified Eagle Medium) (pH = 8.2), including ζ -potentials (mV), hydrodynamic diameter (nm), sedimentation velocity ($\mu\text{m}/\text{sec}$), $\text{Cu}_{\text{dissolved}}/\text{CuO}_{\text{total}}$ weight ratio (%) after 24 h at 25 °C (from (Ortelli et al., 2017)). CIT: Citrate; ASC: Ascorbate; PVP: Polyvinylpyrrolidone; PEI: Polyethylenimine; PRI: Pristine. The reversal of the CuO pristine surface charge sign is due to the presence of phosphate ions (PO_4^{3-}) used in the sample preparation, which are specifically adsorbed onto the CuO NMs surface.

CuO	ζ -potential (mV)			hydrodynamic diameter (nm)			sedimentation velocity ($\mu\text{m}/\text{sec}$)			$\text{Cu}_{\text{dissolved}}/\text{CuO}_{\text{total}}$ weight ratio (%)		
	Milli-Q	PBS	DMEM	Milli-Q	PBS	DMEM	Milli-Q	PBS	DMEM	Milli-Q	PBS	DMEM
PRI- PO_4^{3-}	-9.1 \pm 0.4	-2.3 \pm 2.1	-8.2 \pm 7.4	1093 \pm 50	2756 \pm 347	55 \pm 6	0.12	0.43	0.04	0.2 (1.1)	<0.3 (0.1)	67 (0.5)
CIT	-18.0 \pm 0.3	-3.4 \pm 1.2	-9.7 \pm 0.6	368 \pm 10	271 \pm 43	37 \pm 2	0.1	0.08	0.03	2 (0.5)	1.8 (0.4)	69 (1.0)
ASC	-17.4 \pm 0.3	-8.1 \pm 0.1	-9.2 \pm 0.2	122 \pm 1.4	1314 \pm 525	73 \pm 21	0.0	0.0	0.01	2 (0.5)	<0.3 (0.1)	65 (0.4)
PEI	+28.3 \pm 0.7	+13.8 \pm 0.1	-10.1 \pm 0.7	247 \pm 14	209 \pm 16	45 \pm 14	0.05	0.03	0.1	2.8 (0.6)	2.5 (0.6)	67 (0.5)
PVP	-8.1 \pm 2.3	-0.9 \pm 0.7	-9.4 \pm 0.8	797 \pm 84	2765 \pm 432	53 \pm 25	0.06	0.2	0.03	0.2 (1.0)	<0.3 (0.1)	66 (1.3)

The CuO NM solutions were serially diluted from stock solutions in freshly extracted coelomic fluid in the following concentrations: 0-5-10-50-100-500 μg CuO NM - coated/mL, 0-1-5-10-50-100-500 μg CuO NM/mL and 0-1-5-10-50-100 μg Cu/mL for CuCl_2 .

Cell and coelomic fluid extraction

Eisenia fetida (Oligochaeta, Lumbricidae) earthworms were kept in culture in OECD artificial soil, fed ad libitum with horse manure and under controlled conditions at 18 °C and a photoperiod of 16:8 (light:dark). Selected organisms had similar size (300 - 600 mg) and developed clitellum, as described in OECD standard 222 (OECD,2016). Earthworms were carefully sampled from culture, cleaned with 1X PBS and were transferred to a petri dish with filter paper moistened with PBS for about 1 hour for gut purge. The posterior body part of the worms was massaged to allow expulsion of the content of the gut intestinal tract. Pools of 3-4 worms were subsequently used to obtain the necessary cellular density. Worms were gently placed on a glass petri dish with sterile PBS (1 mL/worm) and an electric current was applied using a 9 V battery for 6 cycles of 2 seconds. The cell suspension was transferred to a centrifuge tube and 1% penicillin-streptomycin and 1% amphotericin was added. Cells were counted in a hemocytometer in order to obtain a density of 10^6 cell/mL, which was seeded in siliconized tubes and left for 24h (dark, 20 °C) to allow acclimation.

Coelomic fluid extraction, used for toxicity exposure, followed the same extraction procedure as for the cells, after which it was filtered through a 0.2 μm filter to remove cells and supplemented with 1% penicillin-streptomycin and 1% amphotericin. The protein concentration was measured (Biowave DNA Life Science Spectrophotometer) and set to 100 μg protein/mL to normalize the protein content. A control with only coelomic fluid was included as well as a control without cells for each treatment to verify NMs interference. Interaction of NMs with coelomic biomolecules was allowed for 24h (dark, 4°C).

In vitro test procedures and flow cytometry

After removal of the medium by centrifugation (5 minutes at 1500 rpm), coelomocytes were exposed to 200 μL of each treatment for 24h and flow cytometry analysis was carried out afterwards. Three independent assays were performed for each test material, using a different pool of worms and the respective batches of coelomic fluid.

For the flow cytometry analysis, 7-aminoactinomycin D (7-AAD; Sigma-Aldrich) and propidium iodide (PI; Sigma-Aldrich), both DNA intercalating fluorescent dyes, were used to assess cell viability and membrane integrity. As these cannot enter cells with intact membranes, measurements will correspond to staining dead cells or cells with compromised membranes. Briefly, cells were loaded with 4 μ L PI and 8 μ L 7AAD and were immediately analyzed by flow cytometry (NovoCyte Flow Cytometer). The 488 nm laser was used for excitation; 7AAD was detected in BL4 (675/30) and PI in BL3 (615/24). For auto-compensation, unstained and singly stained cells were processed. In each replicate, a minimum of 10000 events were gated. To exclude interference of NMs and debris, the solutions with each concentration and treatment were gated out of the analysis, i.e. for each cell exposure concentration there was an equivalent exposure concentration without cells which was used for gating.

Data treatment

Flow cytometry data were analyzed using FlowLogic® Software (Affymetrix), and viability was normalized to control values. One-way analysis of variance (ANOVA) followed by Dunnett's comparison post-hoc test ($p < 0.05$) was used to assess differences between controls and treatments (SigmaPlot, 1997).

RESULTS

Results of the flow cytometry analysis for cell viability are shown in figure 1.

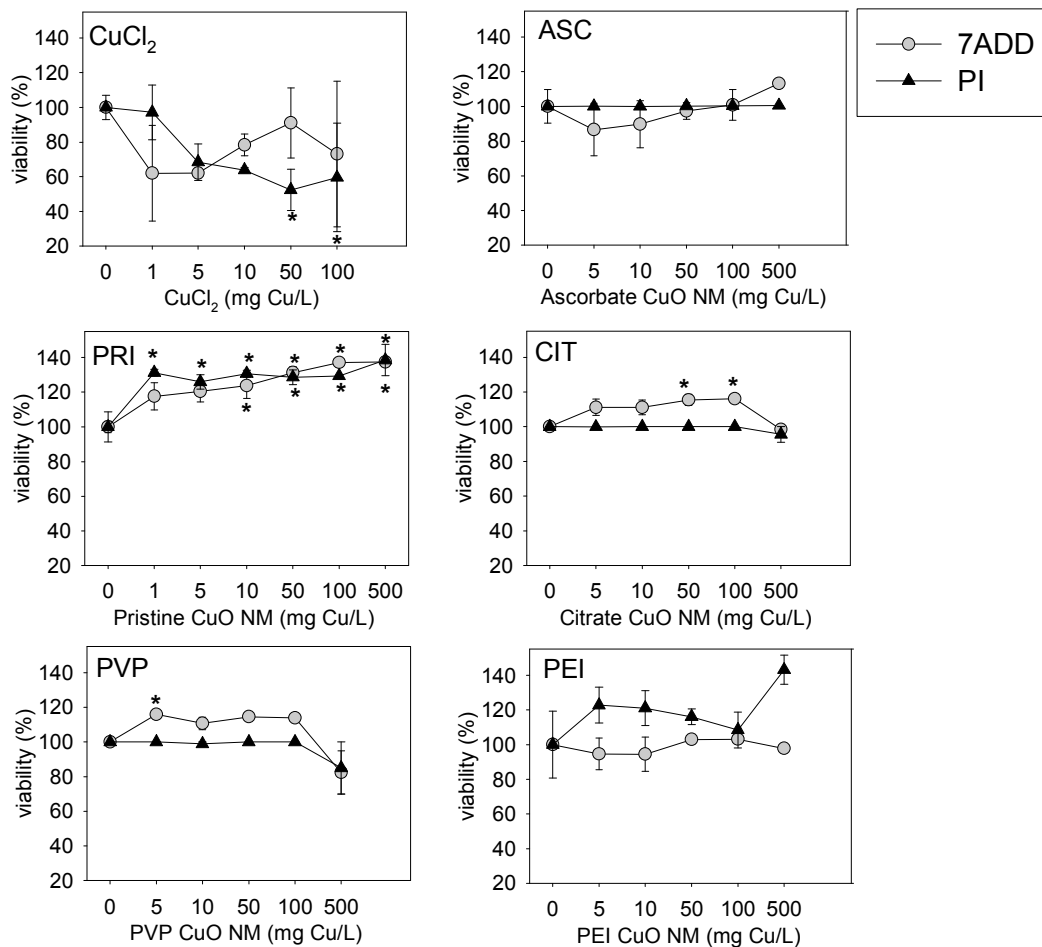


Figure 1: Viability of *Eisenia fetida*'s coelomocytes after 24 hour exposure in coelomic fluid to 0-500 $\mu\text{g Cu/mL}$ range of different CuO NMs - pristine (PRI) and coated (citrate (CIT), ascorbate (ASC), polyvinylpyrrolidone (PVP), polyethylenimine (PEI)), plus CuCl_2 . 7-AAD: 7-aminoactinomycin D PI: propidium iodide. Values are expressed as % normalized to the control average \pm standard error ($\text{AV} \pm \text{SE}$) ($n=3$). *: $p < 0.05$ (between control and treatment).

CuCl_2 affected cell viability in a dose-related manner (shown with PI), whereas none of the CuO NMs caused a significant negative impact.

Representative histograms of the analysis are shown in figure 2. Since displacement of the peaks were observed for some CuO NMs treated samples (i.e. displaced compared to the respective controls), dead populations were only considered after appearance of a second peak.

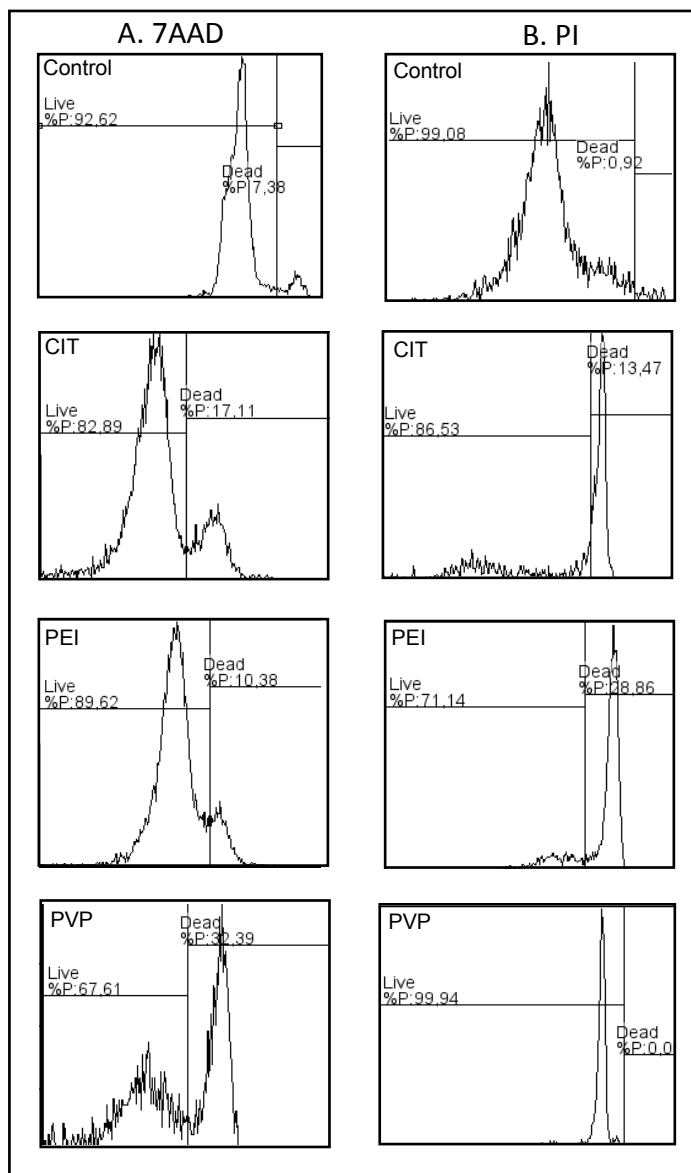


Figure 2: Representative histograms and viability analysis of cells stained with A: 7-aminoactinomycin D (7AAD) and B: Propidium Iodide (PI). CIT: citrate, PEI: polyethylenimine, PVP: polyvinylpyrrolidone CuO NMs.

Figure 3 shows the interference of the tested materials with the cells' signals. The total coelomocyte population was considered, as it was not possible to discriminate between different populations (amoebocytes and eleocytes) in this case: the process used to exclude materials also excludes part of the coelomocytes population (eleocytes) due to overlap.

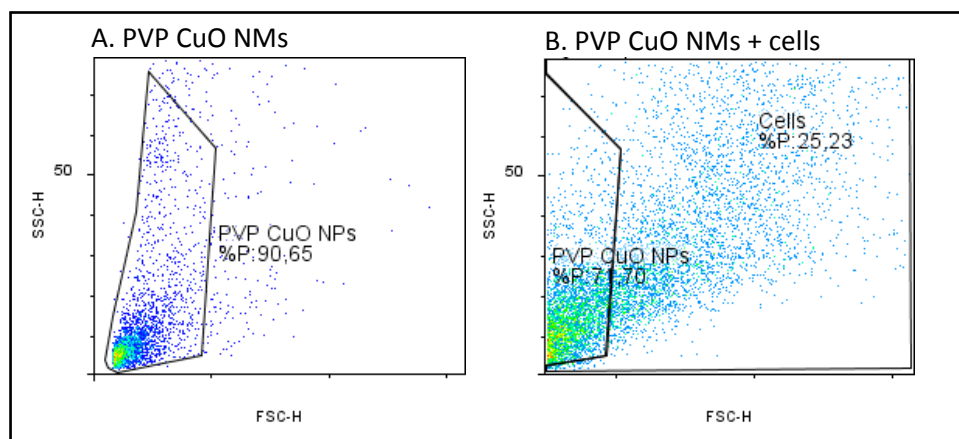


Figure 3: Representation of the overlap between test materials (NMs/CuCl₂) and cells signal. Spectra of materials alone in (A) PVP-CuO NMs. Spectra of the samples containing the cells exposed to the materials for (B) PVP CuO NMs.

DISCUSSION

The present study indicates a difference in toxicity between CuCl₂ and CuO NMs in regards to total *Eisenia fetida*'s coelomocytes population. Whereas CuCl₂ showed some toxicity, no mortality was observed for the particles at similar concentrations. Previous studies have shown that CuO NMs interfered with the immune system in the earthworm *Metaphire posthum* (Annelida: Clitellata: Oligochaeta) exposed *via* the soil (up to 1 g CuO NMs/kg soil) (Gautam et al., 2018). The authors reported sublethal effects, such as decreased phagocytic or catalase activity, but without cell viability decrease. Hence, this confirms that cell viability (a lethal effect) can be less sensitive. However, it may be difficult in our study to rule out viability decrease, especially for eleocytes, which in general in the FSC-SSC plot occupy the exact same areas that we gated based on particle concentration. Another relevant aspect is the exposure, which can be tested *via* 1) the whole organism exposure (*via* soil, realistic) and posteriori cell extraction for measurements or 2) *via* the cells in the *in vitro* system (*via* the coelomic fluid, artificial). Both methods have their pros and cons and ideally should both be included.

CuO NMs can also disturb the immune system in mammals, for instance by interfering with macrophages' normal functions (Triboulet et al., 2015) or recruiting and activating neutrophils (Kim et al., 2011). Studies with human or mouse-derived cells exposed to CuO NMs have described decreased viability (Akhtar et al., 2016; Boyles et al., 2016), occurrence of oxidative stress (Akhtar et al., 2016; Niska et al., 2015), DNA damage (Ahamed et al., 2010), inflammation (Ko et al., 2016) and cell death via apoptosis (Niska

et al., 2015) or necrosis (Rodhe et al., 2015). Earthworm cells (coelomocytes) could be comparatively less sensitive to CuO NMs, as organisms may have to deal with high Cu concentration when ingesting decayed organic material. Gupta and colleagues (2014) reported uptake of zinc oxide ZnO NPs up to 3 mg/L in *E. fetida*'s coelomocytes without induction of DNA damage. *E. fetida* was further proposed as a ZnO NPs scavenger, when aggregation and clustering of ZnO NPs up to the micron-size were observed in coelomocytes, possibly due to ZnO NPs interaction with fulvic compound and humic substances of the coelomic fluid imparting considerable implications in the toxicological profile due to loss of the nano size (Yadav, 2017).

Although there was a concentration response interaction (especially based on PI) between CuCl₂ and cell viability, this happened at relative high concentrations. The "low" decrease with high concentrations can be interpreted in light of Cu being an essential element acting as cofactor for several enzymatic reactions (Festa and Thiele, 2011; Lalioti et al., 2009) and, hence, highly regulated until high doses. Either way, we should bare in mind the interference between the test material and the cell signals, which resulted in a final lower cell count (figure 3) due to exclusion of the overlapping events related to CuCl₂ alone. Additionally, the sensitivity of *E. fetida*'s coelomocytes to Cu has already been shown *in vivo* (Homa et al., 2007; Scott-Fordsmand et al., 2000), hence, *in vitro* effects can be underestimated here.

The importance of CuO NMs surface modifications for toxicity could not be discriminated, since no cell mortality was observed. Again, considering that certain cell populations (especially eleocytes) may have been gated out. The characterization study showed that despite the different surface charge provided by the coatings (negative for CIT and ASC, positive for PEI and neutral for PVP), the interaction with proteins and amino acids present in the biological media (DMEM and MEM) regulated the behaviour of CuO NMs to a similar state, i.e. all zeta potential values were leveraged and no agglomeration occurred for any CuO NMs (Ortelli et al., 2017). Also, higher dissolution rates (ca. 66 % $Cu_{dissolved}/CuO_{total}$ ratio) were found in biological media compared to e.g. PBS (2.5-0.3%) (Ortelli et al., 2017), hence, based on this we would expect toxicity to occur *via* Cu ions. Cytotoxicity of the same ASC, CIT, PEI and PVP-coated CuO NMs was reported in RAW264.7 macrophages with concentrations up to 60 µg Cu/mL (Líbalová et al., 2018); however, since no correlation could be found between measured intracellular Cu and the cytotoxic effect, a simple interpretation of toxicity based on Cu dissolution was rejected. This suggested that CuO NMs may induce toxicity in a nano-specific manner. Inconsistencies in the results in regard to different coatings were also found for Ag NMs.

For instance, CIT was found to be more toxic in mammalian cells than polyethylene glycol (PEG) (Bastos et al., 2016) and PVP (Begum et al., 2016; Wang et al., 2014), but higher sensitivity towards PEG compared to CIT coating was found in human cells (Tlotleng et al., 2016). Hence, variability and scarcity in the results so far hamper the prediction based on surface changes.

It is worth mentioning that we have here used the coelomic fluid instead of an artificial media, providing a more realistic scenario by mimicking the *in vivo* environment. Hayashi et al. (2013) showed the relevance of using physiological relevant fluids in *in vitro* testing, as this increased Ag NMs interaction and consequent accumulation in coelomocytes with *E. fetida*'s coelomic proteins compared to non-native proteins. In an *in vivo* exposure with *Eisenia andrei* exposed for 7 days to CIT-coated Ag NMs in soil (Kwak et al., 2014), the *in vitro* results showed increased aggregation and dissolution with coelomic fluid compared to water, and mild cytotoxicity for CIT-coated Ag NMs with negligible effect of dissolved Ag ions. The artificial biological fluids also show the multiparametric nature of NPs toxicity. For instance, in human keratinocytes selective synergistic toxicity was found between simulated interstitial fluid and CuO NPs, but that was not the case with TiO₂ NPs, and increased agglomeration and deposition occurred with both NPs compared to traditional RPMI media (Cathe et al., 2017). Also, protein interaction with graphene oxide was found to mitigate the cytotoxicity in A549 cells (Hu et al., 2011).

We hypothesize that the interactions with the coelomic proteins may interfere with the potential toxicity of NPs, possibly in a nano-specific manner and independently of the coating. It is possible that lack of mortality is related to challenges of the test design and interference of the NMs in the cell count.

In vitro challenges and way forward

Flow cytometry presents data analysis challenges (Kroll et al., 2009), especially when event count overlaps between test material and cell signal. This means that cell signals may have to be discarded, as it was not possible to discriminate between cells and particles. Flow cytometry is still one of the best techniques to provide a (more) reliable and sensitive analysis (Kumar et al., 2015), and several alternative dyes can be combined to improve results, although it is also well known that dyes bind to particles.

Another important aspect is the exposure period, often too short to allow cell interaction and impact measurement. Time series and longer exposures should be conducted, although this is not always possible without continuous cell lines and long-term cell

viability is an issue. Continuous cell lines, which can proliferate indefinitely, carry practical advantages, but primary cell lines, isolated directly and with limited lifespan, may have increased relevancy and potential. Results from a comet assay (*in vitro*, genotoxicity) in *Enchytraeus crypticus* (Maria et al., 2017) showed that effects of Ag NMs occurred later compared to AgNO₃.

For *in vitro* exposure to NMs, the NMs agglomeration in cell media is a reoccurring matter that must be taken into account when interpreting results. However, since cell media is a complex media, it is difficult to get good measures of agglomeration. It is worth while considering alternative exposure methods, e.g. the use of a tube rotator could improve a more homogeneous exposure and prevent cell and NMs sedimentation.

CONCLUSIONS

In the present study, *Eisenia fetida*'s coelomocytes viability was negatively affected by CuCl₂, but not by CuO NMs, irrespective of the surface modification. However, a key observation here was the rather large overlap between spectra for particles and for cells, which meant that when compensating for NMs in a sample, cells may indeed be also compensated ("gated out"). The use of the coelomic fluid may have further mitigated the toxicity of the NPs due to the formation of a native corona, showing the importance of using relevant biological media for real biomolecule-NPs interactions. The current methodology challenges and way forward were discussed.

ACKNOWLEDGEMENTS

This study was supported by the EU-FP7 SUN: SUstainable Nanotechnologies (Ref. 604305) and acknowledge the materials characterization work made within the SUN consortium partners (Work Package 2). Thanks are due to the support of CESAM (UID/AMB/50017 - POCI-01-0145-FEDER-007638), to FCT/MCTES through national funds (PIDDAC), and the co-funding by the FEDER, within the PT2020 Partnership Agreement and Compete 2020 within the research project NM_OREO (POCI-01-0145-FEDER-016771, PTDC/AAG-MAA/4084/2014), and through FCT via a PhD grant to Maria J. Ribeiro (SFRH/BD/95027/2013).

REFERENCES

- Ahamed, M., Siddiqui, M.A., Akhtar, M.J., Ahmad, I., Pant, A.B., Alhadlaq, H.A., 2010. Genotoxic potential of copper oxide nanoparticles in human lung epithelial cells. *Biochem. Biophys. Res. Commun.* 396, 578–583. doi:10.1016/j.bbrc.2010.04.156
- Akhtar, M.J., Kumar, S., Alhadlaq, H.A., Alrokayan, S.A., Abu-Salah, K.M., Ahamed, M., 2016. Dose-dependent genotoxicity of copper oxide nanoparticles stimulated by reactive oxygen species in human lung epithelial cells. *Toxicol. Ind. Health* 32, 809–821. doi:10.1177/0748233713511512
- Bastos, V., Brown, D., Johnston, H., Daniel-da-Silva, A.L., Duarte, I.F., Santos, C., Oliveira, H., 2016. Inflammatory responses of a human keratinocyte cell line to 10 nm citrate- and PEG-coated silver nanoparticles. *J. Nanoparticle Res.* 18, 205. doi:10.1007/s11051-016-3515-x
- Bastos, V., Ferreira-de-Oliveira, J.M.P., Carrola, J., Daniel-da-Silva, A.L., Duarte, I.F., Santos, C., Oliveira, H., 2017. Coating independent cytotoxicity of citrate- and PEG-coated silver nanoparticles on a human hepatoma cell line. *J. Environ. Sci. (China)* 51, 191–201. doi:10.1016/j.jes.2016.05.028
- Beer, C., Foldbjerg, R., Hayashi, Y., Sutherland, D.S., Autrup, H., 2012. Toxicity of silver nanoparticles - nanoparticle or silver ion? *Toxicol. Lett.* 208, 286–92. doi:10.1016/j.toxlet.2011.11.002
- Begum, A.N., Aguilar, J.S., Elias, L., Hong, Y., 2016. Silver nanoparticles exhibit coating and dose-dependent neurotoxicity in glutamatergic neurons derived from human embryonic stem cells. *Neurotoxicology* 57, 45–53. doi:10.1016/j.neuro.2016.08.015
- Boyles, M.S.P., Ranninger, C., Reischl, R., Rurik, M., Tessadri, R., Kohlbacher, O., Duschl, A., Huber, C.G., 2016. Copper oxide nanoparticle toxicity profiling using untargeted metabolomics. *Part. Fibre Toxicol.* 13, 1–20. doi:10.1186/s12989-016-0160-6

Cathe, D.S., Whitaker, J.N., Breitner, E.K., Comfort, K.K., 2017. Exposure to metal oxide nanoparticles in physiological fluid induced synergistic biological effects in a keratinocyte model. *Toxicol. Lett.* 268, 1–7. doi:10.1016/j.toxlet.2017.01.003

Cooper, E.L., Roch, P., 2003. Earthworm immunity: a model of immune competence: The 7th international symposium on earthworm ecology· Cardiff· Wales· 2002. *Pedobiologia (Jena)*. 47, 676–688.

Festa, R.A., Thiele, D.J., 2011. Copper: An essential metal in biology. *Curr. Biol.* 21, R877–R883. doi:10.1016/j.cub.2011.09.040

Fugère, N., Brousseau, P., Krzystyniak, K., Coderre, D., Fournier, M., 1996. Heavy metal-specific inhibition of phagocytosis and different *in vitro* sensitivity of heterogeneous coelomocytes from *Lumbricus terrestris* (Oligochaeta). *Toxicology* 109, 157–166.

Gautam, A., Ray, A., Mukherjee, S., Das, S., Pal, K., Das, S., Karmakar, P., Ray, M., Ray, S., 2018. Immunotoxicity of copper nanoparticle and copper sulfate in a common Indian earthworm. *Ecotoxicol. Environ. Saf.* 148, 620–631. doi:10.1016/j.ecoenv.2017.11.008

Gomes, S.I.L., Murphy, M., Nielsen, M.T., Kristiansen, S.M., Amorim, M.J.B., Scott-Fordsmand, J.J., 2015. Cu-nanoparticles ecotoxicity - Explored and explained? *Chemosphere* 139, 240–245. doi:10.1016/j.chemosphere.2015.06.045

Gupta, S., Kushwah, T., Yadav, S., 2014. Earthworm coelomocytes as nanoscavenger of ZnO NPs. *Nanoscale Res. Lett.* 9, 259. doi:10.1186/1556-276X-9-259

Harush-Frenkel, O., Debotton, N., Benita, S., Altschuler, Y., 2007. Targeting of nanoparticles to the clathrin-mediated endocytic pathway. *Biochem. Biophys. Res. Commun.* 353, 26–32. doi:10.1016/j.bbrc.2006.11.135

Hayashi, Y., Engelmann, P., Foldbjerg, R., Szabó, M., Somogyi, I., Pollák, E., Molnár, L., Autrup, H., Sutherland, D.S., Scott-Fordsmand, J., Heckmann, L.-H., 2012. Earthworms and humans *in vitro*: characterizing evolutionarily conserved stress and immune responses to silver nanoparticles. *Environ. Sci. Technol.* 46, 4166–73. doi:10.1021/es3000905

Hayashi, Y., Miclaus, T., Scavenius, C., Kwiatkowska, K., Sobota, A., Scott-fordsmand, J.J., Enghild, J.J., Sutherland, D.S., 2013. Species Differences Take Shape at Nanoparticles: Protein Corona Made of the Native Repertoire Assists Cellular Interaction. *Environ. Sci. Technol.* 47, 14367–14375.

Homa, J., Stürzenbaum, S.R., Morgan, A.J., Plytycz, B., 2007. Disrupted homeostasis in coelomocytes of *Eisenia fetida* and *Allolobophora chlorotica* exposed dermally to heavy metals. *Eur. J. Soil Biol.* 43, S273–S280.

Hu, W., Peng, C., Lv, M., Li, X., Zhang, Y., Chen, N., Fan, C., Huang, Q., 2011. Protein corona-mediated mitigation of cytotoxicity of graphene oxide. *ACS Nano* 5, 3693–700. doi:10.1021/nn200021j

Javed, R., Ahmed, M., Haq, I. ul, Nisa, S., Zia, M., 2017. PVP and PEG doped CuO nanoparticles are more biologically active: Antibacterial, antioxidant, antidiabetic and cytotoxic perspective. *Mater. Sci. Eng. C* 79, 108–115. doi:10.1016/j.msec.2017.05.006

Kim, J.S., Adamcakova-Dodd, A., O’Shaughnessy, P.T., Grassian, V.H., Thorne, P.S., 2011. Effects of copper nanoparticle exposure on host defense in a murine pulmonary infection model. *Part. Fibre Toxicol.* 8, 29. doi:10.1186/1743-8977-8-29

Ko, J.W., Park, J.W., Shin, N.R., Kim, J.H., Cho, Y.K., Shin, D.H., Kim, J.C., Lee, I.C., Oh, S.R., Ahn, K.S., Shin, I.S., 2016. Copper oxide nanoparticle induces inflammatory response and mucus production via MAPK signaling in human bronchial epithelial cells. *Environ. Toxicol. Pharmacol.* 43, 21–26. doi:10.1016/j.etap.2016.02.008

Kroll, A., Pillukat, M.H., Hahn, D., Schnekenburger, J., 2009. Current *in vitro* methods in nanoparticle risk assessment: limitations and challenges. *Eur. J. Pharm. Biopharm.* 72, 370–377.

Kumar, G., Degheidy, H., Casey, B.J., Goering, P.L., 2015. Flow cytometry evaluation of *in vitro* cellular necrosis and apoptosis induced by silver nanoparticles. *Food Chem. Toxicol.* 85, 45–51.

Kwak, J. II, Lee, W.-M., Kim, S.W., An, Y.-J., 2014. Interaction of citrate-coated silver nanoparticles with earthworm coelomic fluid and related cytotoxicity in *Eisenia andrei*. *J. Appl. Toxicol.* 34, 1145–1154. doi:10.1002/jat.2993

Lagadic, L., Caquet, T., 1998. Invertebrates in testing of environmental chemicals: are they alternatives? *Environ. Health Perspect.* 106, 593.

Lalioti, V., Muruais, G., Tsuchiya, Y., Pulido, D., Sandoval, I. V, 2009. Molecular mechanisms of copper homeostasis. *Front. Biosci. (Landmark Ed.* 14, 4878—4903. doi:10.2741/3575

Líbalová, H., Costa, P.M., Olsson, M., Farcál, L., Ortelli, S., Blosi, M., Topinka, J., Costa, A.L., Fadeel, B., 2018. Toxicity of surface-modified copper oxide nanoparticles in a mouse macrophage cell line: Interplay of particles, surface coating and particle dissolution. *Chemosphere* 196, 482–493.

Liu, W.-T., 2006. Nanoparticles and their biological and environmental applications. *J. Biosci. Bioeng.* 102, 1–7. doi:10.1263/jbb.102.1

Lynch, I., Salvati, A., Dawson, K. a, 2009. Protein-nanoparticle interactions: What does the cell see? *Nat. Nanotechnol.* 4, 546–7. doi:10.1038/nnano.2009.248

Maiorano, G., Sabella, S., Sorce, B., Brunetti, V., Malvindi, M.A., Cingolani, R., Pompa, P.P., 2010. Effects of cell culture media on the dynamic formation of protein-nanoparticle complexes and influence on the cellular response. *ACS Nano* 4, 7481–91. doi:10.1021/nn101557e

Maria, V.L., Ribeiro, M.J., Guilherme, S., M. Soares, A.M.V., Scott-Fordsmand, J.J., Amorim, M.J.B., 2017. Silver (Nano)Materials cause genotoxicity in *Enchytraeus Crypticus* - as determined by the comet assay. *Environ. Toxicol. Chem.* 9999, 1–8. doi:10.1002/etc.3944

Meyer, J.N., Lord, C.A., Yang, X.Y., Turner, E.A., Badireddy, A.R., Marinakos, S.M., Chilkoti, A., Wiesner, M.R., Auffan, M., 2010. Intracellular uptake and associated toxicity

of silver nanoparticles in *Caenorhabditis elegans*. *Aquat. Toxicol.* 100, 140–150. doi:10.1016/j.aquatox.2010.07.016

Monopoli, M.P., Åberg, C., Salvati, A., Dawson, K.A., 2012. Biomolecular coronas provide the biological identity of nanosized materials. *Nat. Nanotechnol.* 7, 779–786. doi:10.1038/nnano.2012.207

Niles, A.L., Moravec, R.A., Riss, T.L., 2009. *In vitro* viability and cytotoxicity testing and same-well multi-parametric combinations for high throughput screening. *Curr. Chem. Genomics* 3, 33.

Niska, K., Santos-Martinez, M.J., Radomski, M.W., Inkielewicz-Stepniak, I., 2015. CuO nanoparticles induce apoptosis by impairing the antioxidant defense and detoxification systems in the mouse hippocampal HT22 cell line: Protective effect of crocetin. *Toxicol. Vitr.* 29, 663–671. doi:10.1016/j.tiv.2015.02.004

OECD, 2016. OECD Guidelines for the Testing of Chemicals. no. 222. Earthworm reproduction test (*Eisenia fetida*/*Eisenia andrei*). Organization for Economic Co-Operation and Development, Paris, France

Ortelli, S., Costa, A.L., Blosi, M., Brunelli, A., Badetti, E., Bonetto, A., Hristozov, D., Marcomini, A., 2017. Colloidal characterization of CuO nanoparticles in biological and environmental media. *Environ. Sci. Nano* 4, 1264–1272. doi:10.1039/C6EN00601A

Pankhurst, Q.A., Connolly, J., Jones, S.K., Dobson, J., 2003. Applications of magnetic nanoparticles in biomedicine. *J. Phys. D. Appl. Phys.* 36. doi:10.1088/0022-3727/36/13/201

Rodhe, Y., Skoglund, S., Odnevall Wallinder, I., Potáčová, Z., Möller, L., 2015. Copper-based nanoparticles induce high toxicity in leukemic HL60 cells. *Toxicol. Vitr.* 29, 1711–1719. doi:10.1016/j.tiv.2015.05.020

Scott-Fordsmand, J.J., Weeks, J.M., Hopkin, S.P., 2000. Importance of contamination history for understanding toxicity of copper to earthworm *Eisenia fetida* (Oligochaeta: Annelida), using neutral-red retention assay. *Environ. Toxicol. Chem.* 19, 1774–1780.

SigmaPlot, 1997. Statistical Package for the Social Sciences, 11.0. Systat Software, Inc., Chicago, IL, USA.

Su, Y., He, Y., Lu, H., Sai, L., Li, Q., Li, W., Wang, L., Shen, P., Huang, Q., Fan, C., 2009. The cytotoxicity of cadmium based, aqueous phase - Synthesized, quantum dots and its modulation by surface coating. *Biomaterials* 30, 19–25. doi:10.1016/j.biomaterials.2008.09.029

Tejamaya, M., Römer, I., Merrifield, R.C., Lead, J.R., 2012. Stability of citrate, PVP, and PEG coated silver nanoparticles in ecotoxicology media. *Environ. Sci. Technol.* 46, 7011–7017. doi:10.1021/es2038596

Tiede, K., Hassellöv, M., Breitbarth, E., Chaudhry, Q., Boxall, A.B.A., 2009. Considerations for environmental fate and ecotoxicity testing to support environmental risk assessments for engineered nanoparticles. *J. Chromatogr. A* 1216, 503–509.

Tlotleng, N., Vetten, M.A., Keter, F.K., Skepu, A., Tshikhudo, R., Gulumian, M., 2016. Cytotoxicity, intracellular localization and exocytosis of citrate capped and PEG functionalized gold nanoparticles in human hepatocyte and kidney cells. *Cell Biol. Toxicol.* 32, 305–321. doi:10.1007/s10565-016-9336-y

Triboulet, S., Aude-Garcia, C., Armand, L., Collin-Faure, V., Chevallet, M., Diemer, H., Gerdil, A., Proamer, F., Strub, J.M., Habert, A., Herlin, N., Van Dorsselaer, A., Carrière, M., Rabilloud, T., 2015. Comparative proteomic analysis of the molecular responses of mouse macrophages to titanium dioxide and copper oxide nanoparticles unravels some toxic mechanisms for copper oxide nanoparticles in macrophages. *PLoS One* 10, 1–22. doi:10.1371/journal.pone.0124496

Wang, X., Ji, Z., Chang, C.H., Zhang, H., Wang, M., Liao, Y.P., Lin, S., Meng, H., Li, R., Sun, B., Winkle, L. Van, Pinkerton, K.E., Zink, J.I., Xia, T., Nel, A.E., 2014. Use of coated silver nanoparticles to understand the relationship of particle dissolution and bioavailability to cell and lung toxicological potential. *Small* 10, 385–398. doi:10.1002/smll.201301597

Yadav, S., 2017. Potentiality of Earthworms as Bioremediating Agent for Nanoparticles, in: *Nanoscience and Plant–Soil Systems*. Springer, pp. 259–278.

Yue, Z.-G., Wei, W., Lv, P.-P., Yue, H., Wang, L.-Y., Su, Z.-G., Ma, G.-H., 2011. Surface charge affects cellular uptake and intracellular trafficking of chitosan-based nanoparticles. *Biomacromolecules* 12, 2440–2446.

Zhang, Y., Newton, B., Lewis, E., Fu, P.P., Kafoury, R., Ray, P.C., Yu, H., 2015. Cytotoxicity of organic surface coating agents used for nanoparticles synthesis and stability. *Toxicol. Vitr.* 29, 762–768. doi:10.1016/j.tiv.2015.01.017

SUPPORTING INFORMATION

Table S1: Physical-chemical characteristics of the pristine CuO NMs.

Characteristics	Pristine CuO NMs
Manufacturer	Plasma chem
CAS number	1317-38-0
Primary size distribution (average)	3 – 35 (12)
Mode (1 st quartile – 3 rd quartile) [nm]	10 (9.2 – 14)
Shape	Semi-spherical
Average crystallite size [nm]	9.3
Crystallite phases (%)	Tenorite 100 %
Dispersibility in water: D50 [nm]; Average Agglomeration Number (AAN)	135.5 ± 4.6 346
Dispersibility in modified MEM: D50 [nm]; Average Agglomeration Number (AAN)	85.2 ± 2.7 77
Z-potential in UP water [mV]	+28.1 ± 0.6
IsoElectric Point (pH)	10.3
Photocatalysis: photon efficiency	1.5x10 ⁻⁴
Specific Surface Area [m ² g/1]	47.0 ± 1.7
Pore sizes [nm]	13.5 ± 1.6 (BJH) 23.0 ± 0.9 (AVG)
Surface chemistry [atomic fraction]	Cu = 0.46±0.05; O = 0.47±0.05; C = 0.07±0.01
Chemical impurities [mg kg/1]	Na: 505 ± 30; Pb: 36 ± 2; Ag: 13 ± 4

**General Discussion
and
Conclusions**

The molecular effects of silver nanomaterials (Ag NMs) and the salt silver nitrate (AgNO₃) were assessed in *E. crypticus*, in terms of oxidative stress (Chapter I) and genotoxicity (Chapter II). An earlier activation of the antioxidant mechanisms was found for AgNO₃ in comparison to Ag NMs; however, it was not enough to prevent lipid peroxidation (LPO). The same outcome (increase in LPO levels), was observed later for Ag NMs despite the enzymatic activation, that failed in counteracting the ROS imbalance. In terms of genotoxicity, again earlier toxicity was induced by AgNO₃ and the non-monotonic response observed with Ag NMs highlights the risk of exposure to lower-doses of NMs. The later response, both in terms of oxidative stress and genotoxicity, suggests that toxicity of Ag NMs could be related to slower dissolution rates, but a nano-specific effect cannot be discarded given the different effects of the two Ag forms. These studies provide important information regarding the Ag NMs toxicity mechanism in *E. crypticus*, suggesting that oxidative stress is an initiating toxic event which leads to downstream effects, namely DNA damage. This is in line with the mode of action described for other NMs, but it is necessary to evaluate other molecular level endpoints to further understand the cascade of events that leads to organism level effects.

The Comet assay for genotoxicity evaluation is now included in the array of techniques available to assess toxicity in *E. crypticus* and will hopefully benefit future risk assessment studies. Of particular interest will be the integration of this endpoint in Adverse Outcome Pathways (AOP), providing further in-depth understanding of the effect of NMs through several levels of biological organisation.

The effect of Tungsten carbide cobalt nanomaterials (WCCo NMs) and cobalt chloride (CoCl₂) assessed in *E. crypticus*, in terms of survival and reproduction (Chapter III) showed a specific reproductive effect of WCCo, and higher toxicity compared to CoCl₂, for comparable Co concentrations. The exposure characterization provided important information to understand WCCo toxicity. Quantification of Co in the soil:water biofilm (considered an entry route for soil invertebrates) and in the organisms revealed lower Co uptake in WCCo exposure, suggesting a nano-specific or synergistic effect between WC and Co. NMs toxicity testing has been performed using standardized tests developed for conventional chemicals but, and as Chapter I and II show, toxicity of NMs may require longer exposure periods, hence effects can be underestimated. Long-term exposure is a relevant scenario for NMs that is not covered in the current paradigm. The concept of long-term is still vague and involve other aspects, such as multigenerational effects, hence only doubling the exposure period was limited in assessing the true long-term

effects of WCCo and CoCl₂. Nonetheless, it constitutes a preliminary step in order to fill this gap in knowledge.

Multigenerational exposure is scarcely done and was within the scope of the present thesis (Chapter IV). Sublethal concentrations of WCCo NMs didn't impair survival nor reproduction across generations, while the decrease in reproduction induced by CoCl₂ was counteracted in next generations. Uptake of Co was dose-dependent for both chemicals, and while it was maintained throughout the test for CoCl₂, it gradually levelled to control values for WCCo NMs. Results suggest an effective detoxifying mechanism that allowed WCCo-exposed organisms to eliminate the Co, while with CoCl₂, it might have been stored. Transgenerational toxicity was not detected after transference to clean soil, but as only organism-level endpoints (survival and reproduction) were used, other endpoints (e.g., global DNA methylation changes) should also be analysed to account for such effect at lower, more sensitive levels.

Taken together, these results suggest that *E. crypticus* is able to cope with continuous exposure to lower sub-lethal WCCo NMs concentrations (e.g. up to EC50), without impairment in survival or reproduction, at least during the exposure period tested. If it happens at expenses of other physiological functions, or if it is a result of unintentional selection of more resistant organisms, still needs further clarification.

The current procedures and guidelines used in NMs risk assessment provide information that may not account for the true implications of NMs exposure and effects (e.g. long-term effects), the current paradigm needs to change in order to achieve more relevant understanding of the NMs impact.

Copper based nanomaterials (Cu NMs) with different coatings and copper chloride (CuCl₂) were used as a case study to understand the modulatory effect of surface modification (Chapter V). The immune system is an important line of defence for NMs, hence immune cells (coelomocytes) of the earthworm *Eisenia fetida* were used and their viability was assessed. No artificial culture media was used, instead, the native coelomic fluid was extracted to mimic the biological environment. The formation of a biomolecule corona naturally occurs when NMs become in contact with biological fluids. It is possible that the lack of toxicity may be related to the interaction with coelomic proteins and other components present in the fluid, that is, the formation of a protein "corona". However, the composition of the corona is expected to vary with time and among the different surface modifications, and the corona characterization would be important to understand changes in the NMs behaviour. It is possible that the effects could be underestimated due to challenges in the test design. For instance, increased time could be necessary to show

NMs effect (as reported for Ag NMs in Chapters I and II), hence the 24h exposure used could be too short. Flow cytometry was used in this study, and is currently one of the best alternative techniques to common spectrophotometric-based assays that struggle with NMs interference. It is highly relevant in NMs testing, since multi-parameters can be assessed in one single analysis, this way minimizing technical variability.

The technical issues encountered in this case study need to be addressed for future reliable NMs testing but this system is a promising approach to adapt the current *in vitro* testing for more relevant NMs exposures, accounting for the interactions between NMs and biomolecules that occur *in vivo*. As it cannot account for all *in vivo* features, the aim is not to replace NMs *in vivo* testing, at least all of it, but to provide additional information that may explain *in vivo* effects. For instance, molecular mechanisms that may be missed in the time windows of *in vivo* tests may be detected in *in vitro* using shorter-time frames.

In conclusion, the results here presented provide valuable information to increase the knowledge on the selected NMs effects, namely:

- NMs toxicity can be related to nano-specific effects and/or released ions. Slower dissolution rates for NMs may lead to later effects that may be missed when using short exposures.
- The exposure periods currently used in NMs testing may not be enough to predict long-term, multigenerational effects.

An effort was made to address some of the current gaps in nano(eco)toxicology, pushing the nano research one step closer to answers.

Some recommendations for future testing:

- The testing of NMs toxicity should consist of a multi-endpoint approach, but it is often not possible to cover different levels of biological organization in a single test. Hence, the integration of different endpoints can also be made, providing the cascade of events that explains the NMs toxicity mechanisms toxicity.
- The use of realistic scenarios is necessary to understand the risk of exposure to NMs, and the current standard tests used for NMs toxicity evaluation can (and need to) be adapted to cover long-term, persistent effects of NMs.
- The use of *in vitro* testing to predict *in vivo* effects is undeniably attractive, considering the lower costs and time that the first require, however, it is still challenging. A possible strategy to address this issue involves the use of native biological fluids in *in vitro* exposures, as the use of artificial culture media greatly

limits the interactions that are likely to occur between NMs and the organisms' biomolecules.